RNA-binding protein HuD as a potential therapeutic target for Spinal muscular atrophy

Andréanne Didillon

This thesis is submitted as a partial fulfillment of the
M.Sc. program in Cellular and Molecular Medicine
December 20th, 2017

Faculty of Medicine
University of Ottawa

Abstract

Spinal muscular atrophy is caused by mutation of the *SMN1* gene resulting in the selective loss of spinal cord motor neurons. HuD has been shown to interact with SMN and to localize to RNA granules along axons. In conditions where SMN is decreased, like in SMA, HuD's localization to RNA granules affected. Overexpression of HuD in an SMA cell culture model was shown to rescue SMA-like axonal defects. Here, existence of a signaling pathway downstream of PKC leading to the activation of HuD was investigated in MN-1 cells. Stimulation of this pathway using a pharmacological agonist of PKC increased HuD levels and enhanced its binding to GAP-43 and Tau mRNAs. An scAAV9 viral expression system to overexpress HuD *in vivo* was established, laying the foundation for the next phase of the study. Overall, modulating HuD expression and activity would be beneficial and could constitute an attractive therapeutic approach for SMA.

Table of contents

Abstract ii

Table of contents iii

List of figures vii

List of abbreviations ix

Acknowledgements xv

Chapter 1. Introduction 1

1.1 Spinal muscular atrophy (SMA) 1

1.1.1 Survival of motor neuron gene 1

1.1.2 Clinical classification 2

1.1.2.1 Types of SMA 2

1.1.2.2 Disease modifiers 5

1.1.3 Select mouse models of SMA 6

1.1.3.1 The Taiwanese model 7

1.1.3.2 The Burghes models 7

1.1.4 The Survival of motor neuron protein 8

1.1.4.1 SMA: A defective snRNP biogenesis and pre-mRNA splicing disease 10

1.1.4.2 SMA: A motor neuron-specific role for the SMN protein 11

1.2. Embryonic lethal abnormal vision-like (ELAVL) proteins 13

1.2.1 ELAVL4/HuD 14

1.2.1.1 HuD protein structure 14

1.2.1.2 HuD in neuronal differentiation 17

1.2.1.3 Post-translational control of HuD *18*

1.3 Current therapeutic strategies 22

1.3.1 Therapeutic strategies targeting SMN2 ..... *22*

1.3.1.1 Increasing SMN2 transcription *22*

1.3.1.2 Correcting SMN2 splicing *23*

1.3.1.3 Inducing translational read-through and increasing protein stability *24*

1.3.2 SMN1 gene replacement therapies *26*

1.3.3 Non-SMN therapeutic strategies *28*

1.4 Rationale, Hypothesis, and Objectives 29

1.4.1 Rationale *29*

1.4.2 Hypothesis *30*

1.4.3 Objectives *30*

Chapter 2. Materials and methods 31

2.1 Cell culture 31

2.1.1 IncuCyte *31*

2.1.2 Transfection *32*

2.2 SDS-PAGE and Western blotting 32

2.3 Immunoprecipitation (IP) and RNA immunoprecipitation (RIP) 34

2.4 RNA extraction, reverse transcription, and polymerase chain reaction (PCR) 35

2.5 DNA plasmids, vectors, subcloning, and mutagenesis 36

2.5.1 Gibson Assembly® *36*

2.5.2 Transformation *37*

2.5.3 Mutagenesis *38*

2.6 Animal work 39

2.6.1 Animals 39

2.6.2 Genotyping 39

2.6.3 Virus production 40

2.6.4 Facial vein injection 40

2.6.5 Righting reflex test 41

2.6.6 Hind limb suspension test (tube test) 41

2.6.7 Pen test 41

2.7 Statistical analysis 42

Chapter 3. Results 43

3.1 Effect of bryostatin on motor neuron-derived MN-1 cells 43

3.1.1 PKCα and HuD interact in motor neuron-like MN-1 cells 43

3.1.2 HuD is upregulated in motor neuron-like MN-1 cells upon treatment with bryostatin 46

3.1.3. Bryostatin activates PKC downstream signaling in motor neuron-derived MN-1 cells. 48

3.1.4 Bryostatin alters HuD binding to its mRNA targets in motor neuron-like MN-1 cells 49

3.1.5 Bryostatin has poor neuronal differentiation induction capabilities in motor neuron-like MN-1 cells 52

3.2 Establishment of an scAAV9 viral expression system 63

3.2.1 Generation of scAAV-HuD-flag and scAAV-mGFP vectors 63

3.2.1.1 Generation of the scAAV-HuD-flag vector 63

3.2.1.2 Generation of the scAAV-mGFP vector *67*

3.2.2 Overexpression of scAAV-HuD-flag and scAAV-mGFP vectors in MN-1 cells *67*

3.2.3 SMN overexpression in the delta7 mouse model *71*

3.2.3.1 Survival and body mass *71*

3.2.3.2 Behavioural phenotyping in the delta7 mouse model *72*

Chapter 4. Discussion 76

4.1 Summary 76

4.2 Effect of bryostatin on motor neuron-derived MN-1 cells 77

4.2.1 Investigation of a PKCα-HuD-mRNA target pathway in motor neuron-like MN-1 cells *77*

4.2.2 Bryostatin and control of the switch from cell proliferation to neuronal differentiation *82*

4.3 Establishment of an scAAV9 viral expression system 86

4.3.1 CNS gene delivery *88*

4.4 Future directions 90

4.4.1 Bryostatin-activated pathways in motor neurons *90*

4.4.2 HuD overexpression in a mouse model of SMA *91*

4.5 Conclusions 91

References 93

List of figures

Figure 1. Simplified schematic representation of SMA genetics..... 3

Figure 2. Neuronal ELAVL4/HuD gene, transcript, and protein..... 15

Figure 3. PKCα and HuD co-immunoprecipitate in motor neuron-like MN-1 cells. 44

Figure 4. HuD is upregulated following PKC stimulation with bryostatin in motor neuron-like MN-1 cells. 47

Figure 5. PKCα downstream signaling is activated following a short bryostatin treatment in motor neuron-like MN-1 cells. 50

Figure 6. HuD binding to mRNA targets is altered following bryostatin treatment in motor neuron-derived MN-1 cells. 51

Figure 7. HuD overexpression in motor neuron-derived MN-1 cells induces differentiation and neurite extension. 53

Figure 8. HuD overexpression in motor neuron-derived cells induces differentiation and neurite extension. 55

Figure 9. Bryostatin-1 treatment of motor neuron-derived cells has a limited very effect on neuronal differentiation initiation. 56

Figure 10. Bryostatin-1 treatment of motor neuron-derived cells has a limited impact on neuronal differentiation initiation. 57

Figure 11. High concentrations of Bryostatin-1 have a very limited effect on neuronal differentiation induction in motor neuron-derived cells. 58

Figure 12. Prolonged exposure of motor neuron-derived MN-1 cells to high concentrations of Bryostatin-1 results in poor neuronal differentiation initiation.... 59

Figure 13. Effect of a 72-hr bryostatin treatment on motor neuron-derived MN-1 cell morphology. 61

Figure 14. HuD subcloning into the scAAV vector. 64

Figure 15. Correction of SNPs and confirmation of scAAV-HuD expression in motor neuron-derived MN-1 cells. 66

Figure 16. mGFP subcloning into the scAAV vector. 68

Figure 17. mGFP and HuD overexpression in pGIPZ and shSMN motor neuron-derived MN-1 cells. 70

Figure 18. Phenotypic assessment of SMA mice treated with scAAV-SMN. 73

Figure 19. Proximal hind-limb muscle strength and fatigue assessment in delta7 pups treated with scAAV-SMN. 75

List of abbreviations

5'ss - 5' splice site

AAV - Adeno-associated virus

AChE - Acetylcholinesterase

aDMA - Asymmetrical dimethylated arginine ω-N^G,N^G

AKT - Protein kinase B (PKB)

AMV - Avian myeloblastosis virus

aPKC - Atypical protein kinase C

ARE - AU-rich elements

ASO - Antisense oligonucleotide

ATP - Adenosine triphosphate

AUF1 - AU-rich element binding factor 1

BBB - Blood-brain barrier

BDNF - Brain-derived neurotrophic factor

BRF1 - Butyrate-response factor 1

BSA - Bovine serum albumin

CARM1/PRMT4 - Coactivator-associated arginine methyltransferase 1

CB - Cajal body

CBA - Chicken beta-actin promoter

cDNA - Complementary deoxyribonucleic acid

CMV - Cytomegalovirus

CNS - Central nervous system

cPKC - Conventional (or classical) protein kinase C

DAG - Diacylglycerol

DMEM - Dulbecco's modified Eagle medium

DNA - Deoxyribonucleic acid

dNTP - Deoxynucleoside triphosphate

DRG - Dorsal root ganglia

DTT - Dithiothreitol

EDTA - Ethylenediaminetetraacetic acid

eIF4E - Eukaryotic translation initiation factor 4E

elav - Embryonic lethal abnormal vision (*Drosophila melanogaster* gene)

ELAVL - Embryonic lethal abnormal vision-like

EMA - European Medicines Agency

ESE - Exonic splicing enhancer

FBS - Fetal bovine serum

FDA - Food and Drug Administration

FL - Full-length

fne - Found in neurons (*Drosophila melanogaster* gene)

FSTA - Fast skeletal muscle activator

FVB/N - Friend virus B NIH

GAP-43 - Growth-associated protein 43

GAPDH - Glyceraldehyde 3-phosphate dehydrogenase

GAR - Glycine/arginine-rich

GC - Genome content

GDNF - Glial cell-derived neurotrophic factor

GFP - Green fluorescent protein

HB9 - Homeobox 9

HDAC - Histone deacetylase

HLS - Hind-limb suspension score

hnRNP - Heterogeneous nuclear ribonucleoprotein particle

HRP - Horseradish peroxidase

HuA/R - Hu antigene A/R

HuB/Hel-N1 - Hu antigene B

HuC - Hu antigene C

HuD - Hu antigene D

ICV - Intracerebroventricular

IM - Intramuscular

IP - Intraperitoneal

IP - Immunoprecipitation

ISS - Intronic splicing silencer

ISTL1 - Internal stem loop through long-distance interaction 1

IV - Intravenous

KSRP - KH-type splicing regulatory protein

LMN - Lower motor neuron

mGFP: Monomeric green fluorescent protein

MMA - Monomethylarginine ω-N^G

MOE - 2'-O-methoxyethyl

MN - Motor neuron

MN-1 - Motor neuron-like cell line

mRNA - Messenger ribonucleic acid

mRNP - Messenger ribonucleoprotein particle

NAIP - Neuronal apoptosis inhibitory protein

NCALD - Neurocalcin delta

NES - Nuclear export signal

NGF - Nerve growth factor

NLS - Nuclear localization signal

NMJ - Neuromuscular junction

nPKC - Novel protein kinase C

NT-3 - Neurotrophin-3

PABP - Poly(A)-binding protein

PBA - Phenylbutyrate

PBS - Phosphate buffered saline

PBST - Phosphate buffered saline with 0.05% Tween

PCR - Polymerase chain reaction

PKC - Protein kinase C

PKCα - Protein kinase C alpha

PLS3 - Plastin 3

PMSF - Phenylmethanesulphonylfluoride

PRMT - Protein arginine methyltransferase

PVDF - Polyvinylidene difluoride

qPCR - Quantitative polymerase chain reaction

RA - Retinoic acid

RACE - 5’ rapid amplification of cDNA ends

RBP - RNA-binding protein

rbp9 - RNA-binding protein 9 (*Drosophila melanogaster* gene)

RIP - RNA immunoprecipitation

RIPA - Radioimmunoprecipitation assay

RNA - Ribonucleic acid

RNP - Ribonucleoprotein particle

RRM - RNA recognition motif

RT-PCR - Reverse transcriptase polymerase chain reaction

SAHA - Suberoylamilidehydroxamic acid

SAM - S-adenosyl-L-methionine

scAAV - Self-complementary adeno-associated virus

scAAV9 - Self-complementary adeno-associated virus serotype 9

sDMA - Symmetrical dimethylated arginine ω-N^G,N'^G

SDS - Sodium dodecyl sulfate

SDS-PAGE - Sodium dodecyl sulfate polyacrylamide gel

SERF1 - Small EDRK-rich factor 1

SMA - Spinal muscular atrophy

SMN - Survival of motor neuron

SMNΔ7 - SMN without exon 7

snRNP - Small nuclear ribonucleoprotein particle

SOP - Standard operating procedure

sxl - Sex lethal (*Drosophila melanogaster* gene)

TPA/PMA - Tetradecanoylphorbol acetate/phorbol 12-myristate 13-acetate

TSA - Trichostatin A

TTP - Tristetraprolin

UCHL1 - Ubiquitin carboxyl-terminal hydrolase L1

UNRIP - Upstream of N-ras interacting protein

USP9X - Ubiquitin-specific protease 9x

UTR - Untranslated region

VG - Viral genome

VPA - Valproic acid

WT - Wild-type

Acknowledgements

I would first like to thank my supervisor Dr. Jocelyn Côté for taking a chance on me and welcoming me into his laboratory. Your guidance was greatly appreciated and has certainly helped me become a better thinker and a better scientist. I would also like to express my gratitude to the members of my thesis advisory committee Dr. Diane Lagace and Dr. Rashmi Kothary for taking time out of their busy schedule to evaluate my work. Your scientific advice has ensured that I produced rigorous, ethical work.

I would also like to express my appreciation to current and former Côté lab members including Geneviève Paris, Janik Laframboise, Dr. Emma Bondy-Chorney, Dr. Mitch Baldwin, Dr. Alan Morettin, Nasim Haghandish, Fatima Mostefai, Amir Haghandish, and Xheni Konci for their help through the years. All of you have been extremely patient with me and have made the laboratory a welcoming work environment.

Finally, I wouldn't have made it through these last few years without the constant support of my family and close friends. I am extremely grateful to my parents for believing in me and encouraging me to pursue graduate studies. You have made this possible. Thank you also to all of my amazing friends for being there for me. You kept me sane when I thought I was going to go crazy from being captive from the lab. To everyone I crossed paths with, thank you.

Chapter 1. Introduction

1.1 Spinal muscular atrophy (SMA)

Spinal muscular atrophy (SMA) is a severe autosomal recessive disorder characterized by the degeneration of lower motor neurons in the anterior horn of the spinal cord. Clinically, loss of these cells results in progressive, symmetric muscular weakness and leads to paralysis of the proximal voluntary muscles. In the more severe cases, death occurs within two years due to respiratory failure (Crawford et al., 1996). This early-onset neuromuscular disease affects approximately 1 in 6000 to 1 in 10 000 live births and is one of the leading genetic causes of infant mortality (Crawford et al., 1996).

1.1.1 Survival of motor neuron gene

In 1990, two groups (Melki et al., 1990a, Melki et al., 1990b, Brzustowicz et al., 1990) mapped the SMA gene locus to chromosome 5q11.2-q13.3, a highly polymorphic region of the genome. A few years later, Melki's team determined that this region presents a large 500kb element duplication containing at least four genes including *p44*, *NAIP*, and *SMN* and identified the *survival of motor neuron 1* (*SMN1*) gene as the causative gene for SMA (Lefebvre et al., 1995). Indeed, they found that *SMN1* was missing, interrupted, or mutated in patients presenting with all forms on the disease spectrum (Lefebvre et al., 1995, Brahe et al., 1996). The centromeric copy, *SMN2,* is almost identical to *SMN1* except for five nonpolymorphic nucleotide changes. One of these, a single base substitution at position 6 in exon 7 (C6T), alters the splicing pattern

of *SMN2* (Lefebvre et al., 1995) and predominantly yields transcripts lacking exon 7 that translate into a truncated and unstable protein (SMNΔ7) (**Figure 1A**) (Lorson et al., 1999, Monani et al., 1999). This truncated protein is unable to oligomerize properly and is rapidly degraded (Lorson et al., 1998b, Burnett et al., 2009). The remaining pool of stable SMN protein produced by *SMN2* allows for embryonic development and survival. However, it is not sufficient for normal function and long-term survival of the vulnerable α-motor neurons (Lefebvre et al., 1995, Coovert et al., 1997). The *SMN2* copy number and thus the amount of functional SMN protein being produced is generally inversely correlated with disease severity (Coovert et al., 1997, McAndrew et al., 1997, Lefebvre et al., 1997). In humans, the number of *SMN2* copies usually varies between 1 and 6 and is reflected by a large phenotypic heterogeneity in SMA patients. Moreover, it was recently uncovered that not all *SMN2* genes are equivalent. Indeed, a natural mutation in exon 7 of the *SMN2* gene, c859G>C, was identified in patients with mild SMA (Prior et al., 2009). This mutation is thought to disrupt an hnRNP A1 binding site and to create an exonic splicing enhancer (ESE), thus increasing FL-SMN amounts and resulting in a milder phenotype (Prior et al., 2009, Vezain et al., 2010).

1.1.2 Clinical classification

1.1.2.1 Types of SMA

Clinicians, geneticists, and researchers generally agree that SMA patients can be classified into three types based the on age of onset, highest motor milestone achieved, and life expectancy (Munsat, 1991, Munsat et al., 1992, Russman, 2007). Type I SMA is the most severe and common form of the disease. It is also referred to as Werdnig-

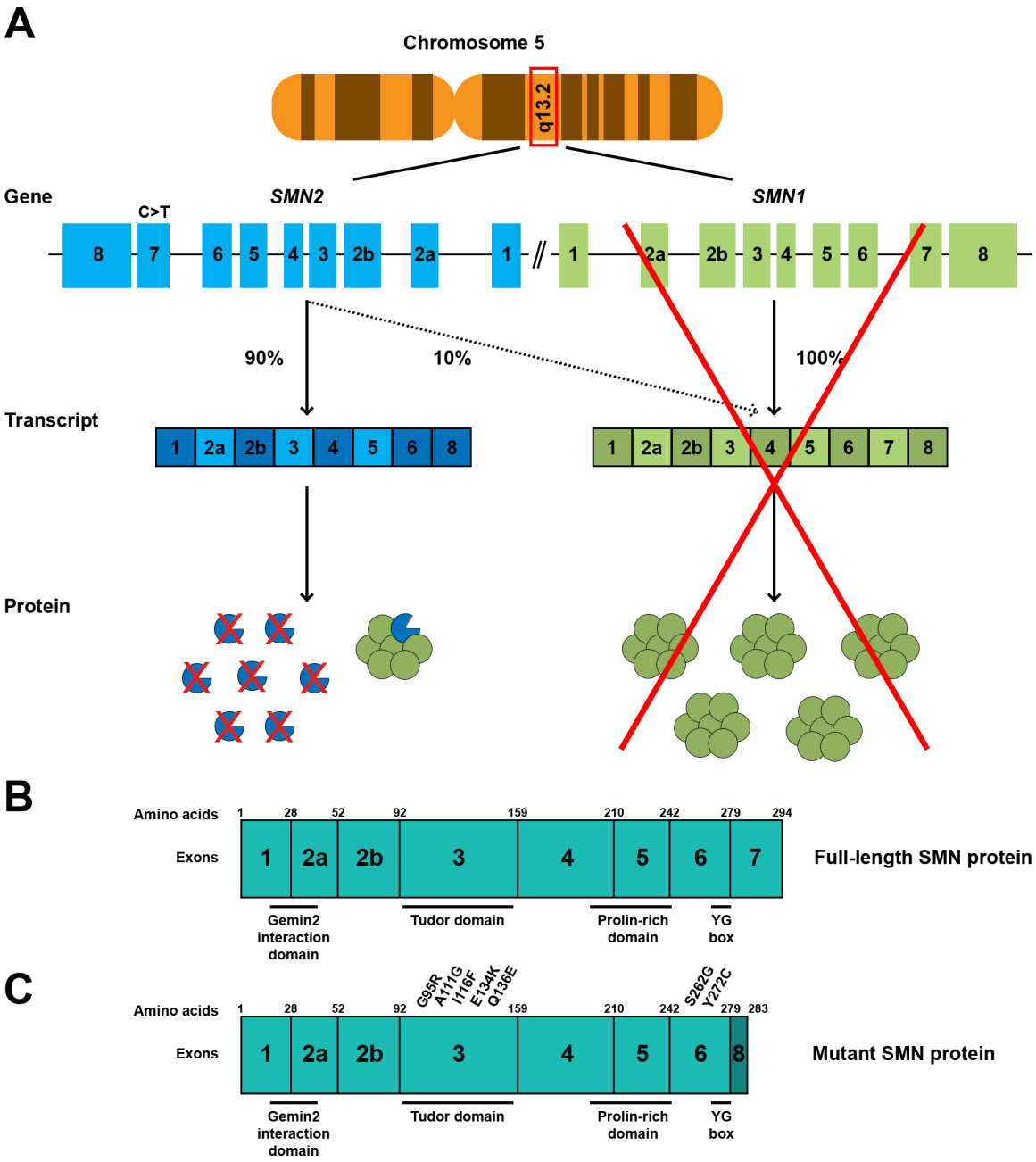

Figure 1. Simplified schematic representation of SMA genetics. ***A***. The 5q13.2 locus houses the *SMN* genes. *SMN1* gives rise to 100% full-length transcripts that get translated into fully functional proteins. On the other hand, *SMN2* has a mutation at position 6 in exon 7 that results in production of a majority of transcripts lacking exon 7. *SMN*Δ7 transcripts are translated into an unstable, truncated protein that is unable oligomerize properly. SMA arises when *SMN2* cannot produce enough SMN protein to compensate for the loss of *SMN1*. ***B***. The SMN protein has 8 coding exons. Major interaction domains are indicated under the protein. ***C***. Mutations found in SMA patients. When exon 7 is excluded (SMNΔ7), the first four amino acids of exon 8 get translated. Disease-linked mutations in the Tudor and the tyrosine-glycine-rich domains are indicated over the protein.

Hoffman disease, after the two neurologists who recorded the first clinical descriptions of the disease at the end of the 19th century (Werdnig, 1891, Hoffmann, 1893, Werdnig, 1894, Hoffmann, 1897, Hoffmann, 1900). Infants with type I SMA can have 1, 2, or 3 *SMN2* copies. They start to show symptoms in the first few months of life, are never able to sit unaided, and rarely live past 2 years of age (Munsat, 1991, Munsat et al., 1992). Fortunately, type I patients born in the more recent years tend to live longer thanks to more proactive clinical care (Oskoui et al., 2007). Children with type II or intermediate SMA can have up to four *SMN2* copies. They usually start presenting symptoms between the ages of 6 and 15 months and are able to sit independently (Munsat, 1991, Munsat et al., 1992). All live past the age of two and 68.5% make it past 25 years of age (Zerres et al., 1997). Type III, also known as Kugelberg-Welander disease (Kugelberg et al., 1956), refers to juvenile patients with 3 or 4 copies of *SMN2*, with disease onset before 3 for type IIIa and after age 3 for type IIIb. Both type IIIa and b are able to walk independently and live well into adulthood (Munsat, 1991, Munsat et al., 1992). Two additional types have gained recognition since the consensus classification was established in the early 1990's. Type 0 usually refers to *in utero* onset and a need for respiratory support at birth. These infants cannot survive with ventilation and die soon after birth (Dubowitz, 1999). Finally, type IV SMA is very rare and refers to individuals with 4 or 5 copies of *SMN2*, symptom onset after 20 years of age, and a normal life expectancy (Pearn et al., 1978, Brahe et al., 1995, Zerres et al., 1995, Moulard et al., 1998).

1.1.2.2 Disease modifiers

In addition to *SMN2* copy number, a few disease modifiers have been identified in the recent years. Among them, Plastin 3 (PLS3), an actin-binding and -bundling protein, was found to be elevated in unaffected *SMN1*-deleted females in families where siblings had the same genetics but presented with different phenotypes (Oprea et al., 2008). Indeed, Stratigopoulos and colleagues established that high expression of PLS3 inversely correlated with disease severity and positively correlated with *SMN2* copy number and gross motor function in postpubertal females (Stratigopoulos et al., 2010). However, a subsequent study determined that this correlation was not valid for all discordant families (Bernal et al., 2011). Work in the zebrafish revealed that overexpression of PLS3 in motor neurons was able to rescue axon length and motor function but had little effect on survival (Oprea et al., 2008, Hao le et al., 2012, Lyon et al., 2014). Work in mouse models unveiled increased profilin IIa levels and decreased PLS3 levels in the intermediate $2B^{-/-}$ mouse model (Bowerman et al., 2009). Although it was not sufficient to rescue the phenotype, knocking-out profilin II induced an increase in PLS3 in an SMN-dependent manner, thus supporting a role for mis-regulation of neuronal actin dynamics in SMA pathology (Bowerman et al., 2007, Bowerman et al., 2009, Bowerman et al., 2010). McGovern and colleagues determined that PLS3 had no beneficial effect on SMA phenotype in the SMNΔ7 model. Indeed, survival, weight, and electrophysiology of the neuromuscular junction were not rescued when human PLS3 was overexpressed in motor neurons, indicating that PLS3 does not offer protection when SMN levels are too dramatically reduced (McGovern et al., 2015). Moreover, Dr. Wirth's team was not able to rescue a severely affected mouse model by overexpressing PLS3 but observed

significant improvements when doing so in a milder model (Ackermann et al., 2013). Using a suboptimal ASO dose combined with PLS3 overexpression, they then were able to rescue survival, endocytosis, increase NMJ size and ameliorate motor abilities (Hosseinibarkooie et al., 2016). Finally, the Lorson laboratory showed that PLS3 was able to extend survival and reduce disease severity in milder SMA models, indicating that a certain SMN threshold might be required for PLS3 to be protective (Kaifer et al., 2017).

Recently, Neurocalcin delta (NCALD), a neuronal calcium sensor protein, was identified as a second disease modifier through genome-wide linkage and transcriptome analysis (Riessland et al., 2017). Dr. Wirth's team showed that low NCALD levels are protective in unaffected *SMN1*-deleted individuals. Downregulation of NCALD ameliorated neurite outgrowth in SMN-deficient cells, corrected phenotype in Smn-deficient zebrafish, and improved axonal outgrowth and NMJ size in a severe mouse model of SMA. Overall, NCALD depletion restored endocytosis and synaptic vesicle recycling impairment associated with SMA pathology (Riessland et al., 2017).

1.1.3 Select mouse models of SMA

In contrast to humans, mice have only one *Smn* gene (DiDonato et al., 1997, Viollet et al., 1997). Homozygous deletion of *Smn* is embryonic lethal; therefore, the disease does not exist naturally in mice (Schrank et al., 1997). To overcome this limitation, two groups used the human *SMN2* gene to create similar but distinct mouse models (Hsieh-Li et al., 2000, Monani et al., 2000, Le et al., 2005).

1.1.3.1 The Taiwanese model

Hung Li's group based in Taiwan introduced a 115-kb genomic fragment which encompasses *SMN2* gene locus, the small EDRK-rich factor 1 (*SERF1*) gene, and part of the centromeric neuronal apoptosis inhibitory protein (*NAIP*) gene onto the *Smn*$^{-/-}$ background (Hsieh-Li et al., 2000). They reported having SMA-like mice with varying disease severity born within the same litter: 'type I' pups surviving up to 10 days, 'type II' living 2-4 weeks, and 'type III' animals having an almost normal lifespan. Varying severity has not been reported anywhere else and is uncommon in SMA families (Monani et al., 2000, Monani et al., 2003, Le et al., 2005). They later backcrossed their mice to obtain a mild model with motor neuron degeneration starting around 6 months (Tsai et al., 2006). This mild model can be backcrossed to FVB/N mice to obtain a phenotypically more severe model using a breeding scheme described by Gogliotti *et al*. (Gogliotti et al., 2010). This severe Taiwanese model has a survival comparable to the delta7, i.e. around 16 days. However, contrary to the delta7 model that will be presented in the next section, the Taiwanese model does not overexpress high levels of SMNΔ7 protein and control and mutant pups are born at a ratio 1:1 (Gogliotti et al., 2010).

1.1.3.2 The Burghes models

Arthur Burghes' team used a similar strategy and rescued the embryonic lethality by inserting a 35.5kb fragment the entire human *SMN2* gene onto the *Smn*$^{-/-}$ (Monani et al., 2000). Burghes' severe model carries two *SMN2* copies and lives on average 5.2 ± 0.2 days (Monani et al., 2000). By generating and comparing low vs high *Smn*$^{-/-}$;*SMN2* copy animals, they showed that additional *SMN2* copies rescue SMA features and confirmed

that disease severity correlates with *SMN2* copy number and that it acts as a disease modifier.

A few years later, the Burghes lab developed a mouse model with a slightly milder phenotype nicknamed the delta7 model (*Smn*$^{-/-}$;*SMN2*;*SMNΔ7*) (Le et al., 2005). This mouse lives on average 13.3 ± 0.3 days, suggesting that SMNΔ7 retains some beneficial function and is not completely detrimental. At postnatal day 5, a weight difference is already apparent and the SMA pups have difficulty righting themselves up after being placed on their back. By day 10, they display difficulty to walk and often fall over. Moreover, they have significantly fewer lumbar MN than non-affected littermates as well as a higher proportion of non-innervated and/or partially innervated NMJs. Overall, they recapitulate some of the major neuronal defects found in SMA (Le et al., 2005). It is now arguably the most widely used and well-characterized mouse model for studying SMA and the development of therapeutic strategies. All mouse models mentioned here have been transferred to and are now maintained by Jackson Laboratories and are available to the SMA community.

1.1.4 The Survival of motor neuron protein

The *survival of motor neuron* protein is composed of 294 amino acids and has a molecular weight of 38kDa (Lefebvre et al., 1995). This ubiquitously expressed multidomain protein has 8 coding exons (**Figure 1B**) (Bürglen et al., 1996). The N-terminal harbors a conserved Gemin2-binding domain, essential to SMN's role in snRNP assembly (Liu et al., 1997, Fischer et al., 1997). *In vitro* binding studies revealed that exon 2 encodes a nucleic acid binding domain (Lorson et al., 1998a). Exon 2b and exon 6

are involved in dimerization of the protein (Young et al., 2000). Furthermore, it was shown that missense mutations found in the tyrosine-glycine-rich motif (YG box in exon 6) in patients with severe SMA result in poor oligomerization of SMNΔ7 with itself (Lorson et al., 1998b). Exon 3 encodes a Tudor domain, a ~60 amino acid conserved domain that recognizes arginine methylation on proteins (Brahms et al., 2001). SMN's Tudor domain consists of five β-strands forming an aromatic cage with a preference for symmetrically dimethylated arginine (sDMA)-containing RG motifs (Selenko et al., 2001, Côté et al., 2005). The domain was shown to be essential for SMN's spliceosome assembly function (Bühler et al., 1999, Côté et al., 2005). Moreover, SMA-causing mutations in the Tudor domain (G95R, A111G, E134K) do not disrupt its structure but change the charge distribution, thus affecting electrostatic interactions (**Figure 1C**) (Selenko et al., 2001, Sun et al., 2005b, Tripsianes et al., 2011, Han et al., 2012). These Tudor domain mutants display greatly reduced binding to SmB, SmD1, SmD3 proteins, leading to inefficient U snRNP biogenesis (Selenko et al., 2001, Sun et al., 2005b). Reduced or abolished capacity to interact with methylated arginine-harboring proteins has been linked with SMA pathology (Côté et al., 2005, Tadesse et al., 2008, Hubers et al., 2011).

Evolutionary conserved from yeast, SMN is expressed in all cells and tissues, with high levels in the nervous system (Lefebvre et al., 1995, Battaglia et al., 1997, Hannus et al., 2000). At the cellular level, the SMN protein is present both in the cytoplasm and the nucleus. SMN is part of a large macromolecular complex that also includes Gemins 2-8 and Unrip. The classical function of this complex is in the cytoplasmic assembly of Sm proteins and U small nuclear RNAs into small nuclear ribonucleoprotein particles

(snRNPs), the core component of the splicing machinery (Liu et al., 1996, Liu et al., 1997, Fischer et al., 1997, Pellizzoni et al., 1998). After remodelling, the Sm core-assembled snRNPs and the SMN complex are imported into the nucleus for further maturation of the snRNPs within Cajal bodies (CB) (Matera et al., 2006). The core SMN complex also accumulates in closely related nuclear bodies termed Gems (Gemini of coiled bodies) in certain cell types (Liu et al., 1996). Immunocytochemistry analyses revealed that Gems are reduced in type I SMA patient-derived fibroblasts and the number of Gems generally inversely correlates with disease severity (Coovert et al., 1997).

1.1.4.1 SMA: A defective snRNP biogenesis and pre-mRNA splicing disease

It remains unclear how a deficiency in SMN protein causes the selective degeneration of alpha motor neurons observed in SMA given that assembly of a functional splicing machinery should be equally essential for all cell types. Two schools of thought have emerged about this question. On one side, there is evidence supporting that disruption of SMN's main function in snRNP assembly causes SMA. Indeed, it was shown that low SMN protein levels result in decreased snRNP biogenesis and in an altered snRNP repertoire (Pellizzoni et al., 1999, Wan et al., 2005, Gabanella et al., 2007). Motor neurons are more sensitive to reduced snRNA levels and an altered snRNP repertoire leads to deficits of fully assembled snRNPs (Gabanella et al., 2007, Zhang et al., 2008). In turn, spliceosomal defects cause aberrant splicing of numerous mRNAs in a cell type-specific manner (Faustino et al., 2003, Zhang et al., 2008). Consequently, splicing of one or more genes that support important motor neuron function(s) might be inefficient, thus explaining the cell-specificity of SMA (Faustino et al., 2003, Eggert et

al., 2006). Notably, a negative feedback loop regulating splicing of *SMN2* was recently uncovered (Jodelka et al., 2010). More specifically, changes in the relative abundance of U1 snRNP worsen *SMN2* exon 7 skipping, leading to even more reduced functional SMN protein levels (Jodelka et al., 2010). Together, these defects could contribute to the specificity of the pathophysiology but the causal link remains to be clearly established.

1.1.4.2 SMA: A motor neuron-specific role for the SMN protein

Alternatively, the second hypothesis supports the idea that SMN plays (an) additional function(s) specific to the highly specialized cells that are motor neurons. Indeed, there is growing evidence that SMN is involved in the transport, regulation, and local translation of mRNA in MN axons. First, in addition to its presence in the nucleus and the cytoplasm, SMN was found to localize to the leading edge of neurites and at the neuromuscular junction, indicative of a potential neuron-specific function (Battaglia et al., 1997, Béchade et al., 1999, Pagliardini et al., 2000, Jablonka et al., 2001, Fan et al., 2002). Zhang and colleagues showed that SMN localizes to granules exhibiting rapid, bidirectional, cytoskeletal-dependent movements in axons and growth cones and that, contrary to the full-length protein, SMNΔ7 accumulates in the nucleus, is absent from processes, and gives rise to shorter neurites when expressed in neurons (Zhang et al., 2003). McWhorter and colleagues confirmed that decreased SMN levels caused defects in motor axons outgrowth and pathfinding *in vivo* (McWhorter et al., 2003). More recent studies showed that SMN is found in neuronal RNA granules along axons, where it associates with cytoskeletal filament systems and interacts with a number of methylated RNA-binding proteins (RBPs) including hnRNP R/Q, FMRP, KSRP, and HuD (Rossoll

et al., 2002, Rossoll et al., 2003, Zhang et al., 2003, Piazzon et al., 2008, Tadesse et al., 2008, Hubers et al., 2011, Akten et al., 2011, Fallini et al., 2011). Interestingly, these complexes sometimes contain Gemins 2 and 3 but always lack Sm proteins and coilin/p80 (Sharma et al., 2005, Zhang et al., 2006). Using a zebrafish model, Carrel and colleagues showed that SMN's potential function in motor axon was independent of its role in snRNP biogenesis. Indeed, SMN mutants A111G and Q282A failed to rescue motor axon defects and longevity when overexpressed in embryos but retained the properties needed for proper snRNP assembly (i.e. oligomerization and Sm binding) (Carrel et al., 2006). They later showed that overexpressing A111G at high levels was able to rescue motor neuron axonal defects in mutant zebrafish (Workman et al., 2009). SMN-interacting RBPs that localize to RNA granules interact with mRNAs to mediate their translocation along axons (Rossoll et al., 2003, Hubers et al., 2011, Fallini et al., 2011, Akten et al., 2011). SMN deficiency results in reduced axonal levels of these SMN-associating RBPs (Helmken et al., 2003, Tadesse et al., 2008, Fallini et al., 2011, Fallini et al., 2014) and in the mislocalization of their mRNA cargo (Rossoll et al., 2003, Fallini et al., 2011, Akten et al., 2011). Microarray analyses revealed that a large number of transcripts associated with axonal growth and synaptic activity are mislocalized due to decreased SMN levels, suggesting widespread defects possibly contributing to pathogenesis (Rage et al., 2013, Saal et al., 2014). Importantly, interaction with most of these RBPs is abolished by disease-linked mutations in the Tudor domain as well as in the YG box of SMN, implying that this function in mRNP assembly and transport may be impaired in SMA patients (Rossoll et al., 2002, Piazzon et al., 2008, Hubers et al., 2011, Fallini et al., 2011). Essentially, low SMN levels result in misregulation of mRNA

transport and local translation which would then lead to impaired motor neuron function, culminating in motor neuron degeneration and pathogenesis.

1.2. Embryonic lethal abnormal vision-like (ELAVL) proteins

For the past years, our laboratory has focused on neuronal RNA granules and their role in the transport, localization, and stability of specific mRNAs along axons (Tadesse et al., 2008, Hubers et al., 2011, Sanchez et al., 2013). Among other things, we showed that SMN is implicated in neurite outgrowth and mediates the proper translocation of HuD and its mRNA targets into axonal RNA granules (Hubers et al., 2011). HuD is a member of the Hu family of genes, homologs of the *Drosophila melanogaster embryonic lethal abnormal visio*n (*elav*) gene and closely related in structure and function to *sex lethal* (*sxl*), *found in neurons* (*fne*), and *RNA-binding protein 9* (*rbp9*) genes (Bell et al., 1988, Robinow et al., 1988, Kim et al., 1993, Good, 1995, Good, 1997, Samson et al., 2003, Colombrita et al., 2013). Deletion of this RNA is lethal in fruit flies where it is required for proper nervous system maintenance (Campos et al., 1985, Robinow et al., 1988). Hu proteins are regulatory factors involved in differentiation, maintenance, and plasticity of neurons. These RBPs preferentially bind to AU-rich RNA elements (AREs) in the 3'-untranslated regions (UTRs) of transcripts (Deschenes-Furry et al., 2006, Deschenes-Furry et al., 2007, Tadesse et al., 2008). Unlike other ARE-binding proteins such as K homology splicing regulatory protein (KSRP), tristetraprolin (TTP), butyrate-response factor 1 (BRF1), and AU-rich element binding factor 1 (AUF1), Hu proteins prevent their mRNA targets from degradation. This increases their stability and prolongs their half-life, thus promoting protein expression (Lu et al., 2004, Deschenes-Furry et al.,

2007, Bird et al., 2013). Hu proteins have been shown to both compete with destabilizing factors and microRNAs and to cooperate with other RBPs for binding to common mRNAs to regulate their expression (Atlas et al., 2004, Kim et al., 2009, Tominaga et al., 2011, Young et al., 2012, Sosanya et al., 2013, Bird et al., 2013, Yoo et al., 2013, Kim et al., 2015).

Hu proteins were first identified as the targets of autoantibodies found in the sera of patients with paraneoplastic encephalomyelitis and sensory neuropathy (Dalmau et al., 1990). In mammals, the family comprises four highly homologous members. The expression of HuB (aka Hel-N1), HuC, and HuD is restricted almost exclusively to the nervous systems, whereas the fourth member HuR, also known as HuA, is expressed ubiquitously (Ma et al., 1996).

1.2.1 ELAVL4/HuD

1.2.1.1 HuD protein structure

HuD was the first member of the ELAVL family to be characterized and is conceivably the best-characterized neuronal RBP (Szabo et al., 1991). Its expression is first detectable in neurogenic precursors at the point of withdrawal from the mitotic cycle, and expression persists in mature neurons (Okano et al., 1997, Clayton et al., 1998, Deschenes-Furry et al., 2003). In humans, the gene is located on chromosome region 1p34 and covers approximately 146kb of DNA (**Figure 2A**) (Muresu et al., 1994, Sekido et al., 1994, Inman et al., 1998). It is divided into seven coding exons (E2 to E8) and was thought until recently to have three alternative noncoding leading exons (Inman et al., 1998). Indeed, using bioinformatics and 5' rapid amplification of cDNA ends (RACE)

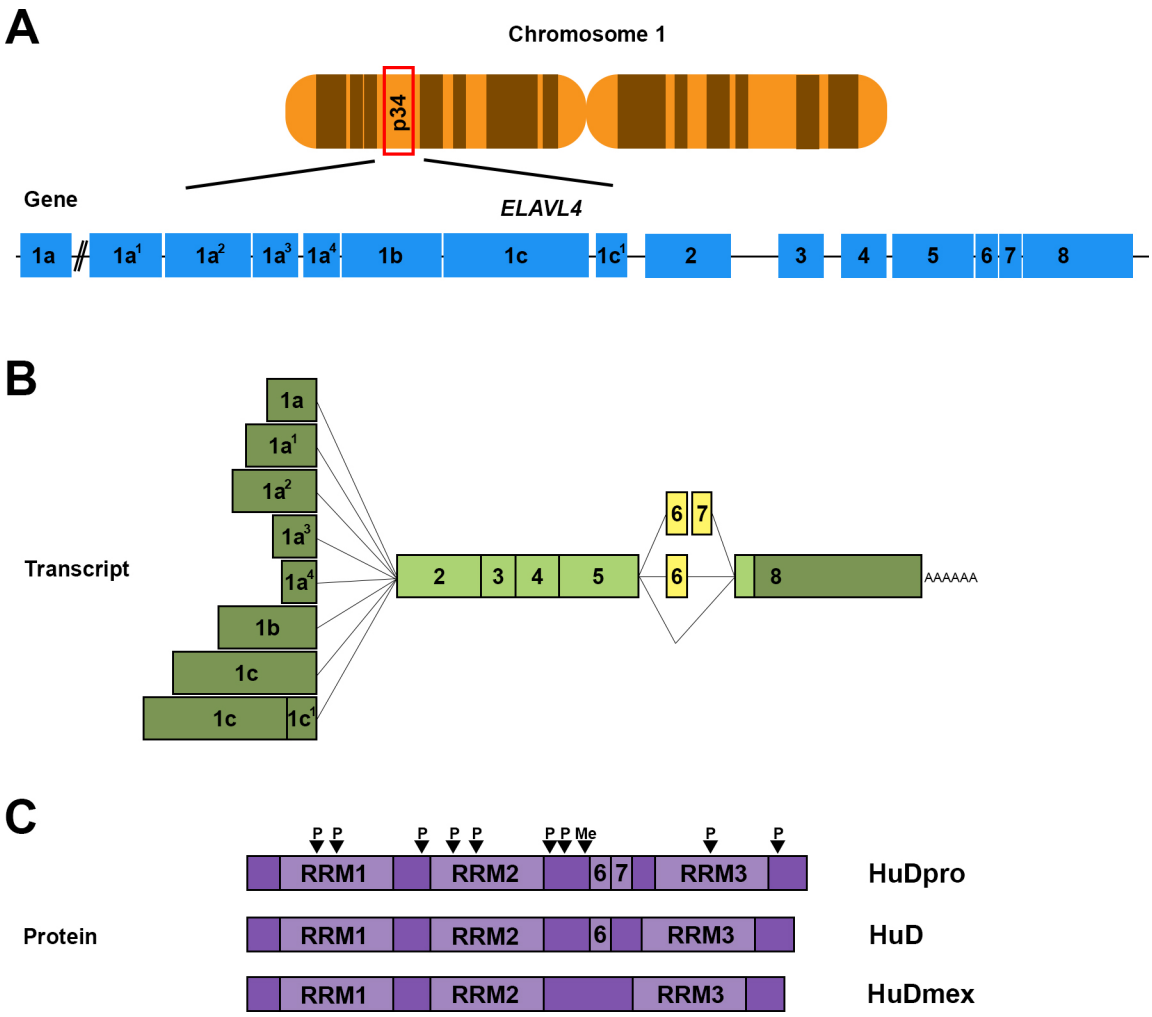

Figure 2. Neuronal ELAVL4/HuD gene, transcript, and protein. ***A***. HuD gene locus is located on chromosome 1p34 and spans 146kb of DNA. ***B***. HuD has 8 different leading exons and is subjected to alternative splicing of exons 6 and 7. ***C.*** This results in the production of three major isoforms, HuDpro and HuD being the most abundantly expressed in the CNS. PKC phosphorylation and CARM1 methylation sites are indicated by black arrowheads**.**

analyses, the Jasmin laboratory uncovered that there are actually eight conserved E1 variants all containing an in-frame translation initiation codon, potentially producing different HuD N-termini (**Figure 2B**) (Bronicki et al., 2012). HuD and the other Hu family members have a molecular weight of ~40kDa and share three ~90 amino acid-long RNA recognition motifs (RRMs) (Inman et al., 1998). RRM1 is encoded by exons 2 and 3, RRM2 by exons 4 and 5, and RRM3 by exon 8 (**Figure 2C)** (Inman et al., 1998). The first and second RRMs bind to *cis*-acting elements in the 3'UTR of mRNAs (Chung et al., 1996, Chung et al., 1997, Ma et al., 1997, Park et al., 2000, Wang et al., 2001). Interestingly, a 2010 study revealed that only a minority of HuD targets actually harbor AREs (Bolognani et al., 2010). Instead, most mRNAs bound by HuD in the mouse forebrain have one of three novel binding motifs. These U-rich and C-rich motifs localize predominantly to the 3'UTR but can occasionally be found in the coding region or the 5' UTR of mRNAs (Bolognani et al., 2010). The third RRM binds to poly(A) tails and stabilizes RBP-mRNA complexes (Ma et al., 1997, Park et al., 2000, Beckel-Mitchener et al., 2002). Moreover, it was shown that HuD has a higher affinity for longer poly(A) sequences (Ma et al., 1997, Beckel-Mitchener et al., 2002). The third RRM also interacts with other proteins, including other Hu family members (Kasashima et al., 2002). Fukao and colleagues showed that the interaction of HuD with eIF4A promotes cap-dependent translation (Fukao et al., 2009). More precisely, HuD competes with miRNAs for binding to eIF4A, thus stabilizing the interaction between eIF4AI&II and mRNA targets and enhancing protein synthesis (Fukao et al., 2014). RRM3 was also shown to be essential for HuD association with polysomes and for its interaction with actively translating mRNAs (Atlas et al., 2007, Fukao et al., 2009). HuD co-localization with poly(A)-

binding protein (PABP) and the cap-binding protein eukaryotic translation initiation factor 4E (eIF4E) supports a potential role for HuD in translation regulation (Tiruchinapalli et al., 2008). A hinge region encoded by alternatively spliced exons 6 and 7 separates the second and third RRMs and encodes a nuclear export signal (NES) as well as a potential nuclear localization signal (NLS) (Inman et al., 1998, Kasashima et al., 1999). The linker region harbors serine/threonine and arginine residues that are subjected to protein kinase C (PKC) phosphorylation and to coactivator-associated arginine methyltransferase 1 (CARM1) methylation, respectively (**Figure 2C**) (Fujiwara et al., 2006, Lim et al., 2012).

1.2.1.2 HuD in neuronal differentiation

HuD expression is mainly cytosolic, with relatively low abundance in the nucleus (Kasashima et al., 1999, Anderson et al., 2001). It is found in growth cones of developing neurons and in axons, dendrites, and synaptic terminals of mature neurons (Aranda-Abreu et al., 1999, Aronov et al., 2002). As mentioned above, HuD localizes to granules along neurites where it interacts with mRNP components, including SMN, mRNAs, motor proteins, and other RBPs (Aronov et al., 2002, Smith et al., 2004, Anderson et al., 2006, Hubers et al., 2011, Akten et al., 2011, Fallini et al., 2012). Through the years, HuD has been found to be involved in almost all aspects of mRNA metabolism in neurons, including nucleocytoplasmic shuttling (Kasashima et al., 1999, Saito et al., 2004, Carmody et al., 2009), mRNA transport and localization (Smith et al., 2004, Atlas et al., 2004, Akten et al., 2011, Yoo et al., 2013, Sosanya et al., 2013, Sosanya et al., 2015), stability (Liu et al., 1995, Chung et al., 1997, Tsai et al., 1997, Anderson et al.,

2000, Mobarak et al., 2000, Beckel-Mitchener et al., 2002, Aronov et al., 2002, Lim et al., 2012), and local translation at growth cones and synapses (Kullmann et al., 2002, Fukao et al., 2009, Lee et al., 2012). In addition, evidence indicates that HuD plays a role in alternative splicing and alternative polyadenylation. Indeed, it has been shown that HuD can promote either exon exclusion (Zhu et al., 2006, Bellavia et al., 2007, Zhu et al., 2008, Ratti et al., 2008, Hinman et al., 2008, Zhou et al., 2011) or inclusion, including of its own exon 6 (Wang et al., 2010, Ince-Dunn et al., 2012). It can also regulate alternative polyadenylation of select transcripts like HuR and Calcitonin (Soller et al., 2003, Zhu et al., 2006, Mansfield et al., 2012, Dai et al., 2012). Through its interaction with its target transcripts, HuD is involved in all facets of neuronal development and plasticity; the protein products of these mRNAs regulate cell proliferation (c-fos, n-myc, c-myc) (Liu et al., 1995, Chagnovich et al., 1996, Ross et al., 1997, Joseph et al., 1998), cell cycle arrest (p21) (Joseph et al., 1998), neuronal growth and survival (NGF, BDNF, NT-3) (Lim et al., 2012), neurite elongation (GAP-43, Tau) (Mobarak et al., 2000, Anderson et al., 2000, Anderson et al., 2001), synaptogenesis (Neuroserpin, NOVA-1), synaptic transmission (AChE) (Deschenes-Furry et al., 2003) as well as spatial learning and memory (Quattrone et al., 2001, Bolognani et al., 2004, Pascale et al., 2004).

1.2.1.3 Post-translational control of HuD

As mentioned above, HuD is subject to post-translational modifications, notably to phosphorylation by PKC. The PKCs are a family of 10-15 serine/threonine kinases categorized into three subfamilies based on the structure of their N-terminal domain which determines secondary messenger specificity (Mellor et al., 1998). Conventional

PKC (cPKC) subfamily members include PKCα, β_I, β_{II}, γ and require calcium (Ca^{2+}), diacylglycerol (DAG), and a phospholipid for activation (Parker et al., 1986, Coussens et al., 1986, Coussens et al., 1987). Novel PKC (nPKC) members include PKCδ, ε, η, θ and require DAG but not Ca^{2+} to be activated (Ono et al., 1987, Osada et al., 1990, Osada et al., 1992). Finally, atypical PKC (aPKC) isoforms PKCι and ζ require neither Ca^{2+} nor DAG for activation (Ono et al., 1989a). When activated, PKC enzymes auto-phosphorylate and translocate from the cytosol to the plasma membrane, where binding of regulatory domains releases the pseudosubstrate from the active site and allows for substrate binding and catalysis (Newton, 2001). PKC activity can be pharmacologically modulated using the phorbol ester tetradecanoylphorbol acetate (TPA), also commonly known as phorbol 12-myristate 13-acetate (PMA), or using the agonist bryostatin. Both act via the same binding site located within the regulatory C1 domain (Smith et al., 1985, Ramsdell et al., 1986). Two of the three PKC subfamilies have C1 domains; therefore, only cPKC and nPKC are sensitive to phorbol esters and bryostatin (Ono et al., 1989b, Kaibuchi et al., 1989). Bryostatins are a family of macrocyclic lactone first isolated from the marine organism *Bugula neritina* for its antiproliferative properties in 1968 (Pettit et al., 1982, Ramsdell et al., 1986). The most studied compound, Bryostatin-1, was chemically characterized in 1982 and its most well-established property is the modulation of PKC activity (Pettit et al., 1982). Bryostatin is structurally unrelated to phorbol esters but competes with it and diacylglycerols for binding to cysteine-rich domains of the C1 region of conventional and novel PKC isoforms. It has been used in many preclinical and clinical trials to evaluate its efficacy at preventing tumor invasion, tumor growth, and angiogenesis (see Kollar et al., 2014 for review). It has also been investigated as a

treatment option for brain injury (Tan et al., 2013, Mizutani et al., 2015, Lucke-Wold et al., 2015), Alzheimer's disease (Lim et al., 2014, Schrott et al., 2015, Marchesi et al., 2016), and depression (Sun et al., 2005a, Alkon et al., 2017) and has been shown to be successful at rescuing hippocampal synapses and spatial learning and memory in adult fragile X mice (Sun et al., 2014). However, high concentrations of drug and/or prolonged exposure of PKC to bryostatin triggers PKC downregulation, ubiquitination, and degradation by the proteasome (Mutter et al., 2000).

PKCs play important roles in diverse signaling cascades and their biological functions include receptor desensitization, transcription regulation, immune response mediation, cell growth regulation, and learning and memory (Amadio et al., 2006). Among others, PKC alpha (PKCα) was shown to regulate HuD's recruitment and stabilizing activity (Pascale et al., 2005). Indeed, PKCα activation in human neuroblastoma SH-SY5Y cells using phorbol esters or bryostatin promoted its interaction with HuD, led to nuclear export of HuD, and increased HuD protein at the level of the cytoskeleton. In turn, this resulted in stabilization of GAP-43 mRNA and in an increase in GAP-43 protein levels, again only in the cytoskeletal fraction (Pascale et al., 2005). Mobarak and colleagues showed that this PKC-HuD-GAP-43 pathway is essential for neurite outgrowth. In rat pheochromocytoma PC12 cells where HuD was knockdown, GAP-43 mRNA and protein levels were decreased and NGF or phorbol ester treatment failed to induce neurite outgrowth (Perrone-Bizzozero et al., 1993, Mobarak et al., 2000). Using mass spectrometry, the Alkon laboratory demonstrated that bryostatin activation of PKCα and PKCε resulted in phosphorylation of HuD on nine residues (Lim et al., 2012).

Another known pathway that regulates HuD expression and function involves protein arginine methyltransferase 4 (PRMT4)/CARM1. The PRMTs are a family of enzymes that catalyze the transfer of a methyl group from S-adenosyl methionine to a guanidine nitrogen atom of arginine residues (Gary et al., 1998). They are divided into three categories based on the type of methyl mark they leave on arginine residues. All PRMTs catalyze monomethylated intermediates (ω-N^G) (Gary et al., 1998). Type I PRMTs (i.e. PRMT1, PRMT2, PRMT3, PRMT4/CARM1, PRMT6, PRMT8) can add a second methyl group to the same terminal nitrogen atom of the guanidino group to form asymmetrically dimethylated arginines (aDMA) (Gary et al., 1998). Type II PRMTs (PRMT5) add a second methyl mark on the other terminal nitrogen atom thus forming symmetrically dimethylated arginines (sDMA) (Gary et al., 1998). Finally, PRMT7 is only able to catalyze the formation of monomethylarginines and is the sole type III PRMT identified so far (Zurita-Lopez et al., 2012, Feng et al., 2013). Arginine methylation plays a role in diverse cellular functions including signal transduction, DNA repair, transcription, protein subcellular localization, and RNA processing (Bedford et al., 2005, Bedford et al., 2009). CARM1 was found to methylate HuD on Arg^{236} (Arg^{248} in the mouse) in PC12 cells. Upon CARM1 knockdown, HuD exhibits a higher binding capacity to p21 mRNA. In turn, p21 is protected from degradation, thus leading to higher p21 levels, cell cycle exit, and neurite outgrowth (Fujiwara et al., 2006, Hubers et al., 2011). Therefore, CARM1 is a negative regulator of HuD-mediated neuronal differentiation in PC12 and motor neuron-derived MN-1 cells (Fujiwara et al., 2006, Hubers et al., 2011). Interestingly, CARM1 methylation activity can be inhibited by phosphorylation of Ser^{229} (Ser^{228} in the mouse) (Higashimoto et al., 2007, Feng et al.,

2009, Lim et al., 2012). More precisely, PKCα and PKCε can directly phosphorylate CARM1, inhibit its enzymatic activity, and thus reduce CARM1 methylation of HuD (Lim et al., 2012). This PKC-dependent inhibition of CARM1 and direct PKC phosphorylation of HuD were found to be important for HuD's mRNA-binding activity and its subsequent effect on dendrite arborisation in hippocampal neurons (Lim et al., 2012).

1.3 Current therapeutic strategies

Increasing full-length SMN levels has been at the centre of most therapeutic approaches developed in the last twenty years, either via enhancing *SMN2* exon 7 inclusion, increasing *SMN* transcription, stabilizing SMN protein, or via gene therapy using a viral approach.

1.3.1 Therapeutic strategies targeting SMN2

1.3.1.1 Increasing SMN2 transcription

The genetic context of SMA makes *SMN2* the ideal therapeutic target. Not only is it found in all patients, but it can be modulated to produce a full-length SMN protein. One way to enhance protein production is to chemically inhibit histone deacetylases (HDAC) from removing acetyl groups from the lysine residues on active chromatin. HDAC inhibitors like phenylbutyrate (PBA) (Andreassi et al., 2004, Hauke et al., 2009), valproic acid (VPA) (Sumner et al., 2003, Brichta et al., 2003, Tsai et al., 2006, Hahnen et al., 2006, Hauke et al., 2009, Harahap et al., 2012), trichostatin A (TSA) (Avila et al., 2007, Narver et al., 2008), and suberoylamilidehydroxamic acid (SAHA) (Riessland et al.,

2006, Hahnen et al., 2006, Hauke et al., 2009) showed promise in animal studies and in patient-derived cell lines, but only modest results in clinical trials (Brahe et al., 2005, Piepers et al., 2011, Swoboda et al., 2010, Darbar et al., 2011). These approaches might not be sufficient to rescue fully the SMA phenotype by themselves but could be beneficial in combination with other drugs or small molecules, Spinraza™ for example (see below).

1.3.1.2 Correcting SMN2 splicing

Modulation of endogenous *SMN2* pre-mRNA to produce FL-SMN protein is an attractive strategy because it allows for a better control of SMN levels, limiting total SMN protein to physiological levels (Goulet et al., 2012). *SMN* exon 7 splicing regulation has been extensively studied (reviewed in Singh et al., 2011, Singh et al., 2015, Singh et al., 2017) and identification of a 15nt-long intronic splicing silencer N1 (ISS-N1) in 2006 by the Singh laboratory opened the door to antisense oligonucleotide (ASO)-based therapies for SMA (Singh et al., 2006). ASOs are short DNA or RNA sequences designed to anneal to a complementary sequence on a gene of interest. They usually mediate splicing by blocking the binding of trans-acting factors that lead to exon inclusion or exclusion. In the case of *SMN2* exon 7 splicing, ASOs targeting the master checkpoint of *SMN2* exon 7 splicing regulation ISS-N1 enhance exon 7 inclusion by a complex mechanism. It involves the disruption of an internal stem loop termed ISTL1 (for internal stem loop through long-distance interaction 1), an inhibitory structure formed by a long distance interaction between the first position of ISS-N1 and a deep intronic sequence designated as ISS-N2 (Singh et al., 2013). ISTL1 also sequesters a portion of the weak 5'

splice site (5'ss) of exon 7. Therefore, ASOs targeting ISS-N1 or ISS-N2 interfere with ISTL1 and make the 5'ss of exon 7 accessible to the spliceosome machinery (Singh et al., 2013). The Krainer group, Ionis Pharmaceuticals, and Biogen developed Spinraza™, an 18nt-long ASO with a 2'-O-methoxyethyl (MOE) backbone (also known as Nusinersen, IONIS-SMN_{RX}, ISIS-SMN_{RX}) targeted at ISS-N1 (Hua et al., 2007, Hua et al., 2008, Hua et al., 2010, Passini, 2011). They received US Food and Drug Administration (FDA) and European Medicines Agency (EMA) approvals for their oligonucleotide in December 2016 and April 2017, respectively, making it the first FDA-approved drug for SMA (Ottesen, 2017, Scoto et al., 2017). Its efficacy has been tested mostly in symptomatic type I and II patients and is now being evaluated in pre-symptomatic infants diagnosed with SMA-causing mutations (Finkel et al., 2016).

1.3.1.3 Inducing translational read-through and increasing protein stability

As mentioned previously, exon 7 exclusion leads to the production of a truncated protein that is unable to compensate fully for the reduced levels of the full-length protein. It has been reported that SMNΔ7 has a turnover rate 2-fold faster than FL-SMN (Burnett et al., 2009). One explanation is the fact that FL-SMN oligomerizes properly and gets stabilized when incorporated into complexes (Burnett et al., 2009). Thus, if SMNΔ7 cannot oligomerize or self-associate correctly and does not get recruited into complexes, all downstream events get disrupted. Therefore, stabilizing SMNΔ7 protein could be a beneficial therapeutic intervention. One way to achieve this is by using aminoglycoside antibiotics. Aminoglycosides work by supressing the accurate recognition of translation stop codons. In the case of the SMNΔ7 protein, these drugs induced the native stop codon

to be read-through and instead use a stop codon situated 18nt downstream from the first one in exon 8. SMA patient-derived fibroblasts treated with tobramycin and amikacin showed an increase in SMN protein levels and Gems, showing that addition of just five extra amino acids could further stabilize the SMNΔ7 protein (Wolstencroft et al., 2005). Moreover, CNS delivery of aminoglycoside-derivative TC007 resulted in SMN induction in the brain and spinal cord, increased lifespan, and increased cell number in the ventral horn (Mattis et al., 2009). These findings and others (Mattis et al., 2009, Heier et al., 2009, Osman et al., 2017) suggest that read-through inducing compounds could be a potential therapeutic approach.

Another way to increase SMNΔ7 stability is to modulate its degradation. Hsu and colleagues identified ubiquitin carboxyl-terminal hydrolase L1 (UCHL1) as a regulator of SMN expression through ubiquitination (Hsu et al., 2010). UCHL1 is significantly increased in type I SMA fibroblasts and directly interacts with SMN in P19 and NSC-34 cells. Overexpression of UCHL1 reduced SMN levels whereas knockdown or inhibition of UCHL1 resulted in increased SMN levels and Gem numbers (Hsu et al., 2010). Similarly, Han and colleagues reported that the ubiquitin-specific protease 9x (Usp9x) modulates SMN levels (Han et al., 2012). In this case, Usp9x interacts directly with SMN but not SMNΔ7 and deubiquitinates it, thus preventing degradation by the proteasome. They showed that knockdown of Usp9x promotes the degradation of SMN and impairs the formation of Gems. Nothing further has been done so far but identification of small molecules able to modulate the activity of these enzymes could be exploited to derive a therapy.

1.3.2 SMN1 gene replacement therapies

In recent years, several preclinical studies have taken advantage of self-complementary adeno-associated viruses (scAAVs) as a tool to efficiently overexpress a gene of interest. Among the different serotypes available, serotype 9 stands out for its efficacy at targeting the CNS (each serotype has a different tropism) (Foust et al., 2009, Bevan et al., 2011, Bucher et al., 2013, Robbins et al., 2014). The Kaspar laboratory showed that AAV9 systemic delivery crosses the blood-brain barrier (BBB) and transduces mostly lower motor neurons (LMN) and dorsal root ganglia (DRG) in the spinal cord as well as neurons and astrocytes in the brain of neonatal mice (Foust et al., 2009). Interestingly, they found the transduction pattern to be strikingly different in the adult CNS. Tail vein injection of scAAV9-GFP in adult mice led to transduction of astrocytes almost exclusively, with very limited signal in spinal cord LMN (Foust et al., 2009). They were able to correct early heart failure in the delta7 mouse by early postnatal IV injection of scAAV9-SMN (Bevan et al., 2010). They also established that the therapeutic window is very limited especially in severe animal models (Foust et al., 2010), as confirmed by another team (Valori et al., 2010). In a dose-response study in the delta7 mouse, they later established that $1.8x10^{13}$vg/kg is the lowest concentration of scAAV9-SMN to use to fully rescue the SMA phenotype (Meyer et al., 2015).

Work from the Barkats laboratory looked at the influence of different routes of administration on spinal cord transduction in neonatal mice and determined that intravenous (IV) delivery is superior to intraperitoneal (IP) and intramuscular (IM) administration for spinal cord gene transfer (Duque et al., 2009). In the same study, they revealed that IV delivery of scAAV9 resulted in spinal cord transduction in adult mice,

confirming that scAAV9 is able to cross the BBB even long after birth (Duque et al., 2009). Also, using a codon-optimized SMN and the strong PGK promoter for more robust expression and better translation efficiency, they were able to get a better phenotypic rescue with a much lower dose than Foust and Valori (Dominguez et al., 2011). The team also found that IM injection of scAAV9-SMN in the delta7 mouse led to MN transduction via retrograde axonal transport and, unexpectedly to systemic expression (Benkhalifa-Ziyyat et al., 2013). Lastly, combining ICV and IV routes, they showed that ICV delivery is very efficient for CNS transduction while IV mostly targets peripheral organs (Armbruster et al., 2016).

The Lorson laboratory was able to decrease disease severity in the Burghes severe model (*Smn*$^{-/-}$;*SMN2*) but concluded that it was too severe for a complete rescue (Glascock et al., 2012a). However, they were able to rescue motor coordination in a slightly less severe model, the delta7 mouse, with both IV and ICV routes of administration (Glascock et al., 2012b) and confirmed once again that therapeutic window in the delta7 mouse is very limited and that the earlier the treatment, the better the rescue (Robbins et al., 2014).

Finally, scAAV9-SMN has made its way into clinical trials thanks to AveXis Inc., Sophia's Cure Foundation, and a team at the Nationwide Children's Hospital in Columbus, Ohio. They developed a self-complementary AAV9 carrying the *SMN* gene under the control of a hybrid CMV enhancer/chicken-b-actin promoter (scAAV9.cba.SMN). The biological agent known as AVXS-101 is now being tested for safety and tolerability after a single intravenous injection in severe SMA patients.

1.3.3 Non-SMN therapeutic strategies

There is now abundant evidence that tissues, organs, and systems other than α-motor neurons and NMJs are intrinsically affected in SMA (Vitte et al., 2004, Shanmugarajan et al., 2009, Shababi et al., 2010, Heier et al., 2010, Michaud et al., 2010, Bowerman et al., 2012b, Bowerman et al., 2012a, Schreml et al., 2013, Bowerman et al., 2014, Gombash et al., 2015, Szunyogova et al., 2016, Sintusek et al., 2016, Thomson et al., 2017, Ottesen et al., 2016, Deguise et al., 2017). SMN-independent strategies and combinatorial therapies (i.e. combining SMN-dependent and SMN-independent approaches) have gained popularity in recent years. Physical exercise has been shown to be beneficial in severe SMA mouse models (Grondard et al., 2005, Biondi et al., 2008, Biondi et al., 2010). More specifically, the Charbonnier group has shown that running reduced motor neuron cell death in the anterior horn of the spinal cord, enhanced *SMN2* exon 7 inclusion, and improved muscle phenotype (Grondard et al., 2005). They determined that physical exercise enhanced NMDA receptor expression and that pharmacological activation of NMDA receptors resulted in improved motor unit maturation, decreased cell death in the spinal cord, and increased SMN expression (Biondi et al., 2008, Biondi et al., 2010). Furthermore, some SMN-independent compounds have made their way into pre-clinical and clinical trials. Among them, Roche's Olesoxime (TRO19622) is currently being tested for long-term tolerability and safety (Bertini et al., 2017) (see also ClinicalTrials.gov: NCT01302600, NCT02628743). This orally active neuroprotectant prevents motor neuron cell death by interacting with outer mitochondrial membrane proteins and modulating permeability transition pore opening in response to oxidative stress. Importantly, Olesoxime crosses the BBB to target

the CNS (Bordet et al., 2010). Moreover, CK-2127107, a fast skeletal muscle troponin activator (FSTA) from Cytokinetics is being tested for a pharmacodynamic effect on measures of skeletal muscle function or fatigability in SMA patients (see ClinicalTrials.gov: NCT02644668). This compound slows down calcium release from fast skeletal muscle troponin, which results in an increased skeletal muscle contractility and improved physical performance (Hwee et al., 2015). Taken together, these findings highlight the importance of better understanding the molecular events leading to pathogenesis and of developing therapies targeting tissues and organs outside of the CNS in order to provide better, more complete care for patients.

1.4 Rationale, Hypothesis, and Objectives

1.4.1 Rationale

Recently, our laboratory showed that CARM1 regulates HuD's RNA-binding activity through methylation, which in turns regulates cell cycle exit. More precisely, CARM1 methylation of HuD on Arg^{248} reduces its affinity for p21 mRNA and promotes cell proliferation (Hubers et al., 2011). Since CARM1 levels are drastically down-regulated during motor neuron differentiation, this results in the pool of HuD becoming hypomethylated. In turn, HuD's affinity for p21 mRNA is increased, leading to its stabilization and promotion of cell cycle exit. In parallel, CARM1 also regulates the interaction between HuD and SMN, which takes place within the Tudor domain of SMN (Hubers et al., 2011). This methylation sensor domain serves as a protein-protein interaction module. Importantly, Tudor domain mutations in type 1 SMA patients result in the loss of its methyl sensor capacity (Côté et al., 2005, Hubers et al., 2011). However,

this phenomenon seems to act more prominently at the level of HuD axonal translocation regulation. In a recent paper, we showed that SMN represses translation of CARM1 (Sanchez et al., 2013). Thus, our current working model is that since CARM1 levels are higher in SMA due to low level of SMN, motor neuron-derived MN-1 cells might have a defect and/or delay in their normal differentiation process.

As mentioned above, we previously demonstrated that increasing HuD protein levels in a cell culture model of SMA allowed for complete rescue of SMA-like neuronal defects. More specifically, HuD overexpression induced neuronal differentiation, as assessed by p21 mRNA upregulation and neurite extension (Hubers et al., 2011). Therefore, increasing the pool of HuD in motor neurons to rescue differentiation defects associated with low SMN expression appears like a promising therapeutic strategy.

1.4.2 Hypothesis

Based on these findings, I propose that RNA-binding protein HuD is a potential therapeutic target for treating SMA. Stimulation and/or overexpression of HuD in cell culture and animal models of SMA will rescue the neuronal defects observed in the pathology.

1.4.3 Objectives

My objectives are to **i)** determine if HuD activity can be stimulated using a pharmacological approach and **ii)** establish an scAAV9 viral expression system to evaluate the benefits of HuD overexpression *in vivo*.

Chapter 2. Materials and methods

2.1 Cell culture

Motor neuron-derived MN-1 cells were cultured in Dulbecco's Modified Eagle Medium (DMEM) (Gibco Cat. #11965-092) supplemented with 10% Premium Fetal Bovine Serum (Wisent Multicell Cat. #080-150), and 1% Penicillin-Streptomycin 100X solution (GE Healthcare HyClone Laboratories Cat. #SV30010). Cells were kept at 37^{o}C with 5% CO_2 and passaged in 100mm plates twice a week at 15% confluency. Cells were seeded for experiments approximately 24h before treatment. Immediately before treatment, cells were washed with 1X PBS and then treated with Bryostatin-1 (Sigma Cat. #B7431) and/or PKCα inhibitor Ro 32-0432 (Santa Cruz Biotechnology, Inc. Cat. #sc-3549) reconstituted in dimethyl sulfoxide (DMSO) (Fisher Scientific Cat. #D139-1) at the indicated concentrations and for the indicated times. SMN knockdown cells were generated using a pGIPZ lentiviral shRNA targeting the sequence 5'-AAGCTTTTATCAATGCTGT -3' in mouse *Smn* (Dharmacon Cat. #RMM-4431-200990831).

2.1.1 IncuCyte

For the IncuCyte experiments, MN-1 cells were seeded in 6-well plates at a density of 125 000 cells/well one day prior to treatment. On treatment day, cells were washed once with 1X PBS before bryostatin medium [DMEM, 2% FBS, 1-1000pM Bryostatin] was added to the wells. Immediately after, plates were placed inside the IncuCyte device equipped with a 20X objective and 16 pictures/well were taken every 2h

for 72h. Neurite outgrowth was measured automatically in real time using the NeuroTrack software.

2.1.2 Transfection

For the overexpression experiments, MN-1 cells were seeded in 6-well plates at a density of 150 000 cells/well one day prior to transfection. On day of transfection, Lipofectamine® 2000 (Invitrogen Cat. #11668-019) in Opti-MEM® I Reduced Serum Media (Gibco Cat. #31985-070) was added to DNA in Opti-MEM® at a ratio of 1:1.66 DNA:Lipofectamine®. The DNA-Lipofectamine® mixture was added to fresh maintenance media after a 5-minute incubation at room temperature. About 6 hours later, cells were washed once in 1X PBS and then induced to differentiate with 16uM retinoic acid (RA) (Sigma-Aldrich Cat. #R2625) and 10ng/mL glial cell-derived neurotrophic factor (GDNF) (PeproTech Cat. #450-10) in DMEM supplemented with 2% FBS. Twenty-four hours after inducing differentiation, plates were imaged (5 pictures/condition/experiment) at 20X magnification using a Canon Powershot G6 camera. Percentage of cells with neurites was calculated by dividing the number of cells presenting neurites measuring at least twice the size of the cell body by the total number of cells in a frame.

2.2 SDS-PAGE and Western blotting

At time point, cells were lysed on ice in radioimmunoprecipitation assay (RIPA) lysis buffer [10mM Tris pH7.4, 100nM NaCl, 1mM EDTA (Fischer Scientific Cat. #S311-500), 1% NP-40, 0.5% NaDOC, 0.1% SDS] supplemented with 10ug/mL

Phenylmethanesulfonyl fluriode (PMSF) (MP Biomedicals Cat. #02195381) and cOmplete, EDTA-free Protease Inhibitor Tablets (Roche Cat. #04693132001). After a 15-minute incubation on ice with periodic vortexing, samples were spun at 13200rpm for 15 minutes at 4^{o}C. Supernatant was transferred to a labeled 1.5mL tube and pellet was discarded. Protein concentration was determined using the DC Protein Assay Reagent package (Bio-Rad Cat. #500-0116).

After quantification, an equal amount of each sample was combined with 5X Laemmli dye [250mM Tris, pH 6.8, 10%SDS, 50% Glycerol, 1.43M β-mercaptoethanol, 0.5M DTT] and heated at 95^{o}C for 8 minutes. Proteins were resolved on a 10% acrylamide gel [30% Acrylamide/bis-acrylamide 29:1 (Bio-Rad Cat. #161-0156), 10% APS (Fischer Scientific Cat. #BP179-100), 10% SDS, TEMED (Bio Basic Cat. #TB0508)] alongside a molecular weight ladder [MW powder (Sigma-Aldrich Cat. #SDS7B2), 4M Urea (Sigma-Aldrich Cat. #U-5378), 1X Laemmli dye)] in 1X SDS running buffer [0.1% SDS, 0.2M Glycine, 25mM Tris-base]. Proteins were then transferred onto an 0.45μm Immobilon-P polyvinylidene difluoride (PVDF) membrane (EMD Millipore Cat. #IPVH00010) in 1X transfer buffer [0.01% SDS, 0.2M Glycine, 25mM Tris-base, 20% Methanol]. Membranes were blocked in 5% non-fat milk in PBS-T [137mM NaCl, 2.7mM KCl, 10.5mM Na_2HPO_4-(H_20), 1.75mM KH_2PO_4, 0.05% Tween-20 (Fischer Scientific Cat. #BP337-500)] and then incubated in primary antibody diluted in 5% non-fat milk in 1X PBST for 1h at room temperature or overnight at 4^{o}C. After incubation, membranes were washed three times for 5 minutes in 1X PBST, incubated in secondary antibody diluted in 5% non-fat milk in 1X PBST for 1h at room temperature before being washed again three times in 1X PBST. After a 2-minute

incubation with Luminata Forte Western HRP substrate (EMD Millipore Cat. #WBLUF0500), bands were detected on HyBlot CL autoradiography films (Denville Scientific Inc. Cat. #E318). Antibodies include mouse anti-HuD (Santa Cruz Biotechnology, Inc. Cat. #sc-48421 and #sc-28299), mouse anti-PKCα (Santa Cruz Biotechnology, Inc. Cat. #sc-208), mouse anti-α-tubulin (Sigma-Aldrich Cat. #T6199), rabbit anti-flag (Cell Signaling Technology Cat. #2368), mouse anti-myc, rabbit anti-phospho-Akt (Ser473) (Cell Signaling Technology, Inc. Cat. #9271), goat anti-Akt (Santa Cruz Biotechnology, Inc. Cat. #sc-1618), rabbit anti-phopsho-p44/42 MAPK (Erk1/2) (Thr202/Tyr204) (20G11) (Cell Signaling Technology, Inc. Cat. # 4376), mouse anti-Erk (BD Transduction Laboratories™ Cat. #610123), HRP-conjugated goat anti-mouse (Jackson ImmunoResearch Laboratories, Inc. Cat. #115-035-174), HRP-conjugated mouse anti-rabbit (Jackson ImmunoResearch Laboratories, Inc. Cat. #211-032-171).

2.3 Immunoprecipitation (IP) and RNA immunoprecipitation (RIP)

At time point, cells were washed once and scraped in 1X PBS. After a 1-minute spin at 13200rpm at 4^{o}C, supernatant was aspirated and cells were lysed on ice in 1% NP-40 lysis buffer [1% NP-40, 150mM NaCl, 50mM 1M Tris pH7.5, 10ug/mL Phenylmethanesulfonyl fluriode (PMSF) (MP Biomedicals Cat. #02195381), cOmplete, EDTA-free Protease Inhibitor Tablets (Roche Cat. #04693132001), 12.5uL Recombinant RNasin® Ribonuclease inhibitors (Promega Cat. #N251B)] for 30 minutes. Samples were spun three times at 13200rpm at 4^{o}C for 15 minutes. After each spin, supernatant was transferred to a new tube. After the third spin, samples were pre-cleared with 20uL Protein A/G PLUS-Agarose beads (Santa Cruz Biotechnology, Inc. Cat. #sc-2003) by

tumbling at 4°C for 30 minutes. Samples were subsequently quantified by Bradford assay and an equal amount of protein (500-1000ug) was added to IgG and IP tubes. Next, 4ug of primary antibody and corresponding control IgG was added to the respective tubes before tumbling samples overnight at 4°C. The next morning, 20uL of bead slurry was added and tubes were tumbled again at 4°C for 60 minutes. Beads were spun down at 6600rpm at 4°C for 1 minute and washed 5 times in 1mL RIPA lysis buffer at 3000rpm at 4°C for 3 minutes. For the IP protocol, 20uL of RIPA buffer and 5X Laemmli were added to each sample after the last wash. Samples were then boiled at 95°C for 8 minutes and resolved by SDS-PAGE (see section 2.2 for details). For the RIP protocol, 1mL of TRIzol Reagent (Ambion Cat. #15596018) was added to each tube before proceeding to RNA extraction, reverse transcription, and polymerase chain reaction (PCR) (see section 2.4 below).

2.4 RNA extraction, reverse transcription, and polymerase chain reaction (PCR)

Total RNA was extracted using TRIzol Reagent (Ambion Cat. #15596018) following the manufacturer's protocol. In short, after a 5-minute incubation at room temperature in TRIzol, 200uL of chloroform was added to each tube. Samples were spun for 15 minutes at 12000rcf at 4°C. After transferring the aqueous phase to a new tube, 500uL isopropyl alcohol and 2uL GlycoBlue were added and the tubes were incubated at room temperature for 10 minutes. Tubes were then spun for 15 minutes at 12000rcf, washed in 75% ethanol, and spun again for 10 minutes at 7600rcf at 4°C. Finally, pellets were air dried for 5 minutes before being resuspended in double distilled water.

To generate complementary DNA (cDNA), 100ng RNA was incubated with 1μM oligo-DT (5'-ttttttttttttttttt -3') for 10 minutes at 65^{o}C, followed by reverse transcription using 10U AMV Reverse Transcriptase enzyme (Promega Cat. #M510F), 20U Recombinant RNasin® Ribonuclease Inhibitors (Promega Cat. #N251B), and 0.5mM dNTP Mix (Promega Cat. #U151B) in AMV RT 5X buffer (Promega Cat. #M515A) for 1h at 42^{o}C.

cDNA was amplified exponentially by PCR using the following primers: p21 F: 5'- cagcgatatccagacattcaga -3'; p21 R: 5'- ctcagacaccagagtgcaagac -3'; GAP-43 F: 5'- tttgtttcttggtgttgttatggc -3'; GAP-43 R: 5'- gaacggaacattgcacacaca -3'; Tau F: 5'- ggtcgaagattggctctactg -3'; Tau R: 5'- gccaaggaagcagacacttc -3'; 18S F: 5'- gtaacccgttgaaccccatt -3'; 18S R: 5'- ccatccaatcggtagtagcg -3'; GAPDH F: 5'- accacagtccatgccatcac -3'; GAPDH R: 5' -tccaccaccctgttgctgta -3'. PCR products were visualized on a 1% agarose gel in 1X TBE buffer with ethidium bromide.

2.5 DNA plasmids, vectors, subcloning, and mutagenesis

2.5.1 Gibson Assembly®

Gibson assembly® was used to subclone HuD-flag and mGFP into the scAAV vector. HuD-flag and mGFP were amplified from their respective vectors of origin using primers designed with the help of the NEBuilder® Assembly tool from New England BioLabs Inc. followed by gel purification (1% agarose gel at 175V) using the Wizard® SV Gel and PCR Clean-Up System (Promega Cat. #A19282). Primers: scAAV-HuD-flag GibF: 5'- ttgtacccgcggccgatccaccggtaccatgttcatacctcttatcttcc - 3'; scAAV-HuD-flag GibR: 5'- tctagtcgacggtatcgataagcttttatttatcgtcgtcatccttataatc -3'; scAAV-mGFP GibF:

5'-ttgtacccgcggccgatccaccggtaccatgagcgggggcgaggag -3'; scAAV-mGFP GibR: 5'-tctagtcgacggtatcgataagcttttatctgagtccggacctgtacagc -3' (PCR conditions: 95℃ for 2min, 25 cycles of 95℃ for 15sec, 59.5℃ for 2sec, and 72℃ for 20sec, followed by a final extension at 72℃ for 600sec). The scAAV-SMN vector, a gift from Dr. Christian Lorson, was cut open with AgeI (NEB Cat. #R0552S) and HindIII-HF (NEB Cat. #R3104S) restriction enzymes. DNA fragments were assembled at 50°C for 30 minutes using 2X Gibson Assembly Master Mix [Isothermal Start Mix (PEG8000 (EM Science Cat. #6510), 1M Tris-HCl, pH8.0, 2M $MgCl_2$), 1M DTT (Promega Cat. #V3155), 25mM dNTPs (Promega Cat. #U151B), NAD+ (NEB Cat. #B9007S), T5 exonuclease (NEB Cat. #M0363S – 10 units/μL), Phusion High Fidelity DNA Polymerase (NEB Cat. #M0530S – 2units/μl), Taq Ligase (NEB Cat. #M0208S – 40units/μL)], 150ng of insert, 75ng of backbone vector in a final volume of 20uL.

2.5.2 Transformation

Following assembly, the new vectors were transformed. Escherichia coli Subcloning Efficiency™ DH5α Competent Cells (Invitrogen Cat. #18265-017) were taken out of the -80°C freezer and thawed on ice for approximately 10 minutes. 3uL of each plasmid vector was added to 150uL of bacteria into a 15mL falcon tube and incubated on ice for 30 minutes. After a 30 seconds heat shock at 42°C, competent cells were incubated on ice for another 2 minutes. After adding 500uL of Lysogeny broth (LB) medium [1% NaCl (Wisent Multicell Cat. #600-082-IK), 0.5% Yeast extract (Bio Basic Cat. #G0961), 1% Tryptone (Fischer Scientific Cat. #BP1421-2)] samples were agitated for 1h at 225rpm at 37°C. Bacteria was grown overnight on LB-Agar plates [4% LB-Agar

(Fischer Scientific Cat. #BP1425-500), 100ug/mL Ampicillin (Sigma-Aldrich Cat. #A9518)]. The next morning, individual colonies were picked and grown in 3mL LB medium. DNA was purified using the PureYield™ Plasmid Miniprep System (Promega Cat. #A1222) and/or using the HiPure Plasmid Maxiprep kit (Invitrogen Cat. #K210007) after a subsequently 16h growth period in 250mL LB medium.

Max Efficiency™ Stbl2 Competent Cells (Invitrogen Cat. #10268-019) were used to amplify the AAV vectors for virus production. Transformation protocol was similar, except for the duration of the heat shock (25sec instead of 30) and the medium used (S.O.C. Medium [2% tryptone, 0.5% yeast extract, 10 mM NaCl, 2.5 mM KCl, 10 mM MgCl2, 10 mM MgSO4, and 20 mM glucose] (Invitrogen Cat. #15544-034)).

2.5.3 Mutagenesis

Following sequencing analysis, single nucleotides were mutated using PrimeSTAR polymerase (Takada Cat. #R040A) and the following primers: g3184a F: 5'-acactcctgtgacttgatcaaccaggattcgtgag -3'; g3194a F: 5'-ctcacgaatcctggttgatcaagtcacaggagtgt -3'; a3763g F: 5'- ccgttgaggctggcgatggccatggcc -3'; a3763g R: 5'- ggccatggccatcgccagcctcaacgg -3' (PCR conditions: 95℃ for 2min, 18 cycles of 95℃ for 20sec, 60℃ for 10sec, and 68℃ for 384sec, followed by a final extension at 68℃ for 300sec). Reactions were treated with DpnI (NEB Cat. #R0176S) for 8h before transformation. Mutations were validated by sequencing at the McGill University and Génome Québec Innovation Centre.

2.6 Animal work

2.6.1 Animals

All animal procedures were performed in accordance with the Canadian Council on Animal Care standards and were approved by the University of Ottawa Animal Care Committee (protocols #CMM-2046 and #CMM-2259). Delta7 breeders (*SMNΔ7*$^{+/+}$;*SMN2*$^{+/+}$; *mSmn*$^{+/-}$) on an congenic FVB/N background were obtained from Dr. Alex MacKenzie (originally purchased from The Jackson Laboratory, stock #005025). Mice were housed up to 5 animals per cage, with ad libitum access to food (Envigo, 2018 Teklad global 18% protein rodent diet) and water. Animals were maintained on a 12h light/dark cycle. Pups were weighed, tattooed, and genotyped on day on birth (P0). Injections and behavioral tests were done in the morning, between 7:30 and 10:30am.

2.6.2 Genotyping

Tail tips were collected in the morning and digested for 1h at 55^{o}C. DNA was extracted using the E.Z.N.A® Tissue DNA Kit (Omega Bio-tek Cat. #D3396-02). PCR reaction: GoTaq® Green Master Mix (Promega Cat. #M712), 5uL of eluted DNA, and the following primers: mSmn WT F: 5′ -tctgtgttcgtgcgtggtgacttt-3′ ; Rev: 5′ -cccaccacctaagaaagcctcaat-3′ ; LacZ F: 5′ -ccaacttaatcgccttgcagcaca-3′ ; Rev: 5′ -aagcgagtggcaacatggaaatcg 3′ ; mSmn F: 5’ -gtgtctgggctgtaggcattgc-3’ ; Rev: 5’ -ggctgtgccttttggcttatctg-3’ (PCR conditions: 95 °C for 5 min, 35 cycles of 94°C for 30sec, 58°C for 30sec, and 72°C for 30sec followed by a final extension at 72°C for 5 min). PCR reactions were visualized on a 1% agarose (Invitrogen Cat. #16500-500) gel

made in 1X TBE buffer [0.05M Tris (Wisent Multicell Cat. #600-125-IK), 0.05M Boric acid (Calbiochem Cat. #2720), 0.8mM EDTA (Fischer Scientific Cat. #S311-500)] containing ethidium bromide (Sigma-Aldrich Cat. #E8751).

2.6.3 Virus production

After subcloning, scAAV-cba-SMN, -HuD-flag, and -mGFP vectors were sent to the Canadian Neurophotonics Platform at Laval University in Québec City for virus production. Stocks [scAAV9-cba-SMN: 1E13 GC/mL; scAAV9-cba-HuD-flag: 4E12 GC/mL; scAAV9-cba-mGFP: 4E12 GC/mL] were shipped to the University of Ottawa on dry ice and stored at -80^{o}C upon receiving. At a later date, viruses were diluted in 1X PBS, aliquoted, and stored again at -80^{o}C.

2.6.4 Facial vein injection

One day after birth, pups received either saline or $2x10^{10}$ vg (i.e. $1.33x10^{13}$ vg/kg for a 1.5g pup) scAAV-SMN serotype 9 in a final volume of 20uL. Virus aliquots were kept at -80^{o}C and thawed on ice right before injection. Pups were anesthetized using isoflurane for 60 seconds and placed on top of a WeeSight™ Transilluminator for facial vein visualization. Injection was performed using a 31G 3/10cc 5/16" insulin syringe (CarePoint Vet Cat. #12-7653). Pups were put on a heating mat for recovery and returned to their home cage once all pups in a litter were awake.

2.6.5 Righting reflex test

Time to right was measured every other day from P2 to P12. Pups were put on their back and time to return to their four paws was recorded. The test consisted of 3 trials with a maximum time of 60 seconds per trial and 5 minutes of rest in between trials. Pups were put back in their home cage during rest periods. See *Treat-NMD Neuromuscular Network SOP #MD_M.2.2.002 - Behavioral Phenotyping for neonates: Righting reflex* for details (DiDonato et al., 2011).

2.6.6 Hind limb suspension test (tube test)

Proximal muscle strength and fatigue was measured every other day from P2 to P12. Pups were put head first in a standard 50mL Falcon tube held straight up. Time spent hanging, number of pulls, and hind limb suspension score (position of the legs and tail) were recorded in 2 consecutive trials. This test was administered at least 10 minutes after the righting reflex test. See *Treat-NMD Neuromuscular Network SOP #SMA_M.2.2.001 - Behavioral Phenotyping for neonates: Hind Limb Suspension Test (a.k.a. Tube Test)* for details (El-Khodor, 2011).

2.6.7 Pen test

Balance and coordination were evaluated every other day starting at P14. In this test, mice were lowered onto a 1cm-wide pen held 20cm above a table. Time spent on the pen was measured 3 times with 5 minutes of rest in between repetitions. See *Treat-NMD Neuromuscular Network SOP #SMA_M.2.1.001 - Use of pen test (balance beam)* to assess motor balance and coordination in mice for details (Kothary, 2010).

2.7 Statistical analysis

Data was analyzed using ImageJ, GraphPad Prism v7.0c, and Microsoft Excel. Unpaired, two-tailed Student t-test was performed on data sets with 3 or more replicates. Significance is indicated * $p<0.05$ and ** $p<0.01$.

Chapter 3. Results

3.1 Effect of bryostatin on motor neuron-derived MN-1 cells

It has previously been reported that a PKC-HuD-mRNA pathway exists in neuronal cells (Mobarak et al., 2000, Pascale et al., 2005, Lim et al., 2012, Lim et al., 2014). Additionally, this pathway can be modulated using bryostatin, a PKC activator currently under investigation as a potential therapy for various pathological conditions affecting the CNS (see Chapter 1). One objective of this study was to determine if such a pathway exists in motor neurons and what are the potential effects of modulating HuD activity using bryostatin in MN-1 cells.

3.1.1 PKCα and HuD interact in motor neuron-like MN-1 cells

In order to determine if a PKC-HuD-mRNA target pathway exists in motor neuron-derived MN-1 cells, a potential interaction between PKCα and HuD was assessed. Endogenous PKCα was immunoprecipitated from MN-1 cells and the immunoprecipitated proteins were resolved by sodium dodecyl sulfate-polyacrylamide gel electrophoresis (SDS-PAGE) and analyzed by western blotting. Antibodies against HuD (**Figure 3A**, lanes 1-3) and PKCα (lanes 4-6) were used to detect the presence of HuD in the PKCα immunoprecipitate, and to confirm the immunoprecipitation PKCα, respectively. Absence of signal in the IgG lane confirmed that the enrichment detected in the IP lane was specific. The reverse co-IP was attempted but detection of PKCα in the HuD immunoprecipitate was unsuccessful (results not shown). This indicates that the two

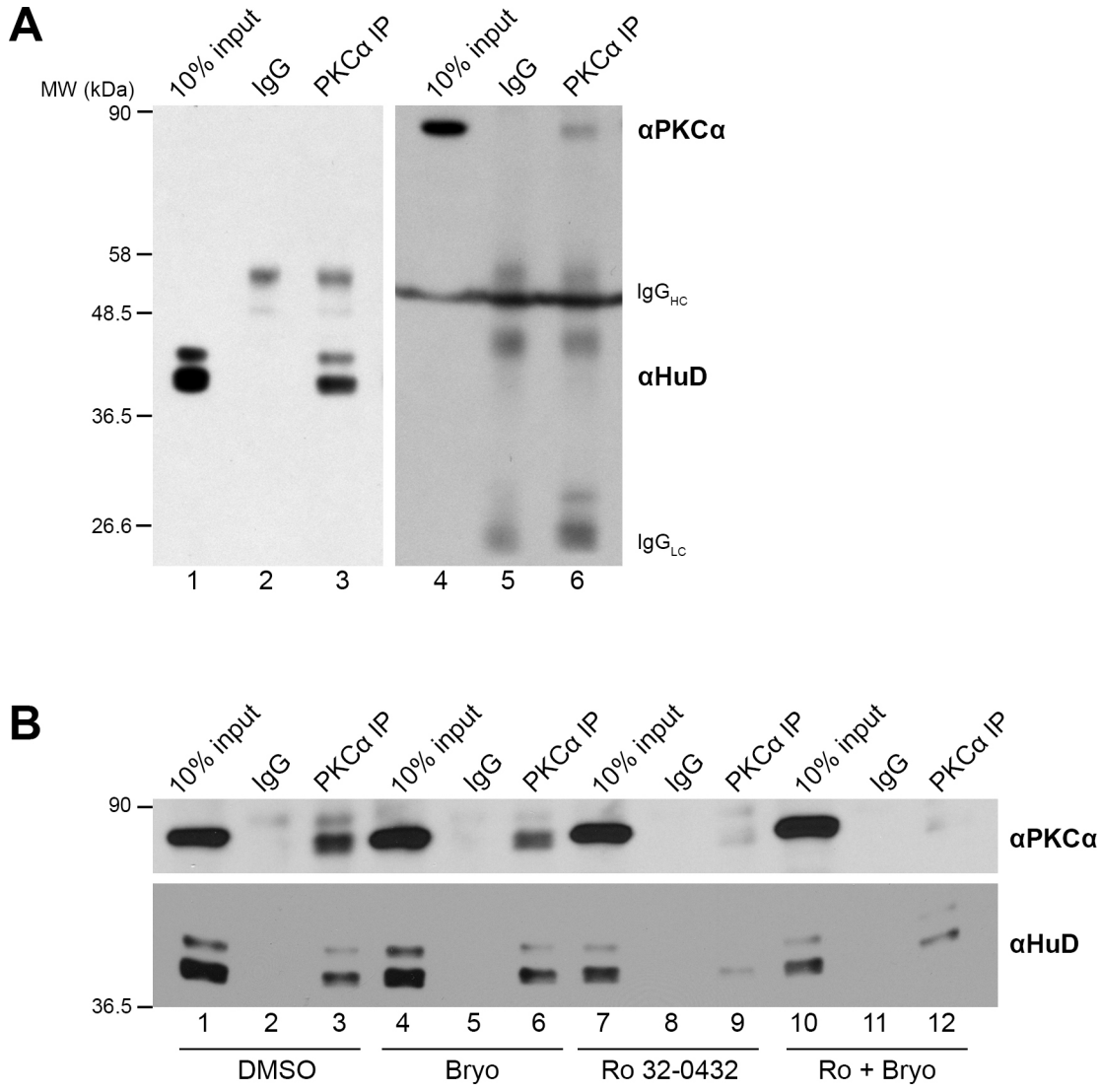

Figure 3. PKCα and HuD co-immunoprecipitate in motor neuron-like MN-1 cells. ***A***. Endogenous PKCα was immunoprecipitated (IP) from MN-1 cells and the immunoprecipitated proteins were resolved by SDS-PAGE and analyzed using antibodies against HuD (left panel) and PKCα (right panel). ***B***. The same experiment was performed with pre-treatment of the cells with 5nM Bryostatin (PKCα activator) for 30 minutes, with 2μM Ro 32-0432 (PKCα inhibitor) for 2h or with both (2h30min).

proteins likely interact in MN-1 cells and that HuD could be a potential substrate of PKCα. Next, we wanted to assess whether the interaction between HuD and PKCα can be modulated using PKCα activator bryostatin or PKCα inhibitor Ro-320432. The same experiment was performed again, this time subjecting the cells to four different conditions: DMSO control, 5nM bryostatin for 30 minutes, 2μM Ro-320432 for 2 hours, and 2μM Ro-320432 pre-treatment followed by 5nM bryostatin treatment. Endogenous PKCα was then immunoprecipitated in these four different conditions and the immunoprecipitated proteins were resolved by SDS-PAGE followed by western blotting. (**Figure 3B**). Based on the literature, it would be expected that the interaction between PKCα and HuD be increased following activation with bryostatin and be decreased following treatment with the inhibitor Ro 32-0432. Here, treatment with bryostatin did not increase the amount of HuD protein co-immunoprecipitated (lane 6, bottom panel) but it decreased the amount of PKCα protein that was immunoprecipitated (lane 6, top panel). Treatment with the Ro 32-0432 inhibitor diminished considerably the amount of both PKCα and HuD proteins in the immunoprecipitate (lanes 9 and 12), to the point where PKCα was almost undetectable in the immunoprecipitate when cells were treated with Ro 32-0432 alone or with Ro 32-0432 and bryostatin. This was the case in all attempts at modulating the PKCα-HuD interaction, making quantification of the relative interaction challenging. Therefore, it could not be determined whether the interaction between HuD and PKCα in MN-1 cells can be modulated using a PKCα activator or inhibitor.

While co-immunoprecipitation of HuD with PKCα was detected endogenously, it does not indicate that HuD is a substrate of PKCα in MN-1 cells. It is possible that the

two proteins are simply part of the same complex but not interacting directly. Thus, in an effort to determine whether HuD is a substrate of PKCα in MN-1 cells, the phosphorylation and methylation statuses of HuD were investigated by SDS-PAGE and western blotting using phospho-serine PKC substrates, phospho-threonine, and CARM1 methyl-specific antibodies on HuD immunoprecipitates from MN-1 cells treated with either bryostatin, Ro 32-432, or both. Unfortunately, it proved difficult to obtain efficient HuD immunoprecipitations and no signal could be detected at the size of HuD in the IP lanes when blotting with the different modification-specific antibodies (results not shown). The phosphorylation status of CARM1 was also assessed using the same paradigm but did not yield any conclusive results (see discussion).

3.1.2 HuD is upregulated in motor neuron-like MN-1 cells upon treatment with bryostatin

Next, we wanted to determine the effect of PKCα activation with bryostatin on HuD protein levels. It was previously shown that bryostatin activation of PKCα induced HuD up-regulation in cell culture and *in vivo* (Pascale et al., 2005, Lim et al., 2012, Marchesi et al., 2016). To determine the effect of bryostatin on HuD protein levels in our cell line, motor neuron-derived MN-1 cells were treated with increasing concentrations of the drug for 15 minutes. After cell lysis, proteins were resolved by SDS-PAGE and, once again analyzed by western blotting (**Figure 4A**). Densitometry analysis of the blots revealed a significant ~1.5-fold increase in HuD protein levels when cells were treated with 1pM bryostatin (**Figure 4B**). HuD levels were also elevated in cells treated with 10 and 100pM bryostatin, although it did not quite reach statistical significance. Since there was a trend in HuD protein levels increasing with bryostatin concentration, cells were

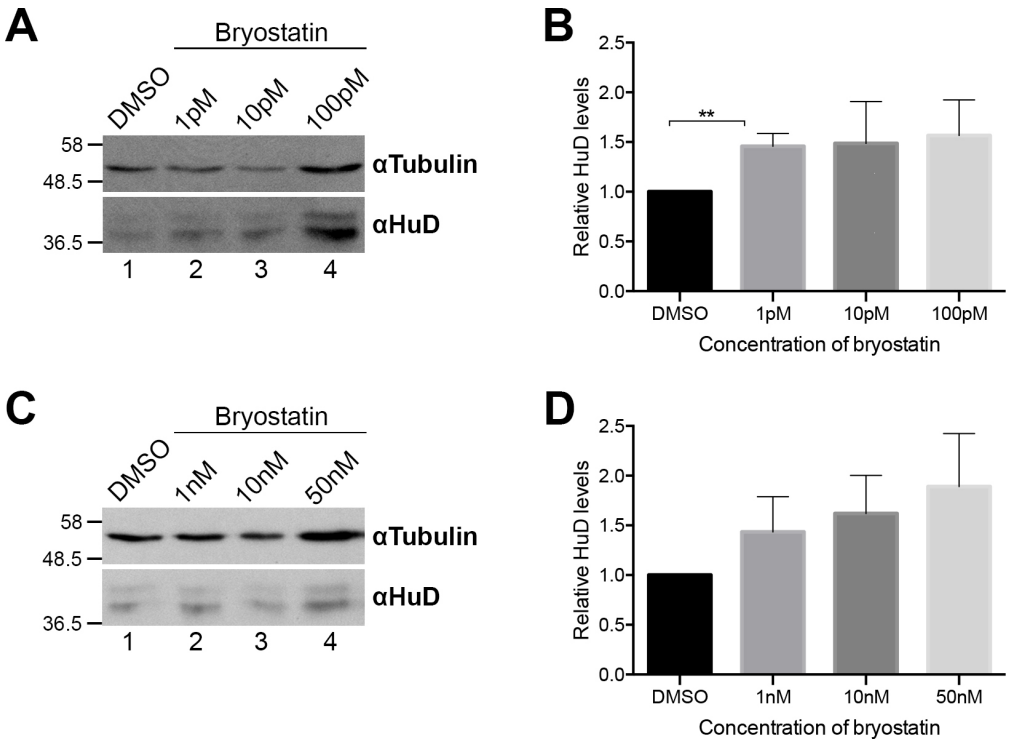

Figure 4. HuD is upregulated following PKC stimulation with bryostatin in motor neuron-like MN-1 cells. ***A***,***C***. MN-1 cells were treated for 15 minutes with increasing concentrations of PKC activator bryostatin. Representative Western blots of HuD and tubulin. ***B***,***D***. Densitometry analysis of the blots revealed a trend in HuD levels increasing with bryostatin concentration. Data are mean ± SEM (1-100pM n=5; 1-50nM n=6), normalized to tubulin and relative to DMSO, two-tailed t-test **p<0.01.

exposed to even higher doses of the drug (**Figure 4C**). The trend was still present when cells were treated with 1, 10, and 50nM bryostatin but the increase in HuD levels was not statistically significant (**Figure 4D**). These findings suggest that one of bryostatin's effects in MN-1 cells is HuD protein upregulation. However, increasing the amount of bryostatin did not seem to promote higher induction of HuD levels.

3.1.3. Bryostatin activates PKC downstream signaling in motor neuron-derived MN-1 cells.

Next, we wanted to determine whether bryostatin activation of PKCα can also modulate other known downstream target(s) of the kinase and what other pathways are potentially activated/inactivated by the pharmacological agent. The serine/threonine kinase Akt/PKB is involved in diverse cellular processes including cell growth and proliferation (Dudek et al., 1997, Franke et al., 1997, Kennedy et al., 1997, Eves et al., 1998, Downward, 1998). TPA-induced activation of PKC has been reported to induce both Akt activation and inactivation, depending on context (Kawakami et al., 2004, Wen et al., 2002, Liu et al., 2006, Fan et al., 2008). Erk/MAPK, also a serine/threonine kinase, is part of the MAPK/Erk signaling cascades involved in cell proliferation, differentiation, and apoptosis among others (reviewed in Shaul et al., 2007, McCubrey et al., 2007, Krishna et al., 2008, Mebratu et al., 2009). Although the effects mediated by Erk signaling are highly context-specific, Erk activation is generally associated with phorbol esters and/or bryostatin-induced PKC stimulation (Racke et al., 1997, Wall et al., 2001, Choe et al., 2002, Matsumoto et al., 2006). Therefore, it would be expected for Erk phosphorylation to be increased following bryostatin treatment. Here, MN-1 cells were

treated with 10nM bryostatin for 30 minutes. Following treatment, proteins were collected and resolved by SDS-PAGE to assess the phosphorylation status of Akt and Erk. Western blotting analysis revealed a decrease in Akt Ser473 phosphorylation upon bryostatin treatment but no change in total Akt, thus resulting in ~50% decrease in the pAkt/total Akt ratio (**Figure 5A,B**). In contrast, bryostatin induced a strong increase in Erk Thr202/Tyr204 phosphorylation while total Erk remained unchanged, resulting in a 2-fold increase of the pErk/total Erk ratio (**Figure 5C,D**). The bryostatin-induced PKC-dependent activation of Erk found here is consistent with the literature (Racke et al., 1997, Wall et al., 2001, Choe et al., 2002, Matsumoto et al., 2006). These findings confirm that bryostatin is indeed active in MN-1 cells and that it activates PKCα, resulting in the downstream modulation of important signaling pathways.

3.1.4 Bryostatin alters HuD binding to its mRNA targets in motor neuron-like MN-1 cells

If the PKC-HuD-pathway is conserved in MN-1 cells, then activation of PKC and upregulation of HuD using bryostatin would be expected to have an effect on the target transcripts of HuD. To assess whether bryostatin treatment of MN-1 cells influences the binding of HuD to some of its mRNA targets, HuD RNA immunoprecipitation (RIP) was performed after treatment with 10nM bryostatin for 30 minutes in MN-1 cells. Endogenous HuD was immunoprecipitated (**Figure 6A**) and total RNA was extracted. Following reverse transcription (RT), polymerase chain reaction (PCR) amplification was used to assess the relative levels of three HuD mRNA targets that are involved in neuronal differentiation. Surprisingly, bryostatin treatment significantly reduced HuD

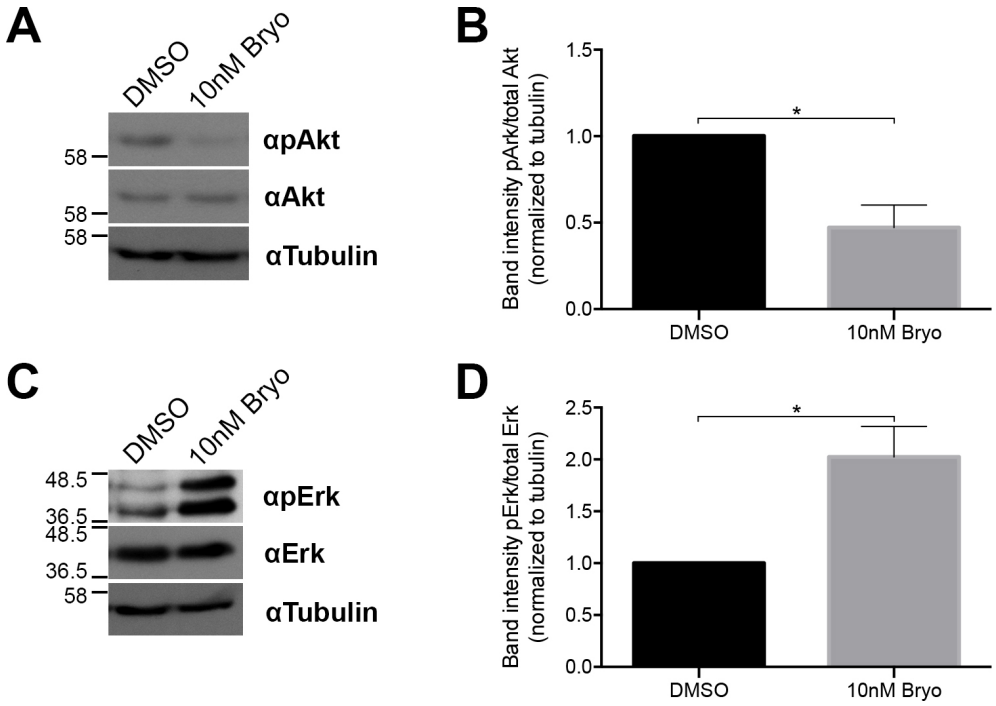

Figure 5. PKCα downstream signaling is activated following a short bryostatin treatment in motor neuron-like MN-1 cells. ***A***,***B***. MN-1 cells were treated with either DMSO or 10nM for 30 minutes and proteins were resolved by SDS-PAGE. Bryostatin treatment reduced Akt phosphorylation. Densitometry analysis of the blots revealed a 50% decrease in the pAkt/Akt ratio. ***C***,***D***. Erk phosphorylation is enhanced by the bryostatin treatment. Densitometry analysis of the blots revealed a 2-fold increase in the pErk/Erk ratio. Data are mean ± SEM (n=3), normalized to tubulin and relative to DMSO, two-tailed t-test *$p<0.05$.

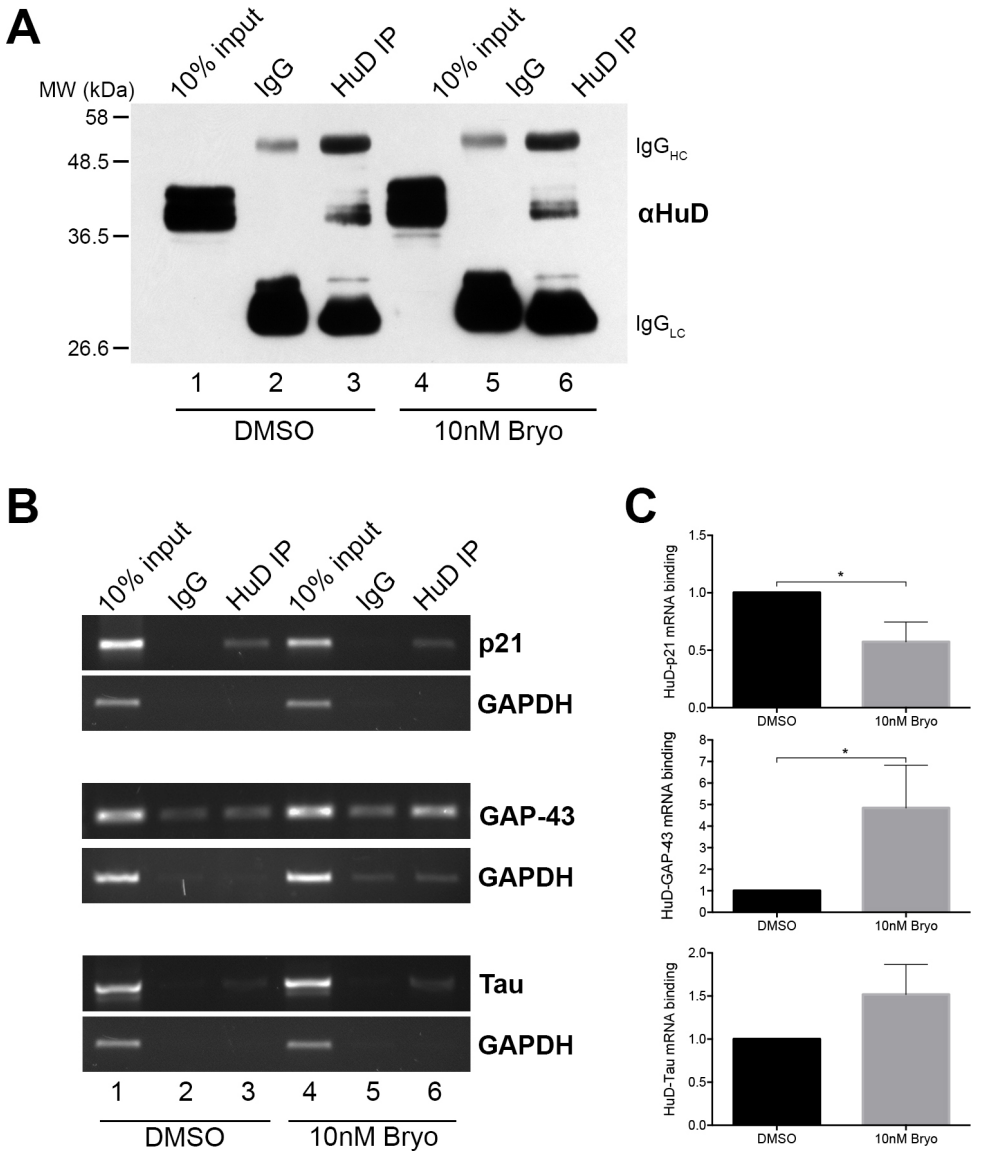

Figure 6. HuD binding to mRNA targets is altered following bryostatin treatment in motor neuron-derived MN-1 cells. ***A***. Endogenous HuD was immunoprecipitated from MN-1 cells treated with either DMSO or 10nM bryostatin for 1hr. ***B***. p21, GAP-43, and Tau binding to HuD was assessed by RT-PCR and GAPDH was used as a negative control. ***C***. Bar graph shows a significant decrease in p21 mRNA levels bound to HuD following bryostatin treatment. HuD binding to GAP-43 and Tau mRNA is increased with bryostatin treatment. Data are mean ± SEM (p21: n=6; GAP-43: n=3; Tau: n=5), normalized to precipitated HuD protein and relative to DMSO, two-tailed t-test *$p<0.05$.

binding to p21 mRNA but enhanced binding to GAP-43 and Tau mRNAs (**Figure 6B,C**, lane 6). Based on previous findings from our laboratory, it was expected that HuD binding to p21 and GAP-43 mRNAs would be enhanced and binding to Tau unchanged, following PKC-induced activation and phosphorylation of HuD and inactivation of CARM1. This will be discussed in later sections.

3.1.5 Bryostatin has poor neuronal differentiation induction capabilities in motor neuron-like MN-1 cells

Since HuD binding to targets involved in neuronal differentiation was altered upon bryostatin treatment, we next wanted to assess the effect of bryostatin on this process in MN-1 cells. In order to be able to evaluate the extent of bryostatin-induced cell differentiation, HuD overexpression was first used as a positive control for neurite extension. As abovementioned, our laboratory has shown in the past that overexpressing HuD induces MN-1 cell differentiation and neurite extension. Here, MN-1 cells were transfected with either an empty myc-pcDNA vector, a low, or a high amount of HuD DNA. Forty-eight hours after transfection, populations overexpressing HuD had 8-12% of cells exhibiting neurites measuring at least twice the length of the cell body, compared to 1-2% for cells overexpressing an empty vector (**Figure 7A,B**). Western blotting was used to confirm HuD overexpression in MN-1 cells (**Figure 7C**, lanes 3 and 4). Densitometry analysis of the blots revealed a ~6-fold increase in HuD protein levels in cells transfected with low and high amounts of DNA, compared to endogenous levels expressed in cells transfected with the empty vector (**Figure 7D**).

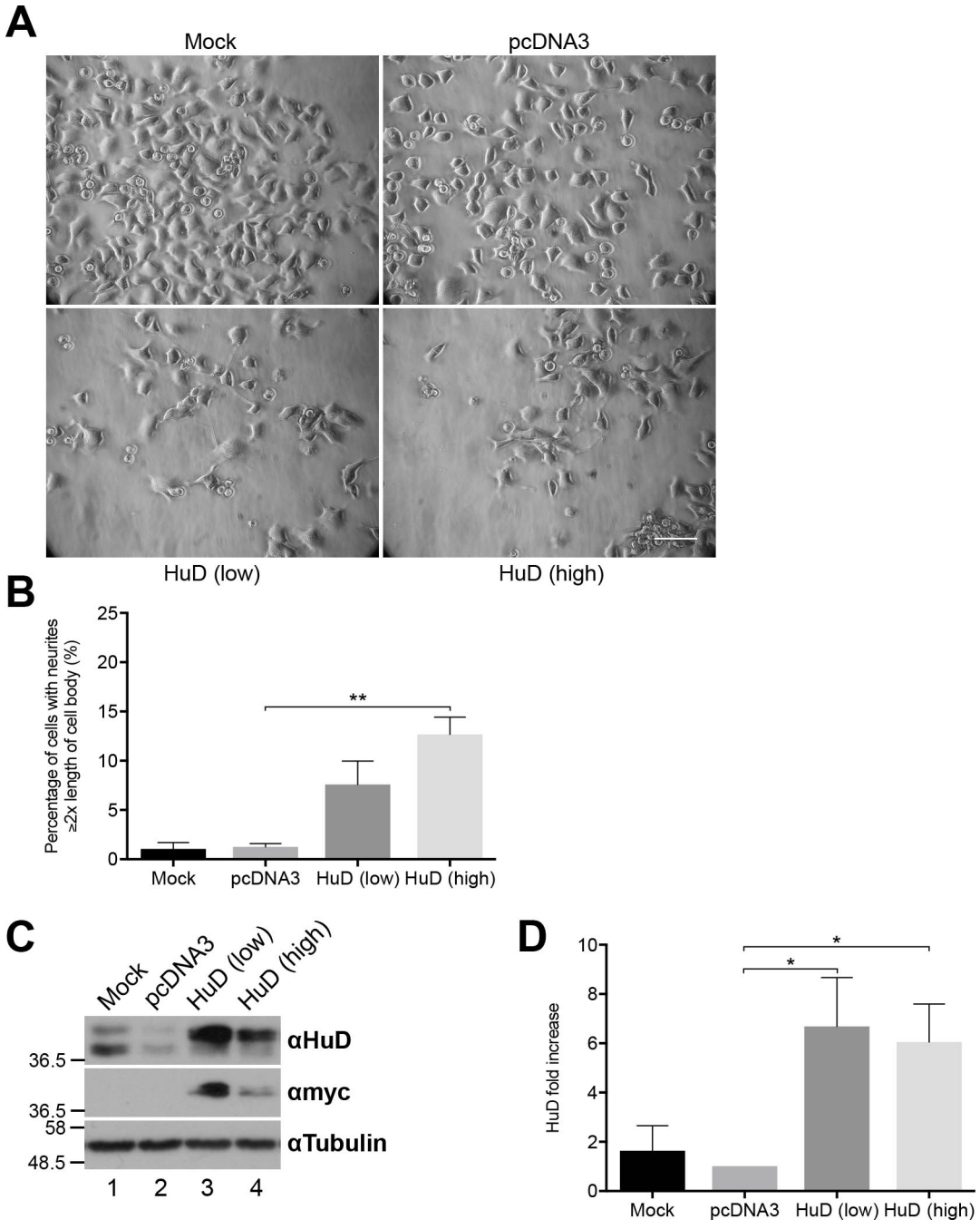

Figure 7. HuD overexpression in motor neuron-derived MN-1 cells induces differentiation and neurite extension. ***A***. Cells transfected with pcDNA3-myc-HuD exhibit a differentiated phenotype 48h post-transfection in comparison to control cells transfected with an empty vector. Scale bar: 100µm. ***B***. Bar graph shows the percentage of cells with neurites measuring at least twice the size of the cell body. ***C***. Cell extracts from empty vector (myc-pcDNA) or myc-HuD transfections were used for immunoblotting with either anti-HuD, anti-myc, or anti-tubulin antibodies. ***D***. Bar graph shows the fold increase in HuD protein levels normalized to tubulin and relative to pcDNA3. Data are mean ± SEM (n=3), two-tailed t-test **p<0.01.

The same experiment was repeated to assess whether longer exposure to low and high levels of HuD would result in the differentiation of an even larger proportion of the cell population. Seventy-two hours after transfection, cells overexpressing low and high amounts of HuD DNA presented significantly more neurites than cells transfected with the empty vector (**Figure 8A**,**B**). Again, there was a positive correlation between the amount of HuD DNA and the number of cells exhibiting a differentiated phenotype. HuD overexpression was confirmed by western blotting analysis (**Figure 8C**,**D**).

In a second step, MN-1 cells were treated with increasing concentrations of bryostatin for 48h and 72h. After a 48-hour treatment with low concentrations of bryostatin (0-5nM), most of the cells exhibited an undifferentiated phenotype (**Figure 9A**). Indeed, only about 1.5-2.5% of cells treated with 0.5, 1, 1,5, 2, or 5nM bryostatin harboured neurites at least twice the length of the cell body (**Figure 9B**). Although statistically significant at 5nM, this increase in the number of cells with neurites did not reflect neuronal differentiation and is likely not biologically meaningful. In comparison, these numbers were around 15% in cells overexpressing HuD at the same time point (**Figure 7A**,**B**). The same analyses were performed after 72h of treatment with the same low concentrations of bryostatin to determine if a larger proportion of the cells would show a differentiated phenotype (**Figure 10A**). On average, about 2-4% of the cells extended long neurites (**Figure 10B**), confirming that low concentrations of bryostatin only have a very modest impact on neuronal differentiation initiation in MN-1 cells.

Since there seemed to be a tendency for the number of cells with neurites to increase with the drug concentration, MN-1 cells were treated with higher concentrations of bryostatin for 48 (**Figure 11**) and 72h (**Figure 12**). Again, the number of differentiated

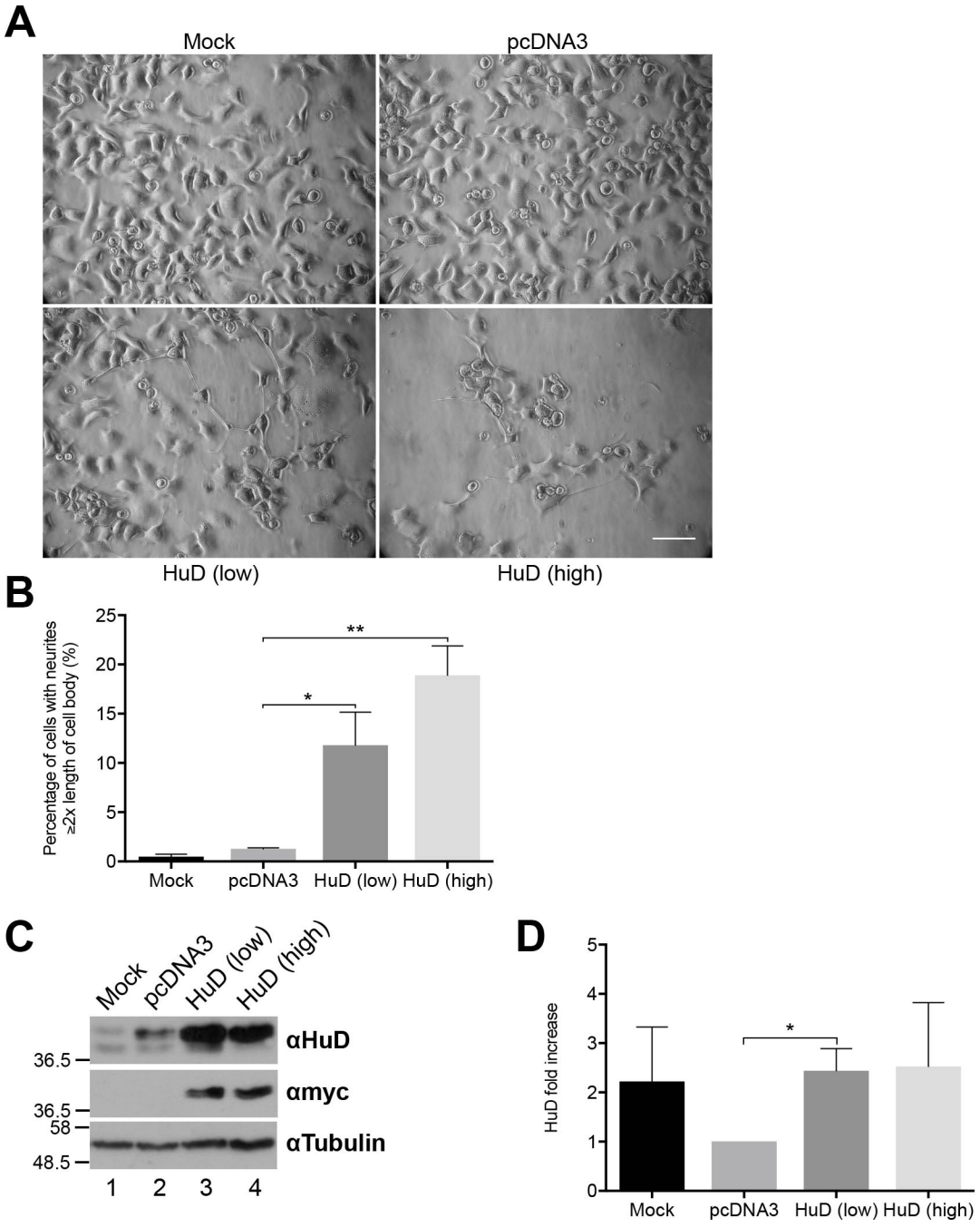

Figure 8. HuD overexpression in motor neuron-derived cells induces differentiation and neurite extension. ***A***. Cells transfected with pcDNA3-myc-HuD exhibit a differentiated phenotype 72h post-transfection in comparison to control cells transfected with an empty vector. Scale bar: 100µm. ***B***. Bar graph shows the percentage of cells with neurites measuring at least twice the size of the cell body. ***C***. Cell extracts from empty vector (myc-pcDNA) or myc-HuD transfections were used for immunoblotting with either anti-HuD, anti-myc, or anti-tubulin antibodies. ***D***. Bar graph shows the fold increase in HuD protein levels normalized to tubulin and relative to pcDNA3. Data are mean ± SEM (n=3), two-tailed t-test *p<0.05; **p<0.01.

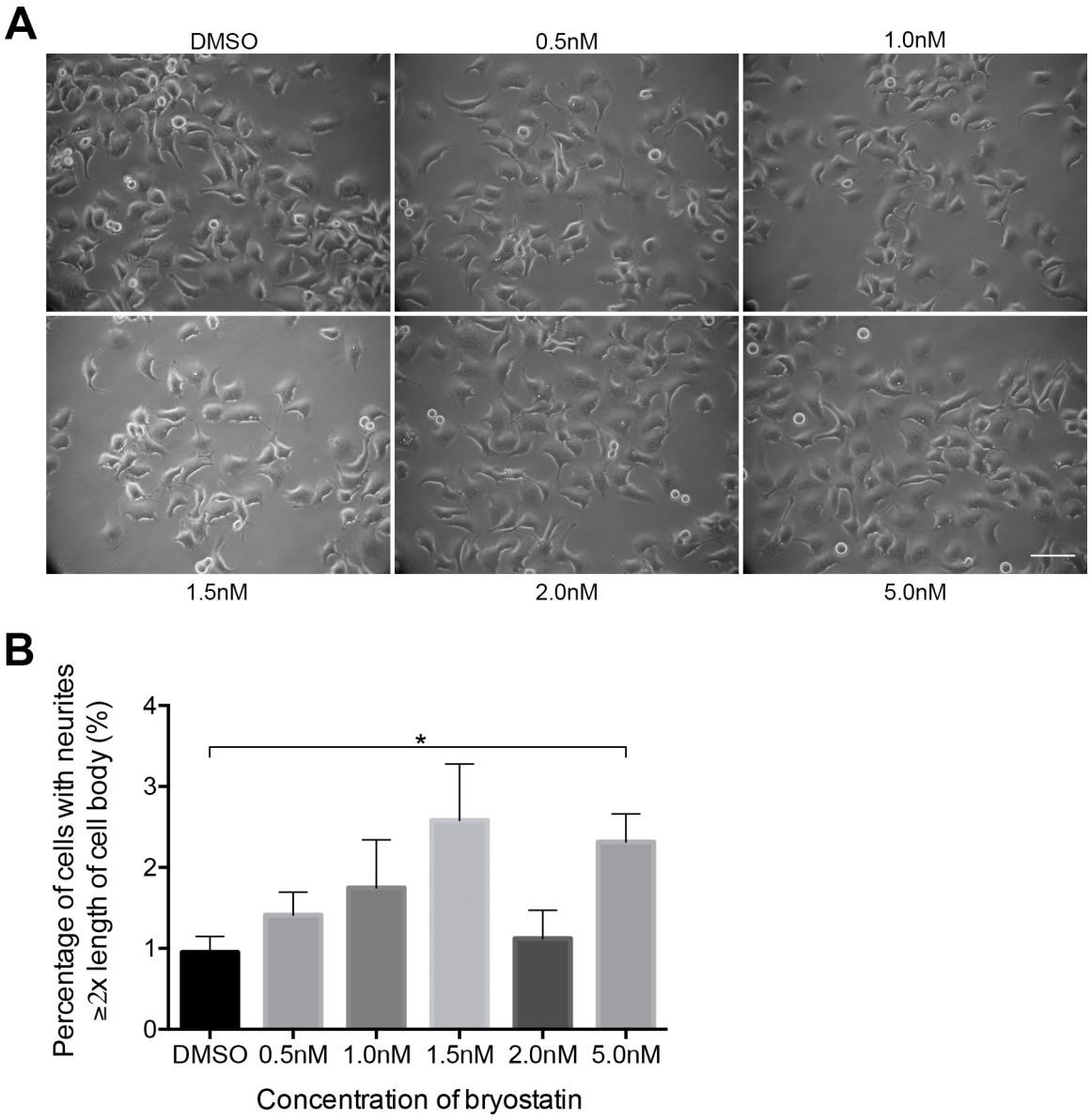

Figure 9. Bryostatin-1 treatment of motor neuron-derived cells has a limited very effect on neuronal differentiation initiation. ***A***. Cells treated with low concentrations of bryostatin for 48h remained mostly undifferentiated. Scale bar: 100µm. ***B***. Bar graph shows the percentage of cells with neurites measuring at least twice the size of the cell body ± SEM (n=4), two-tailed t-test *p<0.05.

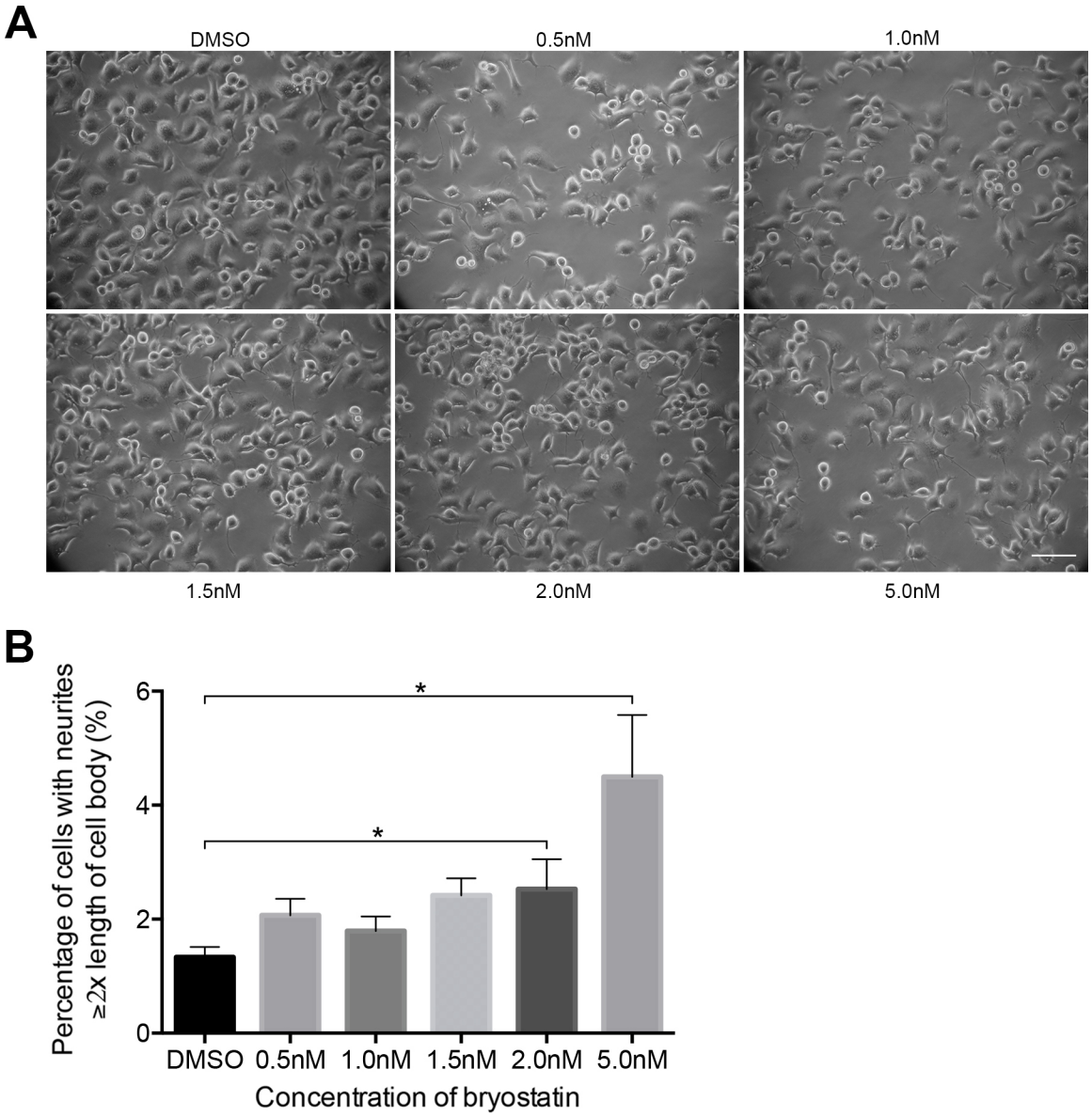

Figure 10. Bryostatin-1 treatment of motor neuron-derived cells has a limited impact on neuronal differentiation initiation. ***A***. Cells treated with low concentrations of bryostatin for 72h remained mostly undifferentiated. Scale bar: 100µm. ***B***. Bar graph shows the percentage of cells with neurites measuring at least twice the size of the cell body ± SEM (n=4), two-tailed t-test *$p<0.05$.

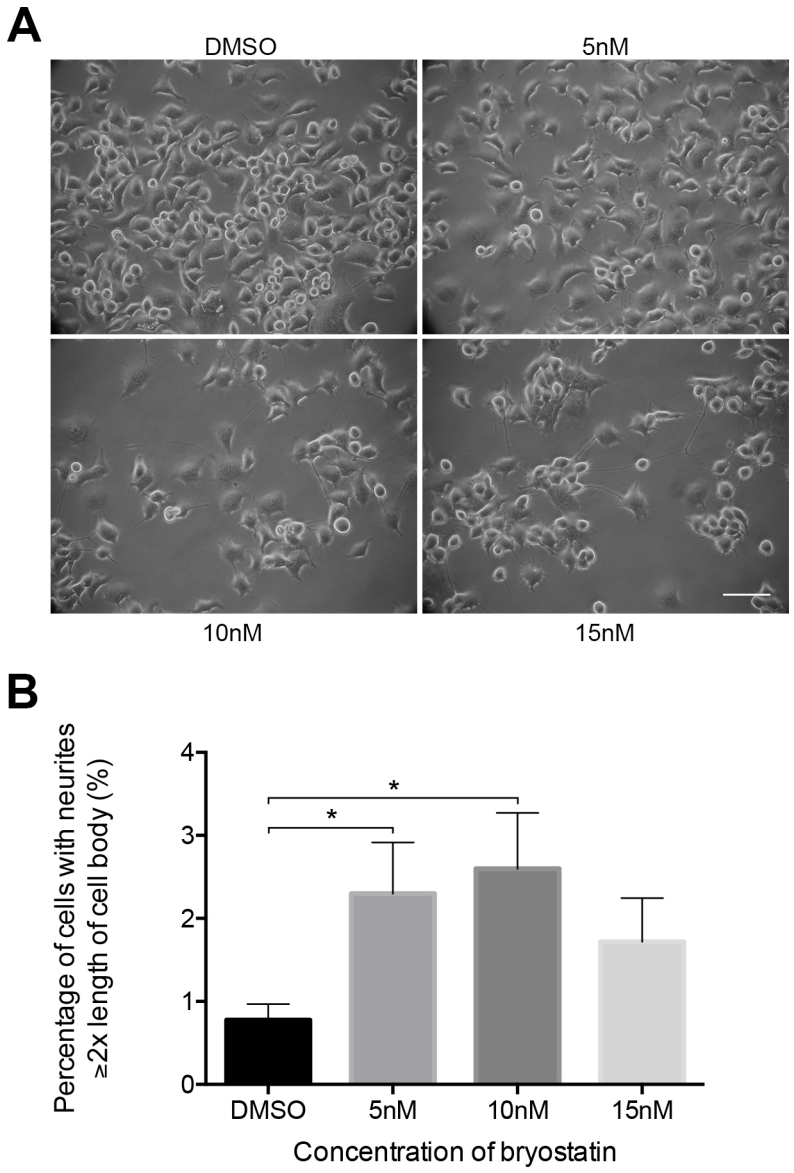

Figure 11. High concentrations of Bryostatin-1 have a very limited effect on neuronal differentiation induction in motor neuron-derived cells. ***A***. Cells treated with higher concentrations of bryostatin for 48h remained mostly undifferentiated. Scale bar: 100µm. ***B***. Bar graph shows the percentage of cells with neurites measuring at least twice the size of the cell body ± SEM (n=5), two-tailed t-test *$p<0.05$.

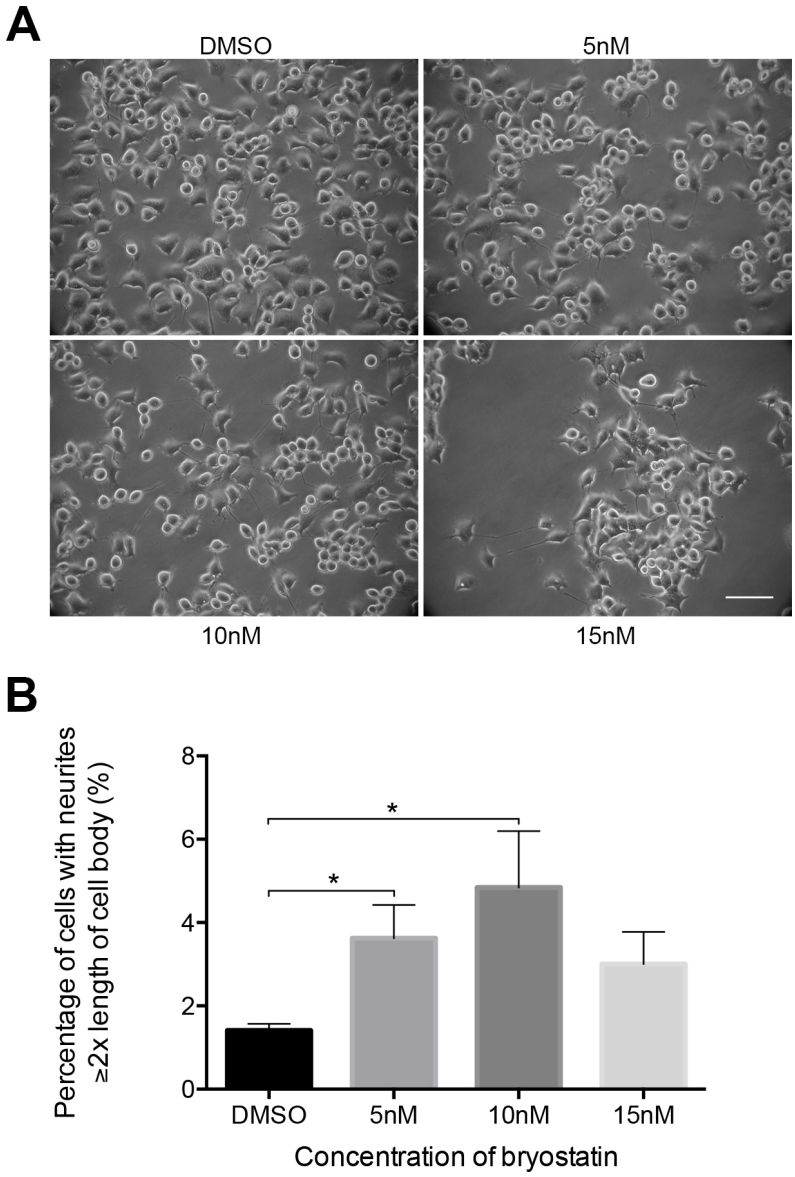

Figure 12. Prolonged exposure of motor neuron-derived MN-1 cells to high concentrations of Bryostatin-1 results in poor neuronal differentiation initiation. ***A***. Cells treated with higher concentrations of bryostatin for 72h remained mostly undifferentiated. Scale bar: 100µm. ***B***. Bar graph shows the percentage of cells with neurites measuring at least twice the size of the cell body ± SEM (n=4), two-tailed t-test *p<0.05.

cells following treatment with 5, 10, and 15nM bryostatin did not compare to the results obtained by HuD overexpression at the same time points. Even higher concentrations of the pharmacological agent were tested (up to 25nM), but it only caused the cells to form aggregates and die (results not shown). These results indicate that prolonged exposure to the range of bryostatin concentrations tested here does not induce neuronal differentiation in MN-1 cells to the same extent as HuD overexpression.

Finally, to gain more insight on the effect of bryostatin on cell proliferation/differentiation, MN-1 cells were treated with a broad range of bryostatin concentrations and placed in an IncuCyte device for 72h. The IncuCyte is a live-cell analysis system that acquires images and information that can be used to assess cell death, invasion, migration, and differentiation among other applications. Here, pictures were taken every 2 hours to accurately (and objectively) track neurite outgrowth over a period of 72h. More specifically, two sets of metrics were analyzed: cell body clusters and neurite length. Cell body cluster area is an estimation of the number of cell bodies in an image and is thus a readout for cell proliferation. Cells treated with 1, 10, 100, and 1000pM followed the same curve as mock treated cells (**Figure 13A**). Although this is only one replicate, there seemed to be a small dose-dependent effect since there was a visible difference in the area covered between DMSO and 1000pM bryostatin treated cells after 72h. Neurite length, i.e. the sum of all neurites extending from cell bodies in an image was plotted. It increased over the first 24h and remained relatively stable at 48 and 72h (**Figure 13B**). However, an increase in neurite length does not necessarily represent an increase in neurite outgrowth since the number of cell bodies is not taken into consideration. Therefore, a more accurate measure of cell differentiation is the ratio of

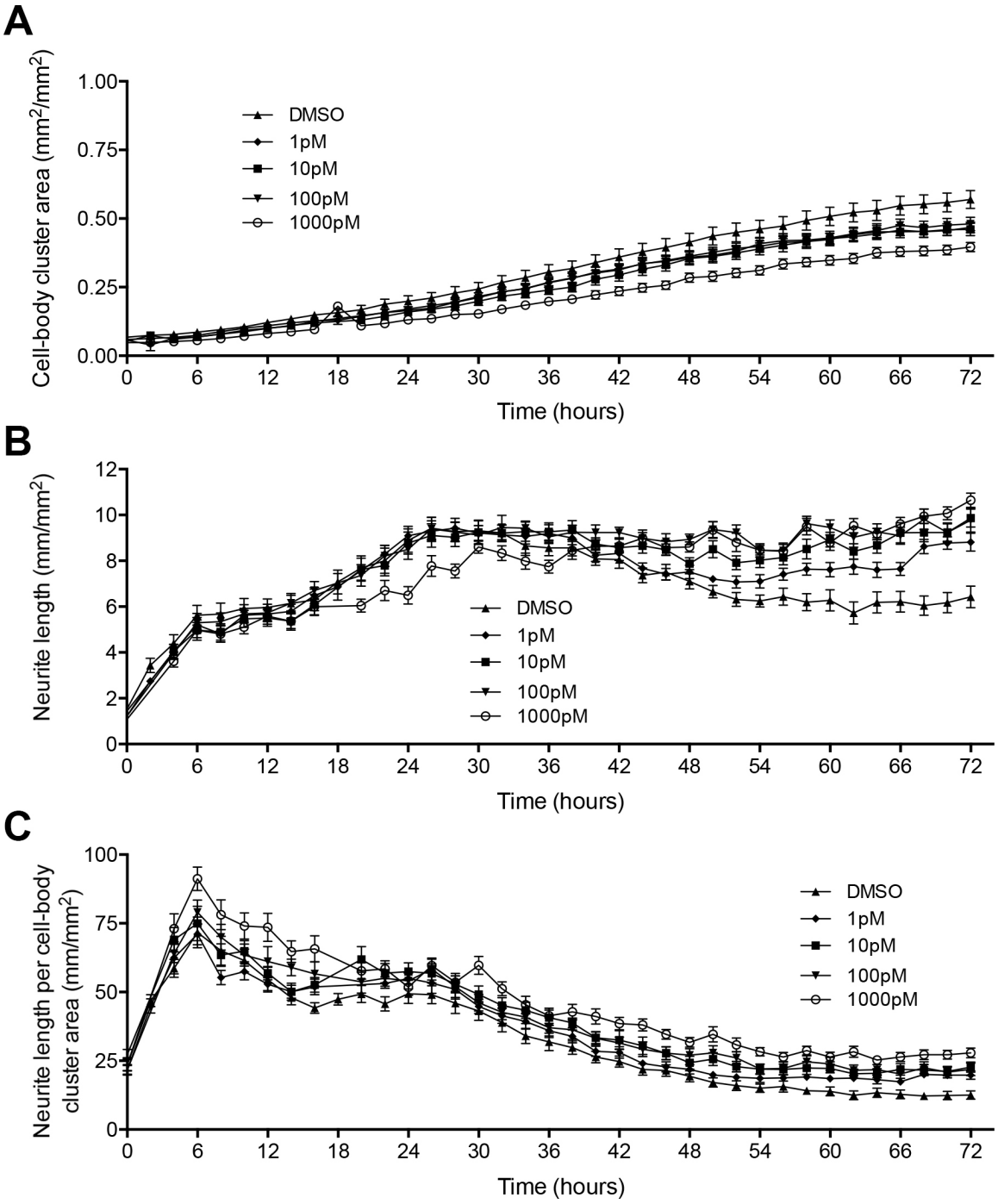

Figure 13. Effect of a 72-hr bryostatin treatment on motor neuron-derived MN-1 cell morphology. ***A***. Cell-body cluster area increases steadily over time for all conditions. Scale bar: 100µm. ***B***. Neurite length increases over the first 24 hours and stays relatively stable afterward. ***C***. Neurite length per cell-body cluster area increases rapidly in the first 6 hours but then decreases slowly over the next 3 days. ***D***. Morphology of MN-1 cells treated with either DMSO (mock) or 1000pM (1nM) bryostatin does not change over the 72-hour treatment. Data are mean ± SEM (16 pictures per condition per time point; n=1).

D

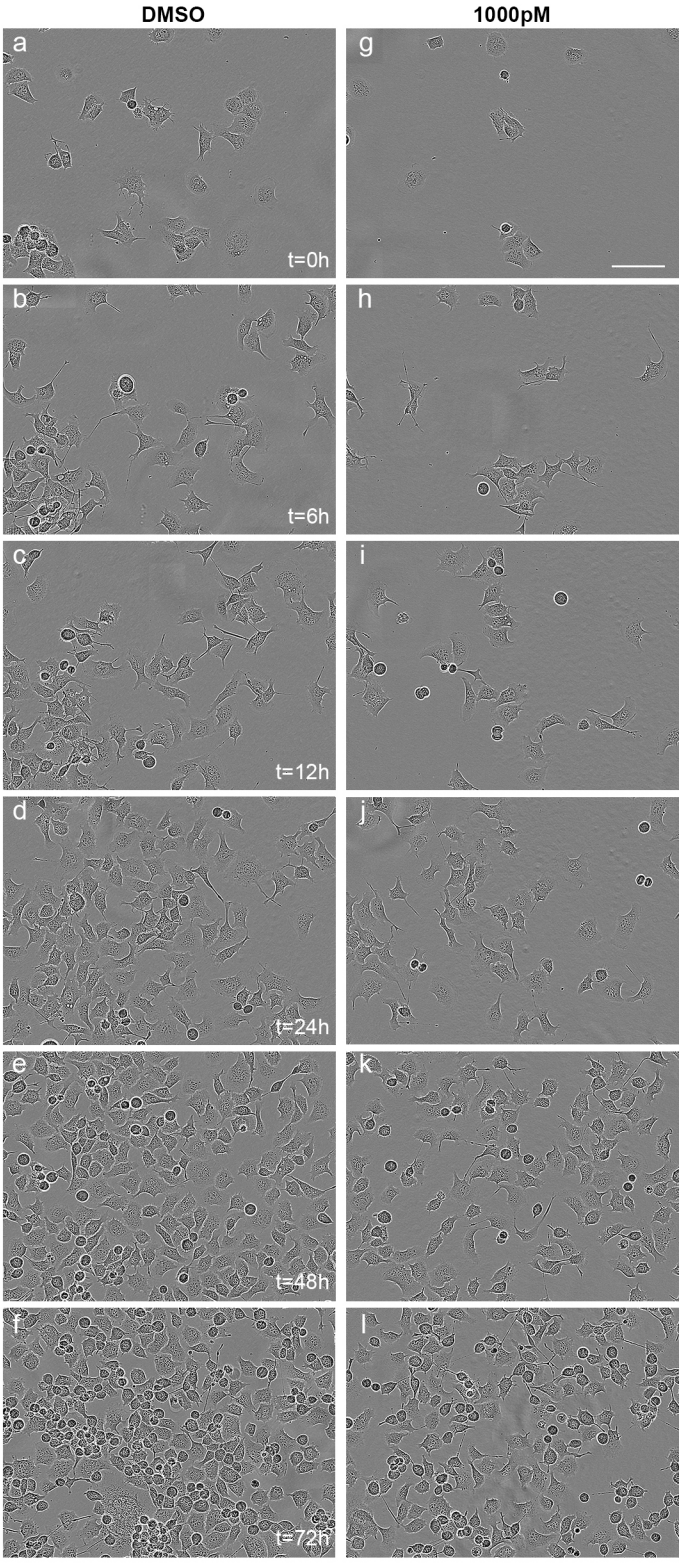

Figure 13. Continued

neurite length per cell body cluster area. Neurite length per cell body cluster area metric analysis revealed a small peak at 6h but a slow decrease thereafter, confirming that cell differentiation was not induced after 24, 48, or 72h for all bryostatin concentrations tested (**Figure 13C**). The slightly slower growth of cells treated with 1000pM (1nM) bryostatin can be visually assessed by looking at pictures of the two conditions side by side (**Figure 13D**). At each time point, there were fewer cells in the bryostatin-treated wells than in the control condition. Overall, these data show that only minimal morphological changes could be documented in MN-1 cells treated with a wide range of bryostatin concentrations for 72h.

3.2 Establishment of an scAAV9 viral expression system

3.2.1 Generation of scAAV-HuD-flag and scAAV-mGFP vectors

3.2.1.1 Generation of the scAAV-HuD-flag vector

Our lab had previously shown that overexpressing HuD rescues SMA-like neuronal defects in a cell culture model of SMA (Hubers et al., 2011). One objective of this project was to determine whether upregulation of HuD in SMA motor neurons can also have positive effects *in vivo*. The first step in this process was to subclone HuD from the pAAV-HuD-FH plasmid into the self-complementary adeno-associated vector (scAAV) using Gibson Assembly® (**Figure 14**). This method is based on homologous recombination between multiple DNA fragments (Gibson et al., 2009). The scAAV-cba-SMN vector (abbreviated to scAAV-SMN) – which is used as a control throughout the whole project – was used as backbone. It was cut open with AgeI and HindIII restriction enzymes (**Figure 14A**). A flag-tagged HuD was amplified from the pAAV-HuD-flag

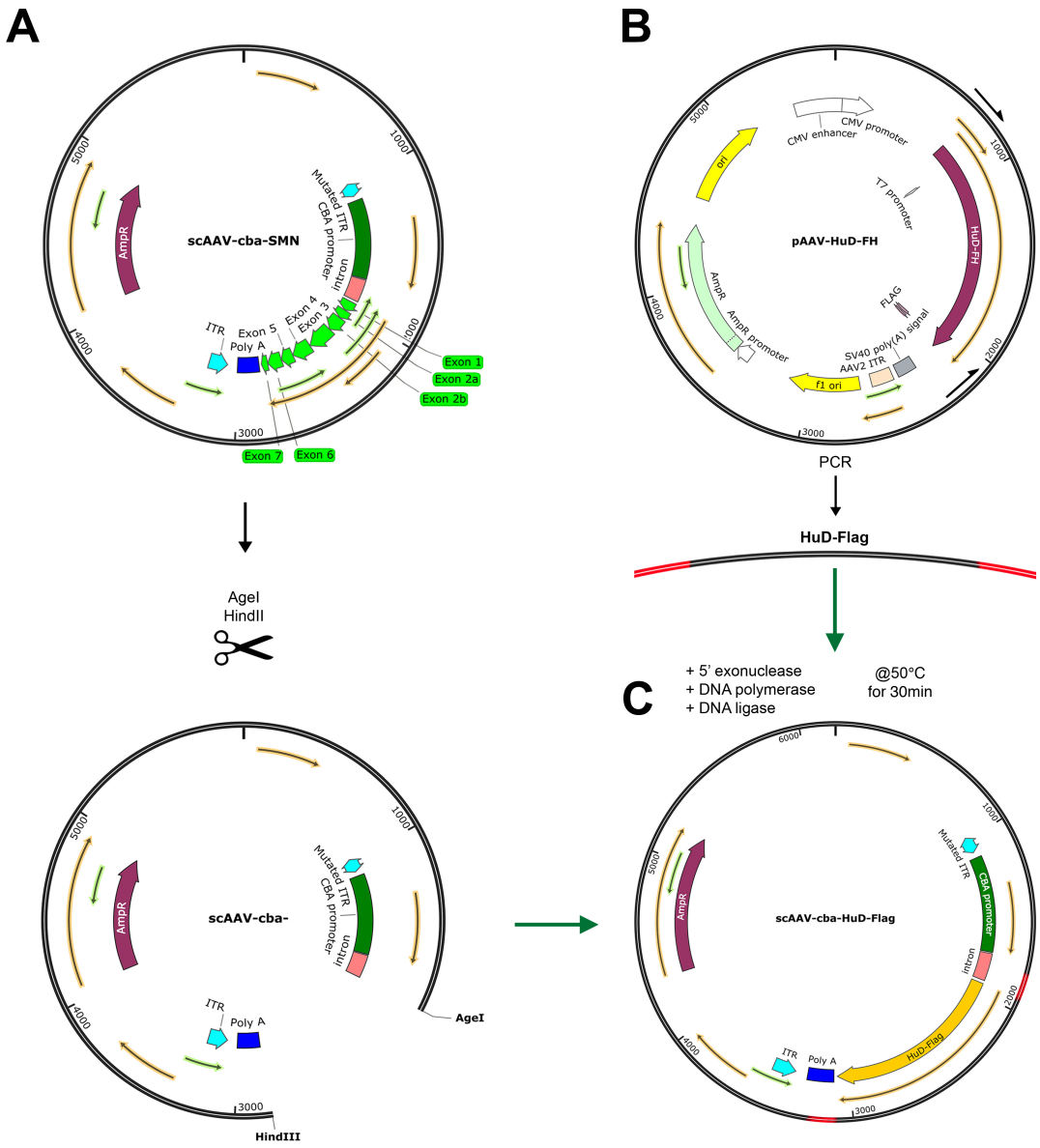

Figure 14. HuD subcloning into the scAAV vector. ***A***. The scAAV-cba-SMN vector is digested open with AgeI and HindIII restriction enzymes. ***B***. In parallel, a PCR is run on the pAAV-HuD-FH vector using Gibson primers, indicated by black arrows. The amplified PCR product has 20-nt overlaps (in red) that are identical to the open ends of the open scAAV-cba vector. ***C***. The DNA fragments are joined through homologous recombination in a single isothermal reaction at 50°C.

vector using Gibson primers designed with the help of the NEBuilder® Assembly tool available on the New England BioLabs Inc. website. These primers generate a PCR fragment with 20-nucleotide overlaps at both ends that are identical to the ends of the linearized vector (**Figure 14B**). The backbone and the insert were then incubated with a mix of three enzymes to ligate the DNA fragments together (**Figure 14C**). In this single isothermal reaction, an exonuclease chews back from the 5' end to create 3' overhangs thus allowing complementary DNA fragments to anneal to each other. Then, a DNA polymerase fills in the gaps with the corresponding nucleotides. Finally, a DNA ligase covalently joins the DNA fragments. Before using the newly synthesized scAAV-cba-HuD-flag (abbreviated to scAAV-HuD) vector *in vitro* or *in vivo*, its integrity was verified. Sequencing revealed that the HuD ORF in the pAAV-HuD-FH vector ordered from Vigene Biosciences was actually a clone (BC036071) of transcript variant 2 (NM_001144774.2) containing 4 single nucleotide mutations (**Figure 15A**). Two of them, at positions 497 and 1024, were missense mutation and could have had detrimental effects, whereas the other two were silent and thus did not change the amino acid sequence. Using site-directed mutagenesis and the QuickChange® primer design tool from Agilent Technologies, the two missense mutations were corrected back to wild-type to ensure that they did not affect HuD's function. Then, before sending the vector for virus production, expression of the scAAV-HuD vector was tested MN-1 cells. Forty-eight hours after transfection, proteins were collected and both HuD and the flag tag were successfully detected by western blotting (**Figure 15B**), confirming once again the integrity of the sequence and giving us assurance that the protein can be expressed in mammalian cells.

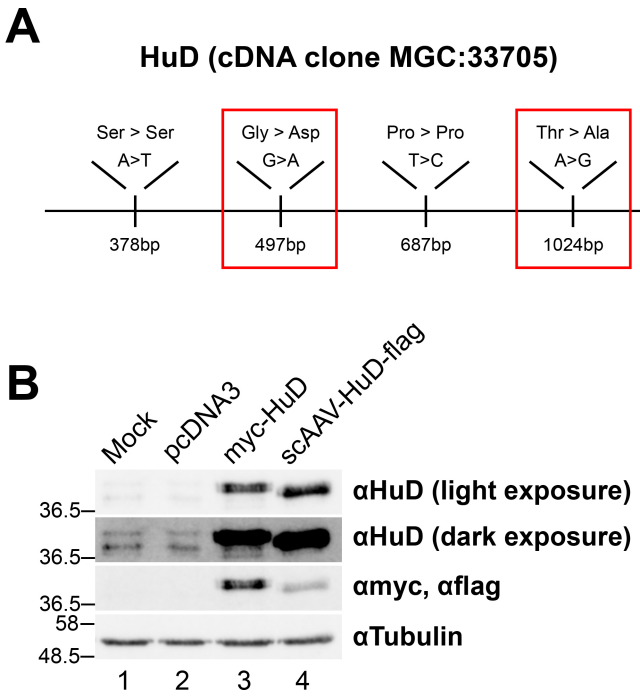

Figure 15. Correction of SNPs and confirmation of scAAV-HuD expression in motor neuron-derived MN-1 cells. ***A***. Sequencing revealed that the HuD ORF in pAAV-HuD-FH was actually a clone of transcript variant 2 (NM_001144774.2) containing 4 single nucleotide mutations (BC036071). ***B***. After correcting the 2 missense mutations back to wild-type, the vector was overexpressed in MN-1 cells. Both HuD and the flag tag (lane 4) are detectable by immunoblotting.

3.2.1.2 Generation of the scAAV-mGFP vector

Similar to HuD, mGFP was subcloned into the scAAV backbone by Gibson Assembly® (**Figure 16**). mGFP was first amplified by PCR from the pLenti-C-mGFP-PRMT7 vector using Gibson primers designed using the NEBuilder® Assembly tool (**Figure 16B**). It was then ligated into the open backbone (**Figure 16C**), amplified, and purified. It was sent along with the HuD vector to be sequence-verified by Genome Quebec (not shown) before being used in cell culture or *in vivo*.

3.2.2 Overexpression of scAAV-HuD-flag and scAAV-mGFP vectors in MN-1 cells

As mentioned above, our lab had previously shown that overexpressing HuD in SMN knockdown cells rescues the neurite extension delay/defect associated with the pathology. Hence, a rescue experiment was performed in shSMN MN-1 cells to validate that the new scAAV-HuD plasmid can rescue SMA-like neuronal defects. pGIPZ scramble and shSMN MN-1 cells were transfected with either scAAV-mGFP or scAAV-HuD. Surprisingly, cell morphology remained mostly unchanged in both undifferentiated pGIPZ and shSMN cell lines transfected with scAAV-HuD (**Figure 17A**, top 6 panels). Neurite analysis revealed that only about 3-4% of pGIPZ and shSMN cells presented neurites measuring at least twice the length of the cell body 32h after transfection (**Figure 17B**). In contrast, 13-17% of pGIPZ and 7-11% of shSMN transfected cells treated with retinoic acid (RA) and GDNF for 24h extended long neurites (**Figure 17A**, bottom 6 panels and **B**). Statistical analysis confirmed that RA+GDNF treatment induced differentiation, which as expected was less efficient in shSMN cells, but that expression of HuD did not seem to have any statistically significant effects on the process.

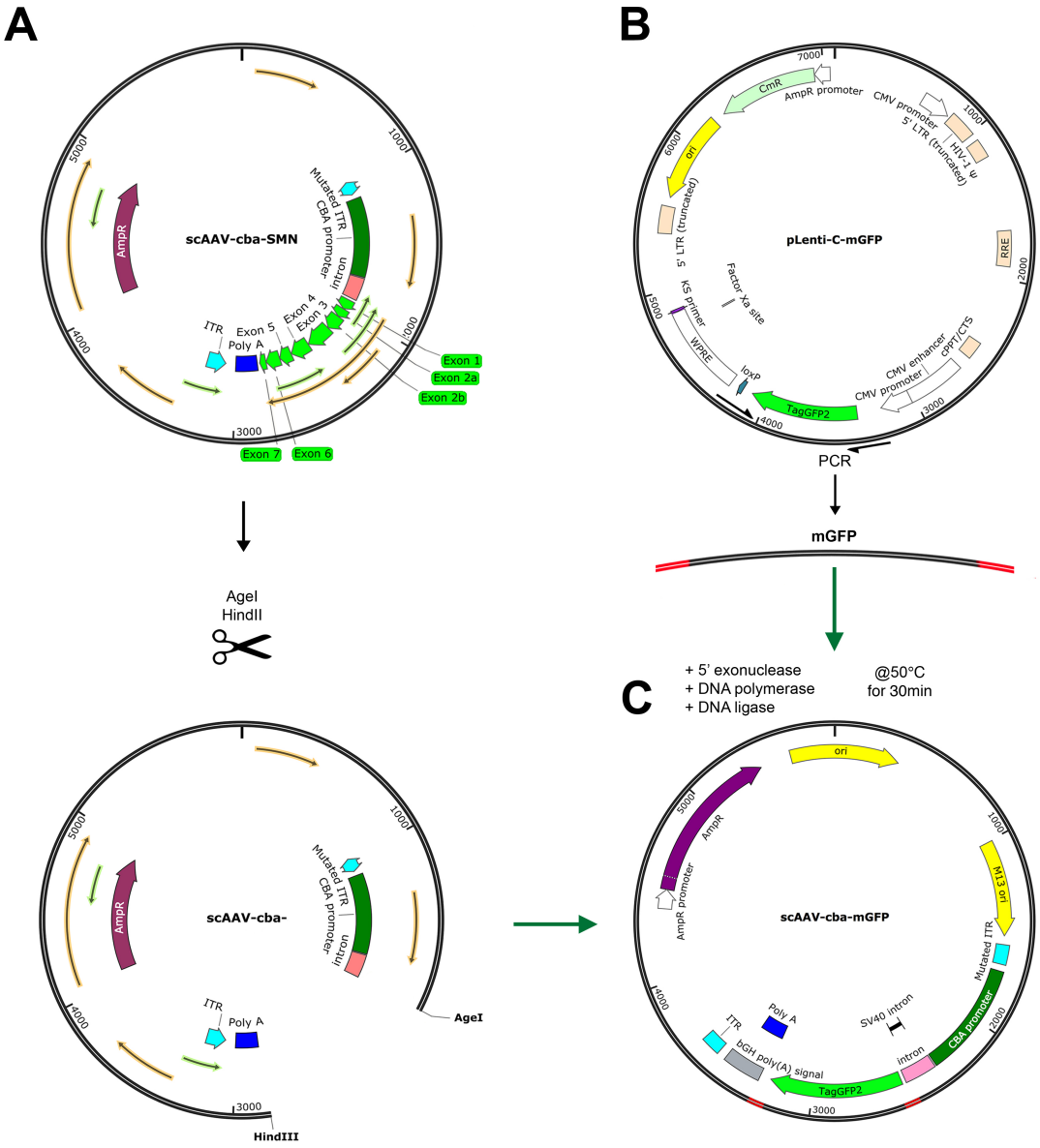

Figure 16. mGFP subcloning into the scAAV vector. ***A***. The same scAAV-cba-SMN vector is digested with AgeI and HindIII enzymes. ***B***. Similar to HuD subcloning, a PCR is run on the pLenti-C-mGFP vector using Gibson primers, indicated by black arrows. The PCR product has 20-nt overlaps identical to the open ends of the linearized vector. ***C***. The fragments are joined through homologous recombination to generate scAAV-cba-mGFP.

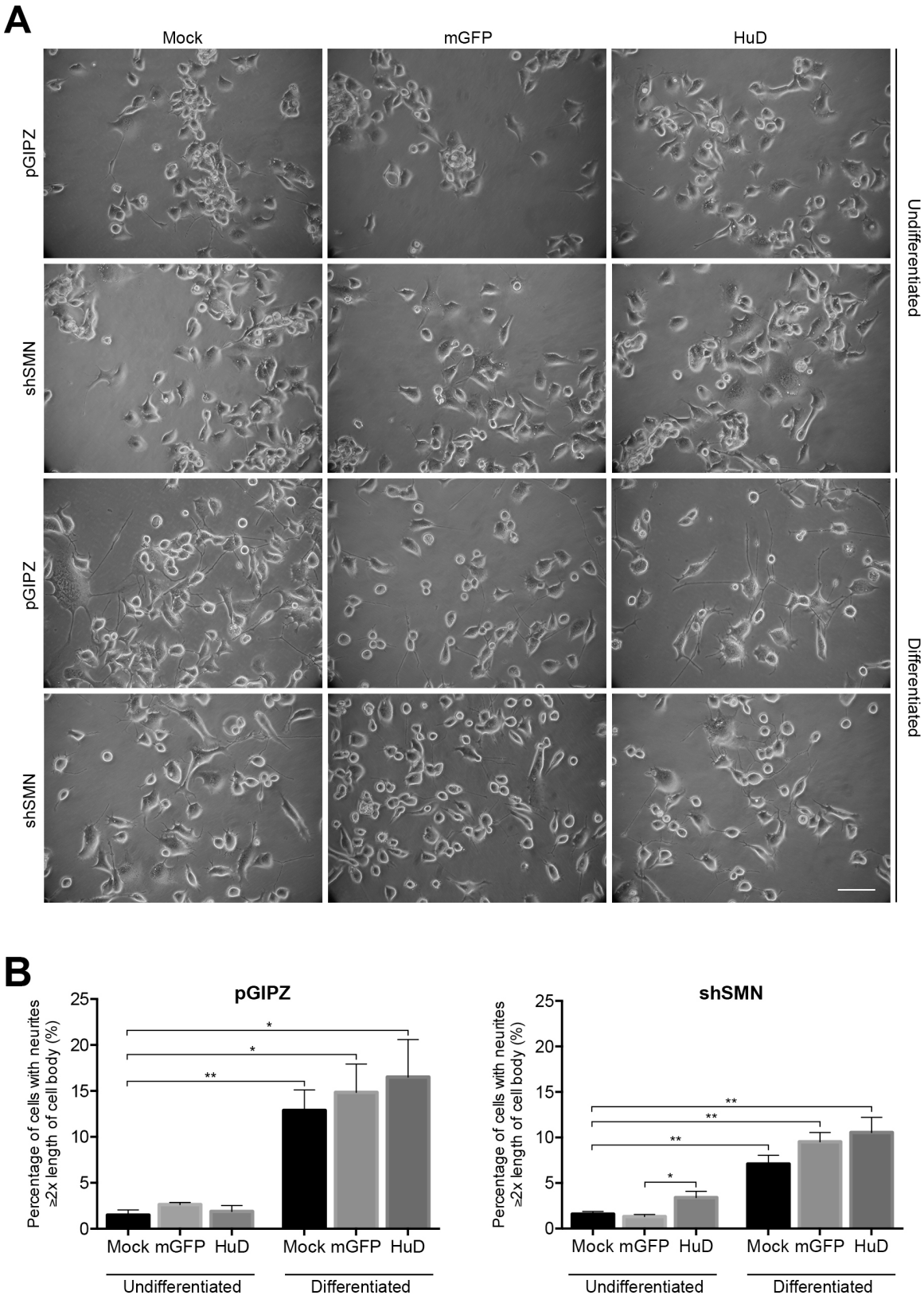
A
Mock
mGFP
HuD
pGIPZ
shSMN
pGIPZ
shSMN
Undifferentiated
Differentiated
B
pGIPZ
shSMN
Percentage of cells with neurites ≥2x length of cell body (%)
0
5
10
15
20
25
*
*
**
**
**
**
*
Mock mGFP HuD
Mock mGFP HuD
Undifferentiated
Differentiated

Figure 17.

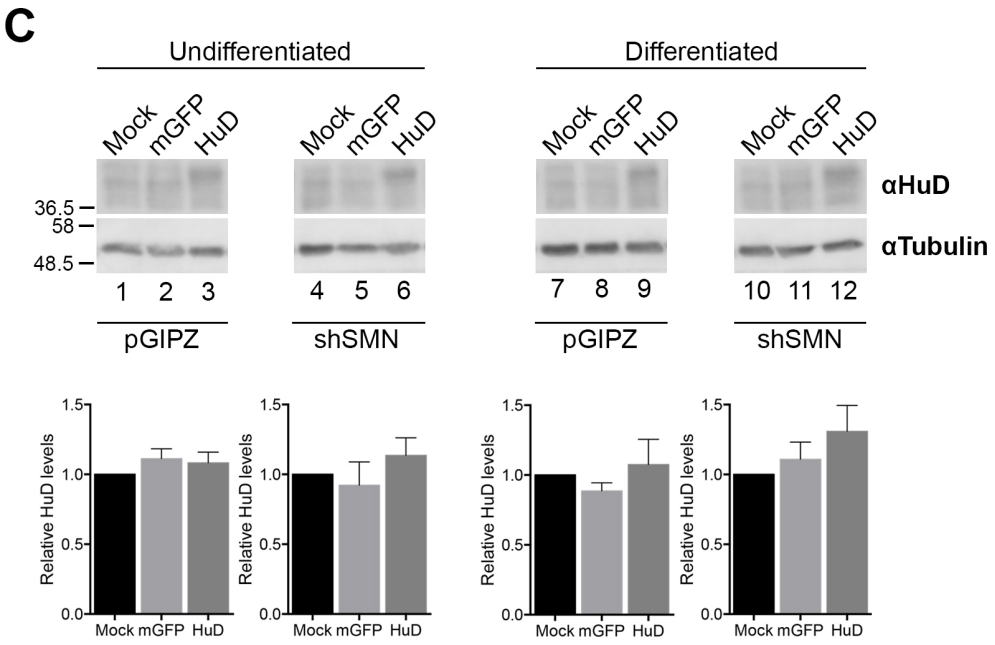

Figure 17. mGFP and HuD overexpression in pGIPZ and shSMN motor neuron-derived MN-1 cells. ***A***. pGIPZ cells treated with RA and GDNF showed a differentiated phenotype after 24h. HuD overexpression failed to induce neurite extension in pGIPZ and shSMN MN-1 cells after 24h. Scale bar: 100µm. ***B***. Bar graph indicates the percentage of cells with neurites measuring at least twice the length of the cell body ± SEM (n=3), two-tailed t-test *p<0.05; **p<0.01. ***C***. Cell extracts from mock-, mGFP-, and HuD-transfected pGIPZ undifferentiated (lanes 1-3), shSMN undifferentiated (lanes 4-6), pGIPZ differentiated (lanes 7-9), and shSMN differentiated (lanes 10-12) cells were used for immunoblotting with anti-HuD and anti-tubulin antibodies. Bar graphs show the corresponding fold increase in HuD protein levels normalized to tubulin and relative to mock. Data are mean ± SEM (n=3).

HuD protein levels were assessed by western blotting to determine whether transfection was successful (**Figure 17C**, top panels). Densitometry analysis of the blots did not reveal a significant increase in HuD levels in HuD-transfected conditions (**Figure 17C**, graphs). These experiments will need to be repeated to confirm HuD overexpression.

3.2.3 SMN overexpression in the delta7 mouse model

In order to evaluate and compare HuD's effect *in vivo*, it was first necessary to establish a baseline using an already validated dose of scAAV9-SMN (Glascock et al., 2012b). Thus, eleven SMA pups received $2x10^{10}$vg of scAAV9-SMN systemically via facial injection at postnatal day (P1). Eleven wild-type (WT) littermates received an equal volume of saline as control. The mice were followed until endpoint and motor functions were tested every other day starting on P2. It should be noted that all data past P28 is only n=1 for both WT and SMA mice. Data is not available yet for untreated, mGFP-, and HuD-injected SMA pups.

3.2.3.1 Survival and body mass

The first phase of our study focused on the effect of overexpressing SMN in SMA pups on their survival and weight gain. The majority of SMA pups injected with scAAV9-SMN survived past the expected 13-14 days for untreated SMA pups (Le et al., 2005). Kaplan-Meier plot revealed that SMN-injected pups had a median survival of 21 days (**Figure 18A**). Only one mouse lived past 40 days. In comparison, IV treated SMA mice from the 2012 study by the Lorson laboratory had a median survival of 34 days, with 2 mice (out of 6) living past 200 days (Glascock et al., 2012b).

Body mass was recorded daily at the beginning of each session (**Figure 18B**). Wild-type pups gained weight regularly, sometimes more than a gram per day. In comparison, scAAV9-SMN-injected SMA pups gained a lot less weight and their body mass peaked at P11. The weight difference between WT and SMN-injected SMA pups was statistically significant as early as P3 (**Figure 18B**, inset).

3.2.3.2 Behavioural phenotyping in the delta7 mouse model

To evaluate the benefits of the treatment on the SMA phenotype, select functional tests were performed from P2 to endpoint. The objective here was to establish these tests in our laboratory and acquire experience at administering the functional tests to get an accurate and consistent readout throughout the next phases of the study. First, the righting reflex test measures the time needed by a mouse to return unto its four paws after being place on its back. It evaluates general body strength and the maximum time allowed in this study was 60 seconds. At first, scAAV9-SMN-treated SMA pups had difficulty right themselves up whereas control littermates improved quickly over the first few days and were able to get their four paws flat on the table almost instantly at P8 (**Figure 18C**).

Starting on P14, mice were subjected to the pen test. It evaluates motor balance and coordination to assess how these functions are impaired in SMA models and/or ameliorated following treatment. In this test, mice were lowered onto a 1cm wide pen held 20cm above a table and time spent balancing was recorded. In the beginning, SMN-injected SMA pups were often too weak to stay balanced more than a few seconds. They did show improvement, but never reached the maximum of 60s allowed per repetition. In comparison, WT mice quickly learned to balance on the pen and eventually reached the

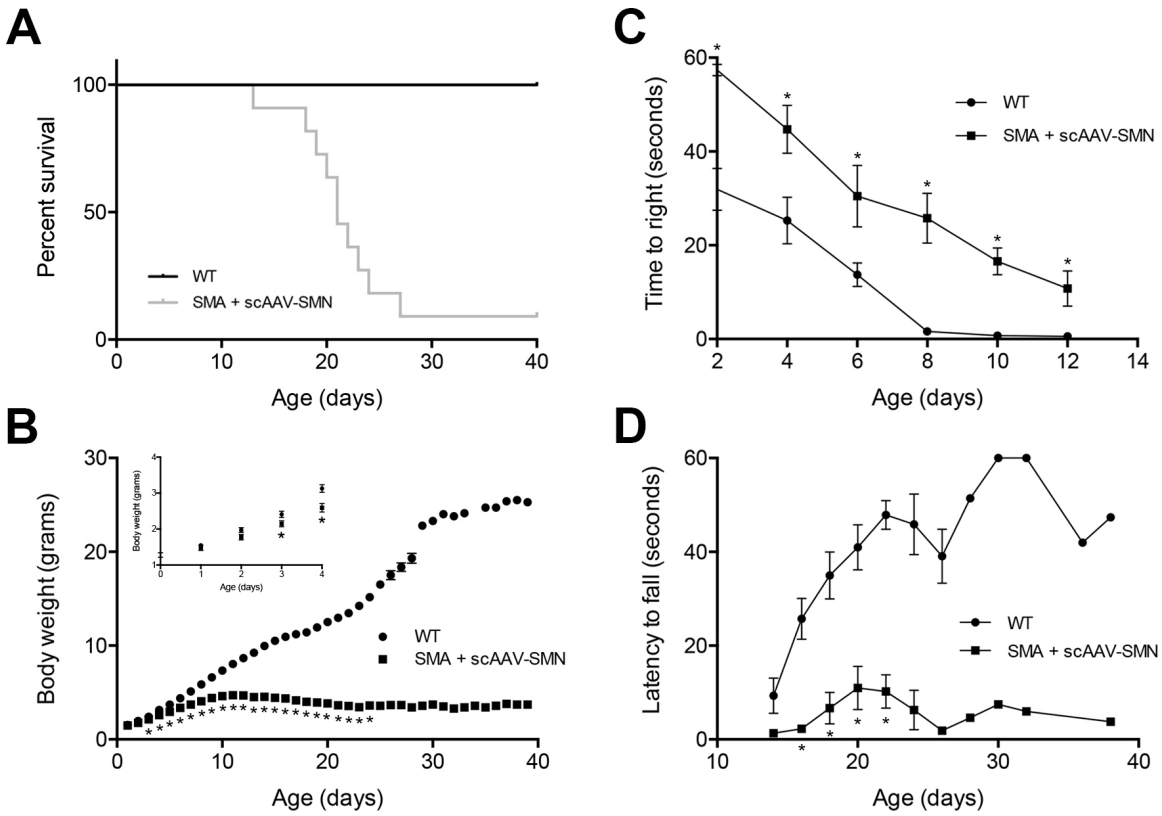

Figure 18. Phenotypic assessment of SMA mice treated with scAAV-SMN. ***A***. Kaplan-Meier survival curve of scAAV-SMN-injected SMA pups and WT controls. ***B***. Daily weights were measured starting from day of birth (P0). Weight difference between SMN-injected SMA pups and WT was statistically significant as early as P3 (inset). ***C***. Time to right was evaluated every other day starting at P2. ***D***. Motor balance and coordination were evaluated every other day starting at P14 using the pen test. Data are mean ± SEM (wild-type: n=11; SMA: n=11), two-tailed t-test *p<0.05.

time limit (**Figure 18D**). It should be noted that not enough data was collected past P22 to perform statistical analysis.

Finally, the hind-limb suspension test (also known as tube test) was used to evaluate muscle strength, weakness, and fatigue in proximal hind-limb muscle. In this test, pups are suspended head first over the rim of a 50mL Falcon tube. The test consists of two consecutive trials and is designed to capture fatigue. Three parameters were evaluated: latency to fall, the number of pulls, and the hind-limb score (HLS), a score based on the distance between the hind paws and the positioning of the tail. Until P8, SMN-injected SMA pups performed similarly to WT littermates in terms of latency to fall (**Figure 19A**). From P10 onward, SMA pups spent significantly less time hanging of the rim of the tube than control pups. They also attempted to pull themselves fewer times (**Figure 19B**). Lastly, SMA pups scored lower than WT pups on the HLS from P4 onward and their score worsened with disease progression (**Figure 19C**). Overall, it is impossible to fully interpret these behavioural phenotyping findings in the absence of data for uninjected and/or mGFP-injected pups on these tests. Together, these *in vivo* data helped establish a routine protocol for the administration of functional tests to evaluate the extent of the rescue achieved following the injection of scAAV-HuD in delta7 mice.

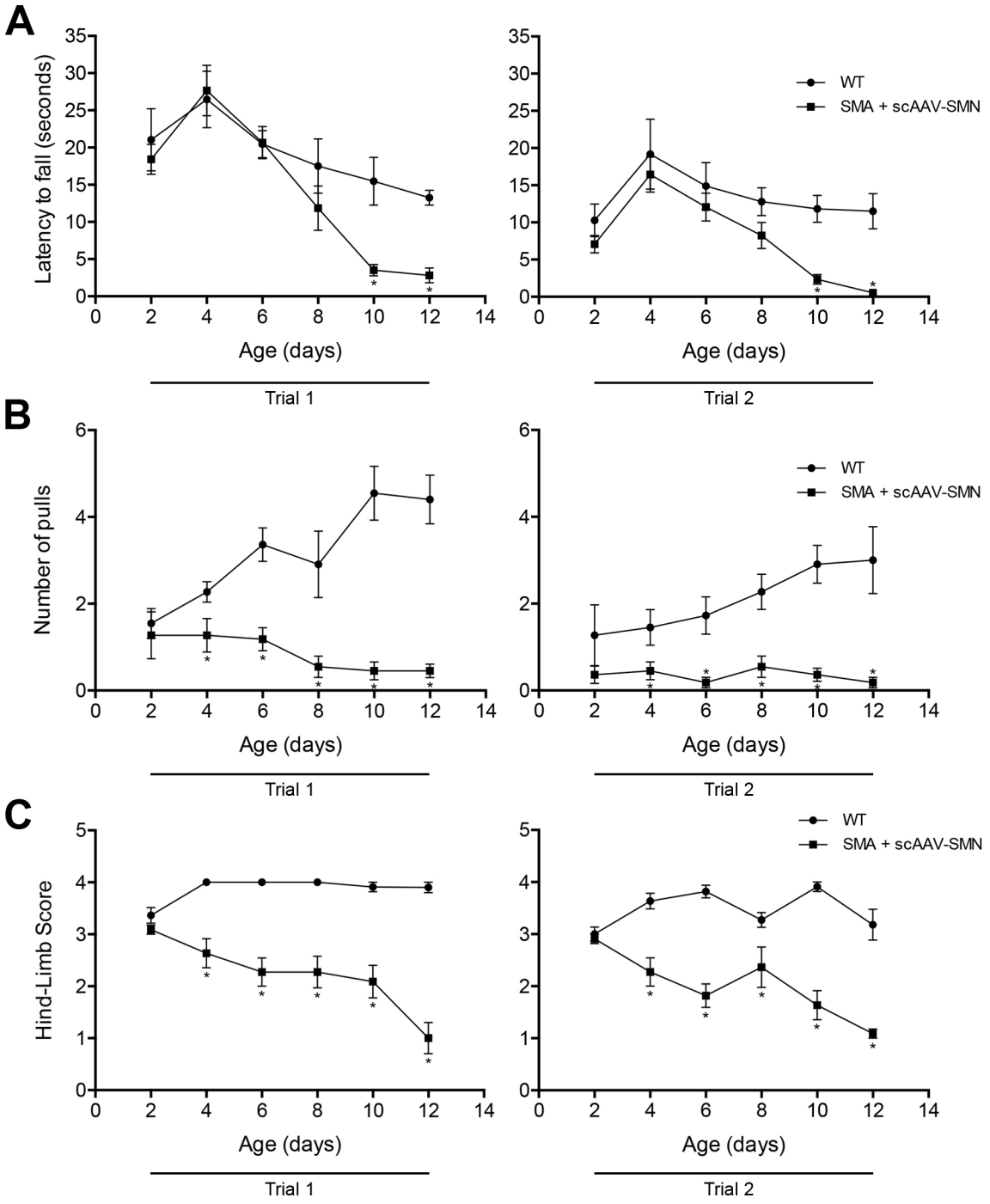

Figure 19. Proximal hind-limb muscle strength and fatigue assessment in delta7 pups treated with scAAV-SMN. ***A***. Time spent hanging was significantly shorter for SMA pups starting at P10 compared to control pups in both trials. ***B***. Number of pulls for WT pups increases over time whereas SMA pups fail to improve. The difference is statistically significant starting at P4. ***C***. Hind-limb suspension (HLS) score is lower in SMA mice starting at P4 and worsens with time. See Treat-NMD SOP #SMA_M.2.2.001 for details (El-Khodor, 2011). Data are mean ± SEM (wild-type: n=11; SMA: n=11), two-tailed t-test *p<0.05.

Chapter 4. Discussion

4.1 Summary

In this study, existence of a PKCα-HuD-mRNA target pathway was investigated in motor neuron-derived MN-1 cells. The data presented here suggest that PKC signaling is present in MN-1 cells and can be modulated by the activator bryostatin. Indeed, bryostatin-induced PKC activity increased HuD's expression level and modulated HuD's binding to selective mRNA targets. Bryostatin treatment in MN-1 cells also led to the activation of Erk and inhibition of Akt kinases, confirming that the drug is active in motor neuron-like cells and that it can be used to modulate PKC signaling.

The second objective of this study was to establish an scAAV9 viral expression system to evaluate the benefits of HuD overexpression *in vivo*. A flag-tagged HuD was successfully inserted in the scAAV vector and its expression was tested in MN-1 cells. Although data collection for its *in vivo* effects is very preliminary, a good baseline was established using scAAV-SMN. While injection of a low dose did not provide a complete rescue, it still improved survival and weight gain. Moreover, a protocol was established for the administration of functional tests to accurately evaluate and quantify the extent of the rescue achieved following virus injection. This lays the foundation for a study where a potential synergistic effect of combining HuD and SMN administration will be evaluated.

Together, these results support the idea that early increase of HuD activity and expression may allow for a better rescue of motor neurons. Increasing the number of cells that can be kept alive may help improve the overall outcome of therapeutic treatments combining CNS and systemic approaches.

4.2 Effect of bryostatin on motor neuron-derived MN-1 cells

4.2.1 Investigation of a PKCα-HuD-mRNA target pathway in motor neuron-like MN-1 cells

Work from different laboratories has examined a PKCα-dependent signaling cascade involved in mRNA stabilization and neuronal differentiation (Mobarak et al., 2000, Pascale et al., 2005, Lim et al., 2012). A model has been established where PKCα phosphorylates HuD, leading to its upregulation and to mRNA target stabilization. Mobarak and colleagues have shown that PKC-mediated neurite outgrowth in PC12 cells requires the presence of not only HuD but also GAP-43, a gene involved in neuronal development, regeneration, and plasticity (Mobarak et al., 2000). Indeed, they found that PC12 cells transfected with the antisense construct pDuH presented reduced GAP-43 mRNA and protein levels. Additionally, both NGF and phorbol esters failed to induce GAP-43 mRNA stabilization and protein up-regulation when HuD was knockdown, resulting in a defective differentiation. Another group revealed that bryostatin-induced phosphorylation of HuD had a positive impact on GAP-43 (Pascale et al., 2005). More precisely, they showed that a 15-minute treatment with 100nM bryostatin in human neuroblastoma SH-SY5Y cells led to HuD nuclear export, upregulation, and phosphorylation specifically in the cytoskeleton compartment, where it co-localized with PKCα. It was accompanied by stabilization of GAP-43 mRNA by HuD and in an early increase in GAP-43 protein levels. Importantly, all of these effects were abolished by inactivation of PKCα pharmacologically or via knockdown (Pascale et al., 2005). These results suggest that phosphorylation of HuD by PKCα plays an important role in HuD-

regulated gene expression during neuronal differentiation and importantly, that it can be modulated using small molecules.

In the current study, the existence of a similar pathway was investigated in motor neuron-derived MN-1 cells. These cells generated from the fusion of mouse embryonic spinal cord motor neurons and neuroblastoma cells (Salazar-Grueso et al., 1991) have been used by our laboratory and others as a an alternative to primary motor neurons, which are challenging to grow and work with in culture (Tadesse et al., 2008, Hubers et al., 2011, Sanchez et al., 2013). To this day, these cells have not been extensively characterized and it is not precisely known what pathways have been conserved from the two original cell lines. Here, an interaction between endogenous HuD and PKCα was detected by co-immunoprecipitation, but evidence that PKCα phosphorylates HuD directly or that the interaction can be modulated using bryostatin could not be obtained. One reason why PKCα and HuD might be hard to detect in the immunoprecipitate after treatment with bryostatin and/or the Ro inhibitor has to do with their subcellular localization once activated. Indeed, PKCα translocates to the cellular and nuclear membranes and associates with the cytoskeleton after activation. Therefore, any activated protein would locate to the insoluble fraction and not be detectable by western blotting when only the soluble fraction is probed. Future experiments should include both the insoluble and soluble fractions to get a better sense of the entire bryostatin-induced activation. In addition, conditions for the HuD IP will need to be optimized. Finally, a good modification-specific antibody against phospho- and methylarginine-HuD would need to be developed since there are none commercially available currently.

To investigate the next part of the pathway, RIP followed by RT-PCR was performed. It revealed a decrease in the binding of HuD to p21 mRNA after a 15-minute bryostatin treatment. This was surprising at first since our initial hypothesis supported a role for bryostatin-induced activation of HuD in cell cycle exit and/or neuronal differentiation. Indeed, it was expected that inactivation of CARM1 via bryostatin-induced PKCα phosphorylation (which was not validated) would lead to a higher proportion of the HuD pool to be unmethylated. In turn, this would result in a higher affinity of HuD for p21 mRNA, stabilization of the transcript, and eventually to cell cycle exit, as we and others have shown previously (Fujiwara et al., 2006, Hubers et al., 2011). However, bryostatin did not induce an increase in binding to p21 mRNA levels nor neurite extension. Assuming that the PKCα-HuD portion of the pathway is conserved in MN-1 cells, one explanation could be that CARM1 is not a substrate of PKCα in this cell line. Indeed, it has been established that CARM1 can be phosphorylated and inactivated by certain kinases (Higashimoto et al., 2007, Feng et al., 2009). Moreover, it was shown in rat hippocampal neurons that both HuD and CARM1 are phosphorylated by PKCα (Lim et al., 2012). This dual effect of the kinase inhibited CARM1 and decreased CARM1 methylation of HuD, resulting in the stabilization of HuD's mRNA targets and enhanced dendritic arborisation in these cells (Lim et al., 2012). Additionally, we and others have shown that CARM1 is an important regulator of the switch from cell proliferation to neuronal differentiation (Fujiwara et al., 2006, Hubers et al., 2011). We have found that CARM1 protein (but not mRNA) is downregulated during MN-1 differentiation and that methylation of its substrates is also decreased. Reduced methylation of HuD resulted in a higher binding affinity to p21 and GAP-43 mRNAs. On

the other hand, binding of HuD to Tau and Nova-1 mRNAs was found to be insensitive to CARM1 methylation (Hubers et al., 2011). Therefore, instead of the hypothetic dual effect on HuD and CARM1, PKCα could be phosphorylating only HuD and not inactivating CARM1. Thus, the effect of PKCα on HuD alone might be insufficient to induce the switch from proliferation to neuronal differentiation. To investigate this avenue, it would be fundamental to determine if CARM1 is a substrate of PKCα in MN-1 cells by the means detailed above for HuD.

An increase in the binding of HuD to known mRNA targets GAP-43 and Tau was detected here after a short 15-minute treatment with bryostatin. The protein products of these mRNAs are important players in neurite outgrowth. Thus, it would make sense for these mRNAs to get stabilized if activation of the PKC-HuD pathway using bryostatin contributed to cell differentiation, which does not seem to be the case at the concentrations and time points tested in this study. Increased binding to HuD suggests a subsequent stabilization of the transcript(s). Therefore, absolute (not only those bound to HuD) should also be examined. Assessing the transcripts' stability over time while activating or inhibiting individual actors in the pathway using RNA interference or pharmacological agents such as bryostatin, Ro 32-432,7 or a CARM1 inhibitor would unquestionably give us more insight on how each segment of the pathway is conserved. In parallel, it would also be of importance to determine if this increase in binding is associated with an increase in the protein product of these mRNAs. Pascale and colleagues were able to detect an increase in GAP-43 levels, even after a 15-minute bryostatin treatment, suggesting that the effect was at the post-transcriptional level (Pascale et al.).

Because phosphorylation and inactivation of CARM1 activity by PKCα could not be confirmed, it is not possible to conclude on whether these findings are in accordance with was previously shown by our laboratory. As abovementioned, we had found HuD binding to p21 and GAP-43 mRNAs to be sensitive and Tau and Nova-1 to be insensitive to CARM1 methylation (Hubers et al., 2011). Assuming that CARM1 is inhibited by the bryostatin treatment, our results would suggest that HuD binding to Tau mRNA is sensitive to methylation by the PRMT, at the concentrations and time points tested. The use of a CARM1-specific inhibitor would allow us to determine whether the PRMT is involved in this stabilization pathway. In another set of experiments, overexpression of WT, methylmimetic, or unmethylable HuD in an shHuD cell line could confirm that the effects detected here are truly mediated by HuD and are affected by CARM1 methylation.

Alternatively, bryostatin could have a HuD variant-specific activity. Hayashi and colleagues have looked at the expression, localization patterns, neurite-inducing abilities, and pre-mRNA and translational activities of the different HuD splicing variants (Hayashi et al.). Sv1, which is the general form, was shown to localize only to the cytoplasm, to have neurite-inducing activity in neuroblastoma cells, and translational activity on p21. On the other hand, sv4, a shorter isoform present both in the nucleus and the cytoplasm and missing a portion of the NLS or NES, had stronger growth-arresting activity and lower neurite inducing activity (Hayashi et al.). Some PKC phosphorylation sites and the one CARM1 methylation site are located within the linker region of HuD, where sv1 and sv4 differ (see figure 2). Thus, if for example sv4 is the most abundant splicing variant expressed in MN-1 cells, modulation of PKC (and CARM1) activity with

bryostatin might not influence HuD activity in the same manner as it would with a variant more susceptible to phosphorylation and methylation.

4.2.2 Bryostatin and control of the switch from cell proliferation to neuronal differentiation

As stated previously, it has been reported in many neuronal cell lines that HuD overexpression is sufficient to induce cell differentiation (Kasashima et al., 1999, Mobarak et al., 2000, Hubers et al., 2011). In this study, a 15-minute (1pM) bryostatin treatment in MN-1 cells led to a modest increase in HuD protein levels. This is consistent with previous studies where bryostatin induced up-regulation of HuD both *in vitro* and *in vivo* (Pascale et al., 2005, Lim et al., 2012, Marchesi et al., 2016). One important control that was neglected in the current study was to confirm that the increase in HuD protein levels can be prevented by pre-treating the cells with the PKC inhibitor Ro 32-0432. This would have helped establish that the effect on HuD levels are indeed through PKC. Since a short bryostatin treatment induced a slight HuD up-regulation, we wanted to assess whether this up-regulation would be accompanied by induction of neuronal differentiation. Motor neuron-derived MN-1 cells treated with a range of bryostatin concentrations for 48 and 72h showed miminal changes in morphology. Data acquired using the IncuCyte device confirmed that prolonged exposure to the drug had little effect on cell morphology. This is in accordance with what was reported by Jalava and colleagues. They found that a 72-hour treatment with 10nM bryostatin in SH-S5Y5 cells failed to induce neuronal differentiation (Jalava et al., 1990). Their cells did exhibit neurites after 6h of treatment, but the morphology reverted back to an undifferentiated

phenotype shortly after. This is only one of many reports that have looked into bryostatin's differentiation-inducing activity. A number of studies have found that bryostatin induces cell differentiation in a variety of cell lines (Kraft et al., 1989, Lilly et al., 1990, Hu et al., 1993, al-Katib et al., 1993b, al-Katib et al., 1993a, Hu et al., 1994, Li et al., 1997), while others have reported the opposite effect (Kraft et al., 1986, Kraft et al., 1987, Sako et al., 1987, Jalava et al., 1990). Overall, bryostatin's activity seems to be cell type, concentration, treatment duration, and PKC isoform-dependent (Lorenzo et al., 1997, Gschwend et al., 2000). One important element to keep in mind here is that MN-1 cells are not proper motor neurons. Therefore, repeating these experiments in primary or iPSC-derived motor neurons would be important and might result in a different outcome.

It has been reported that prolonged exposure to and/or high concentrations of bryostatin actually have an inhibitory effect on PKCα signaling. After a short exposure to bryostatin, PKC gets activated, autophosphorylated, and translocates to the membrane. Then, after the initial activation and translocation of PKC to the membrane, the kinase is down-regulated and degraded (Mutter et al., 2000). Thus, bryostatin might activate PKC during the first few hours of treatment before getting down-regulated and degraded by the proteasome (Lee et al., 1996), explaining the undifferentiated phenotype after three days of treatment. Since short or long exposure of MN-1 cells to bryostatin did not seem to induce cell cycle exit and differentiation, it would be interesting to determine whether bryostatin treatment can enhance specifically neurite extension. If cells are already committed to the neuronal lineage and in the process of differentiating, then maybe stimulation of HuD activity following HuD overexpression would result in an increased number of cells with long neurites. In support of this idea, Lim and Alkon found that

bryostatin enhanced dendritic arborisation in rat hippocampal neurons. Cells treated with bryostatin showed increased dendritic branching and length, an effect that was enhanced further by the co-administration of a CARM1 inhibitor (Lim et al., 2012). This would fit with our findings that HuD protein levels are upregulated, binding to p21 (a key regulator of cell cycle exit) is decreased, and binding to GAP-43 and Tau (both involved in neurite extension) is increased following treatment with bryostatin.

With fifteen different isoforms, each one with common and specific interacting partners, PKC signaling is involved in a wide range of cellular functions. It has been shown to be involved in receptor desensitization, membrane structure event modulation, transcription regulation, immune response, cell growth regulation, and learning and memory to name a few. Since PKC isoforms and substrates are expressed in a cell type specific manner, it is possible that some PKC isoform(s) usually activated by bryostatin might not be expressed in MN-1 cells. In fact, it is not known which PKC isoforms are expressed in MN-1 cells. One important experiment that should have been done early on in this study is to confirm the expression and activation by bryostatin of PKCα but also of other PKC isoforms. Furthermore, knowing that bryostatin activates both the classical/conventional and novel PKC subfamilies, it is difficult to conclude that the effects seen in the study are solely PKCα specific. They could be due to activation of one or more PKC isoforms. Indeed, PKCε, another kinase known to phosphorylate HuD was found to be involved in a similar bryostatin-inducible stabilization pathway (Lim et al., 2012, Lim et al., 2014). Therefore, determining the PKC isoforms expressed in MN-1 cells and activated by bryostatin would give us a more complete picture of the players potentially involved in PKC-dependent mRNA stabilization pathway(s). Furthermore,

this could contribute to determine whether some PKC isoforms have a selective activity towards CARM1 and help elucidate why CARM1 does not seem to be inhibited by bryostatin treatment in MN-1 cells.

Finally, it would have been important to assess whether small molecule-mediated activation of HuD through the PKCα pathway could have beneficial effects on SMA axonal defects, as planned originally. Our laboratory has shown previously that methylation of HuD by CARM1 is required for its interaction with the Tudor domain of SMN (Hubers et al., 2011). This adds another layer to the current model where on one side PKCα phosphorylates both HuD and CARM1 and controls the methylation of HuD by CARM1 by blocking the PRMT's activity. This increases the binding of HuD to some of its targets, leading to transcript stabilization, protein upregulation, and contributing to neurite extension. On the other side, while CARM1 methylation modulates the binding of HuD to some of its targets such as p21, it also modulates HuD's interaction with SMN and its proper recruitment into RNA granules along axons. This is of major importance in the context of SMA pathology, where CARM1 has been found to be abnormally up-regulated in the absence of SMN (Sanchez et al., 2013). Therefore, repeating some of these experiments in an SMA context would be important to determine if there is any benefit to increasing HuD levels and activity using bryostatin. On paper, bryostatin is an attractive therapeutic drug: it activates PKC at picomolar concentrations and lacks the tumor promoting activity of phorbol esters. Moreover, it has been shown to induce mature synapse growth and to prevent neuronal cell death (Hongpaisan et al., 2011, Hongpaisan et al., 2013). Although its relative safety has been demonstrated in the past, bryostatin might not be the best candidate drug for SMA. In a series of papers, the

Charbonnier laboratory uncovered that there exists a competition between the PI3K/Akt/CREB and MEK/Erk/Elk-1 pathways for *SMN2* regulation in type I SMA mice spinal cord (Branchu et al., 2013). They found that Erk was constitutively overactivated and Akt decreased in spinal cords from severe SMA-like mice (Biondi et al., 2010). More precisely, they showed that MEK/Erk/Elk-1 pathway inhibition *in vivo* using U0126 and/or Selumetinib resulted in a shift towards Akt/CREB pathway activation (likely through CaMKII), in increased SMN expression in the spinal cord, and in a significant increase in survival (Branchu et al., 2013). Similar results were observed in the spinal cord and skeletal muscle of severe SMA-like mice following IGF-1R reduction (Biondi et al., 2015). Therefore, treatments that would activate Erk signaling further, such as bryostatin, should be thoroughly studied, especially in the context of SMA.

4.3 Establishment of an scAAV9 viral expression system

There is increasing evidence that CNS delivery of ASOs to correct *SMN2* splicing does not compensate fully for the SMN deficiency in the periphery. A systemic approach or a combination of SMN-dependent and SMN-independent therapies have the potential to provide a more effective treatment regimen. In the past, our laboratory has shown that overexpressing HuD was sufficient to induce neuronal differentiation and to rescue SMA-like defects in motor neuron-derived cells. Thus, the second objective of this study was to evaluate the therapeutic potential of HuD *in vivo*. To this end, a self-complementary adeno-associated viral vector was designed to deliver our gene of interest systemically. ScAAVs are engineered to skip the second DNA strand synthesis to produce a faster, more robust transduction than ssAAV vectors found in nature (Ferrari et

al., 1996, Fisher et al., 1996, McCarty et al., 2001, Wang et al., 2003). AAVs have very low pathogenicity and immunogenicity, making them an attractive tool for gene therapy.

Before scAAV-HuD could be expressed in the mouse, it had to be tested in a cell culture model of SMA. Surprisingly, pGIPZ and shSMN cells transfected with scAAV-HuD did not extend long neurites, as expected based on previous experiments. One explanation might be that cell morphology was analyzed before neuronal differentiation was fully underway. Pictures were taken approximately 24h after inducing differentiation with RA+GDNF and about 32h after transfection. In comparison, results presented in figures 7 and 8 are pictures of cells taken 48 and 72h after transfection, respectively. Therefore, it would be expected that a larger proportion of cells would extend neurites at similar time points. Additionally, the fact that there is a difference in the number of cells with neurites between populations transfected with low and high amounts of HuD DNA suggests that there is a correlation between the levels of HuD and the proportion of differentiated cells. As shown by the blot quantification in figure 17C, HuD levels were not significantly increased 32h post-transfection, whereas cells collected after 48h expressed levels ~6-fold higher compared to endogenous levels (see figure 7D). This suggests that there could be a threshold to surpass to induce neurite extension and might partially explain the relatively undifferentiated morphology of the cells transfected with scAAV-HuD. Transfection conditions (amount of DNA, ratio of transfection reagents, incubation times, cell batch) are currently being tested to determine the optimal settings for this new vector.

4.3.1 CNS gene delivery

The goal of the first phase of this study was to establish an scAAV9 viral expression system to evaluate the benefits of HuD overexpression *in vivo*. To this end, overexpression of SMN in the delta7 mouse model was used to determine the optimal titer to use to get a partial rescue. While a full rescue might seem desirable, a lower dose has better chances of revealing small differences and requires smaller volumes to be injected. Moreover, it gives us room to study the effect of a combined SMN+HuD approach. The dose selected was chosen based on literature and it allowed us to compare and interpret our preliminary results. The viral titer used in the current study had a modest but significant impact on survival of the delta7 mouse. This allowed us to establish a good baseline and to acquire experience at administering the functional tests to get an accurate and consistent readout throughout the next phases of the study. In comparison to a study published by the Lorson laboratory where they used the same vector, titer, and mouse model, our SMA pups treated with scAAV-SMN had a shorter survival (Glascock et al., 2012b). The discrepancy in survival between our results could be due to multiple factors. First, even though the vector used to produce the virus is exactly the same, the virus itself was made by distinct services. This means that the protocol used, the purity, and the titer of the virus probably differed in some points. Also, although AAV has been proven to be very stable (Croyle et al., 2001), it is possible that the freeze/thaw cycles that the virus went through when aliquoted and then injected could have affected its titer. A more probable explanation as to why our mice were not rescued to the same extent as the mice in the 2012 study could be the incomplete delivery of the viral load. Indeed, when removing the needle from the facial vein, there was often

formation of a droplet of blood at the site of injection, possibly resulting in a partial delivery of the dose. It is also possible that our mice have a more severe phenotype than the Lorson mice. Indeed, even though most research groups originally got their delta7 mice from Jackson Laboratories, different groups have reported slightly different survival and disease severity. These differences are likely due to local factors. Indeed, it has been documented that housing conditions (i.e. number of mice in a cage, light/dark cycle, diet, etc.) can influence the general well-being of the mice as well as performance on tests (El-Khodor et al., 2008, Butchbach et al., 2010, Burghes et al., 2011, Butchbach et al., 2014, Walter et al., 2017). Our litters contained 6-10 pups, whereas SMA pups from the 2012 Lorson study were raised with two heterozygous littermates to control for litter size. Since there is less competition for milk and maternal attention, SMA pups from smaller litters tend to present a slightly milder phenotype. This could influence the overall survival and weight gain results. At last, recent findings from Dr. Melissa Bowerman's investigations into circadian rhythms in severe SMA mice revealed that a controlled light exposure influenced SMA phenotype and had beneficial effects of survival and weight gain. More precisely, SMA pups exposed to light pulses after birth were on average bigger than unexposed pups, while there was no effect of control mice (Walter et al., 2017). These are all elements that can influence the survival of SMA pups and that should obviously be kept as constant as possible throughout the course of the study to control for variability.

4.4 Future directions

4.4.1 Bryostatin-activated pathways in motor neurons

Further investigations could include determining CARM1's involvement in this PKC-HuD-mRNA pathway in motor neurons. In primary hippocampal neurons, bryostatin-induced PKC activation led to inactivation of CARM1 and reduced methylation of HuD by the PRMT. As we have shown previously, HuD hypomethylation increases its binding to selective targets, leading to transcript stabilization and protein upregulation in MN-1 cells. On the other hand, methylation of HuD by CARM1 is required for its interaction with the Tudor domain of SMN and for proper recruitment into RNA granules along axons. Interestingly, a number of mRNAs have been found to be mislocalized along axons in SMA. Moreover, we have shown that CARM1 is upregulated in SMA. Therefore, it would be of interest to determine whether treatment with bryostatin alone or in combination with a selective CARM1 inhibitor can rescue the axonal localization of key mRNAs SMA-like conditions. Exploring the effects of combining bryostatin and CARM1 inhibition on neurite length in primary motor neurons and/or iPSC-derived motor neurons would also be informative both in wild-type and SMA-like conditions. In a separate set of experiments, the effects of activating or inhibiting important signaling pathways such as the MEK/Erk/Elk-1 and PI3K/Akt cascades could be investigated further. Both pathways are involved in cell cycle regulation, cell proliferation, and neurite extension. Taken together, these data would contribute to determine if bryostatin activation of PKC is involved in cell cycle exit and/or neurite outgrowth, two processes that have been found to be defective in SMA. This would then provide needed insight into the rationale design of a potential

pharmacological strategy to complement and improve treatment options currently being develop for SMA.

4.4.2 HuD overexpression in a mouse model of SMA

In light of the results presented here, it has become evident that a slightly higher titer will be necessary in the next phase of the study. Expression of the virus in different tissues at P4, P7, and P14 is currently being assessed to confirm transduction and expression *in vivo*. Motor neuron counts, NMJ morphology, and muscle fiber size analyses at the same time points will complement these measures. Finally, the combined administration of SMN and HuD will be evaluated in the last phase of the study. This should provide evidence for a protective effect of HuD on motor neurons and a potential synergistic effect of a combinatorial approach. Ultimately, an earlier treatment targeting HuD might be able to preserve a greater proportion of motor neurons, which could be crucial for an SMN-targeted therapy to be even more efficient consequently.

4.5 Conclusions

The data presented in this thesis indicate that PKC signaling is active in motor neuron-derived MN-1 cells. Importantly, it can be modulated pharmacologically using a small molecule. Treatment with bryostatin induced HuD upregulation and increased its binding to selective mRNA targets, providing evidence for the existence of a PKC-HuD-mRNA stabilization pathway in these motor neuron-like cells. *In vivo* data suggest that our scAAV9 system led to the efficient expression of SMN in the delta7 mouse, resulting in an improved survival and weight gain. Moreover, a baseline was established for the

functional tests that will be used to accurately evaluate the rescue achieved following virus injection. Together, these results support my initial hypothesis and fulfill my objectives. Again, our working model is that activating and/or increasing HuD protein levels early on would be protective to motor neurons. Thus, ensuring that a high number of motor neurons are kept alive from the start would increase the chances of a better rescue by the co-administration of other therapies and provide superior treatment options for neurodegenerative diseases such as spinal muscular atrophy.

References

ACKERMANN, B., KRÖBER, S., TORRES-BENITO, L., BORGMANN, A., PETERS, M., HOSSEINI BARKOOIE, S. M., TEJERO, R., JAKUBIK, M., SCHREML, J., MILBRADT, J., WUNDERLICH, T. F., RIESSLAND, M., TABARES, L. & WIRTH, B. 2013. Plastin 3 ameliorates spinal muscular atrophy via delayed axon pruning and improves neuromuscular junction functionality. *Hum Mol Genet,* 22**,** 1328-1347.

AKTEN, B., KYE, M. J., HAO LE, T., WERTZ, M. H., SINGH, S. K., NIE, D., HUANG, J. P., MERIANDA, T. T., TWISS, J. L., BEATTIE, C. E., STEEN, J. A. & SAHIN, M. 2011. Interaction of survival of motor neuron (SMN) and HuD proteins with mRNA cpg15 rescues motor neuron axonal deficits. *Proc Natl Acad Sci U S A,* 108**,** 10337-10342.

AL-KATIB, A., MOHAMMAD, R. M., DAN, M. E., HUSSSEIN, M. E., AKHTAR, A., PETTIT, G. R. & SENSENBRENNER, L. L. 1993a. Bryostatin 1-induced hairy cell features on chronic lymphocytic leukemia cells in vitro. *Exp Hematol,* 21**,** 61-65.

AL-KATIB, A., MOHAMMAD, R. M., KHAN, K., DAN, M. E., PETTIT, G. R. & SENSENBRENNER, L. L. 1993b. Bryostatin 1-induced modulation of the acute lymphoblastic leukemia cell line Reh. *J Immunother Emphasis Tumor Immunol,* 14**,** 33-42.

ALKON, D. L., HONGPAISAN, J. & SUN, M. K. 2017. Effects of chronic bryostatin-1 on treatment-resistant depression in rats. *Eur J Pharmacol,* 807**,** 71-74.

AMADIO, M., BATTAINI, F. & PASCALE, A. 2006. The different facets of protein kinases C: old and new players in neuronal signal transduction pathways. *Pharmacol Res,* 54**,** 317-25.

ANDERSON, K. D., MORIN, M. A., BECKEL-MITCHENER, A. C., MOBARAK, C. D., NEVE, R. L., FURNEAUX, H. M., BURRY, R. W. & PERRONE-BIZZOZERO, N. 2000. Overexpression of HuD, but not its truncated form HuD I+II, promotes GAP-43 gene expression and neurite outgrowth in PC12 cells in the absence of nerve growth factor. *J Neurochem,* 75**,** 1103-1114.

ANDERSON, K. D., SENGUPTA, J., MORIN, M., NEVE, R. L., VALENZUELA, C. F. & PERRONE-BIZZOZERO, N. I. 2001. Overexpression of HuD accelerates neurite

outgrowth and increases GAP-43 mRNA expression in cortical neurons and retinoic acid-induced embryonic stem cells in vitro. *Exp Neurol,* 168**,** 250-8.

ANDERSON, P. & KEDERSHA, N. 2006. RNA granules. *J Cell Biol,* 172**,** 803-8.

ANDREASSI, C., ANGELOZZI, C., TIZIANO, F. D., VITALI, T., DE VINCENZI, E., BONINSEGNA, A., VILLANOVA, M., BERTINI, E., PINI, A., NERI, G. & BRAHE, C. 2004. Phenylbutyrate increases SMN expression in vitro: relevance for treatment of spinal muscular atrophy. *Eur J Hum Genet,* 12**,** 59-65.

ARANDA-ABREU, G. E., BEHAR, L., CHUNG, S., FURNEAUX, H. M. & GINZBURG, I. 1999. Embryonic lethal abnormal vision-like RNA-binding proteins regulate neurite outgrowth and tau expression in PC12 cells. *J Neurosci,* 19**,** 6907-6917.

ARMBRUSTER, N., LATTANZI, A., JEAVONS, M., VAN WITTENBERGHE, L., GJATA, B., MARAIS, T., MARTIN, S., VIGNAUD, A., VOIT, T., MAVILIO, F., BARKATS, M. & BUJ-BELLO, A. 2016. Efficacy and biodistribution analysis of intracerebroventricular administration of an optimized scAAV9-SMN1 vector in a mouse model of spinal muscular atrophy. *Mol Ther Methods Clin Dev,* 3**,** 16060.

ARONOV, S., ARANDA, G., BEHAR, L. & GINZBURG, I. 2002. Visualization of translated tau protein in the axons of neuronal P19 cells and characterization of tau RNP granules. *Journal of Cell Science,* 115**,** 3817-3827.

ATLAS, R., BEHAR, L., ELLIOTT, E. & GINZBURG, I. 2004. The insulin-like growth factor mRNA binding-protein IMP-1 and the Ras-regulatory protein G3BP associate with tau mRNA and HuD protein in differentiated P19 neuronal cells. *J Neurochem,* 89**,** 613-26.

ATLAS, R., BEHAR, L., SAPOZNIK, S. & GINZBURG, I. 2007. Dynamic association with polysomes during P19 neuronal differentiation and an untranslated-region-dependent translation regulation of the tau mRNA by the tau mRNA-associated proteins IMP1, HuD, and G3BP1. *J Neurosci Res,* 85**,** 173-83.

AVILA, A. M., BURNETT, B. G., TAYE, A. A., GABANELLA, F., KNIGHT, M. A., HARTENSTEIN, P., CIZMAN, Z., DI PROSPERO, N. A., PELLIZZONI, L., FISCHBECK, K. H. & SUMNER, C. J. 2007. Trichostatin A increases SMN expression and survival in a mouse model of spinal muscular atrophy. *J Clin Invest,* 117**,** 659-71.

BATTAGLIA, G., PRINCIVALLE, A., FORTI, F., LIZIER, C. & ZEVIANI, M. 1997. Expression of the SMN gene, the spinal muscular atrophy determining gene in the mammalian central nervous system. *Hum Mol Genet,* 6**,** 1961-1971.

BÉCHADE, C., ROSTAING, P., CISTERNI, C., KALISCH, R., LA BELLA, V., PETTMANN, B. & TRILLER, A. 1999. Subcellular distribution of SMN protein possible involvement in nucleocytoplasmic and dendritic transport. *Eur J Neurosci,* 11**,** 293-304.

BECKEL-MITCHENER, A. C., MIERA, A., KELLER, R. & PERRONE-BIZZOZERO, N. I. 2002. Poly(A) tail length-dependent stabilization of GAP-43 mRNA by the RNA-binding protein HuD. *J Biol Chem,* 277**,** 27996-8002.

BEDFORD, M. T. & CLARKE, S. G. 2009. Protein arginine methylation in mammals: who, what, and why. *Mol Cell,* 33**,** 1-13.

BEDFORD, M. T. & RICHARD, S. 2005. Arginine methylation an emerging regulator of protein function. *Mol Cell,* 18**,** 263-72.

BELL, L. R., MAINE, E. M., SCHEDL, P. & CLINE, T. W. 1988. Sex-lethal, a Drosophila sex determination switch gene, exhibits sex-specific RNA splicing and sequence similarity to RNA binding proteins. *Cell,* 55**,** 1037-1046.

BELLAVIA, D., MECAROZZI, M., CAMPESE, A. F., GRAZIOLI, P., TALORA, C., FRATI, L., GULINO, A. & SCREPANTI, I. 2007. Notch3 and the Notch3-upregulated RNA-binding protein HuD regulate Ikaros alternative splicing. *EMBO J,* 26**,** 1670-1680.

BENKHALIFA-ZIYYAT, S., BESSE, A., RODA, M., DUQUE, S., ASTORD, S., CARCENAC, R., MARAIS, T. & BARKATS, M. 2013. Intramuscular scAAV9-SMN injection mediates widespread gene delivery to the spinal cord and decreases disease severity in SMA mice. *Mol Ther,* 21**,** 282-290.

BERNAL, S., ALSO-RALLO, E., MARTINEZ-HERNANDEZ, R., ALIAS, L., RODRIGUEZ-ALVAREZ, F. J., MILLAN, J. M., HERNANDEZ-CHICO, C., BAIGET, M. & TIZZANO, E. F. 2011. Plastin 3 expression in discordant spinal muscular atrophy (SMA) siblings. *Neuromuscul Disord,* 21**,** 413-419.

BERTINI, E., DESSAUD, E., MERCURI, E., MUNTONI, F., KIRSCHNER, J., REID, C., LUSAKOWSKA, A., COMI, G. P., CUISSET, J.-M., ABITBOL, J.-L.,

SCHERRER, B., DUCRAY, P. S., BUCHBJERG, J., VIANNA, E., VAN DER POL, W. L., VUILLEROT, C., BLAETTLER, T., FONTOURA, P., ANDRÉ, C., BRUNO, C., CHABROL, B., DECONINCK, N., ESTOURNET, B., FONTAINE-CARBONNEL, S., GOEMANS, N., GORNI, K., GOVONI, A., GUGLIERI, M., LOCHMULLER, H., MAGRI, F., MAYER, M., MÜLLER-FELBER, W., RIVIER, F., ROPER, H., SCHARA, U., SCOTO, M., VAN DEN BERG, L., VITA, G. & WALTER, M. C. 2017. Safety and efficacy of olesoxime in patients with type 2 or non-ambulatory type 3 spinal muscular atrophy: a randomised, double-blind, placebo-controlled phase 2 trial. *The Lancet Neurology,* 16**,** 513-522.

BEVAN, A. K., DUQUE, S., FOUST, K. D., MORALES, P. R., BRAUN, L., SCHMELZER, L., CHAN, C. M., MCCRATE, M., CHICOINE, L. G., COLEY, B. D., PORENSKY, P. N., KOLB, S. J., MENDELL, J. R., BURGHES, A. H. & KASPAR, B. K. 2011. Systemic gene delivery in large species for targeting spinal cord, brain, and peripheral tissues for pediatric disorders. *Mol Ther,* 19**,** 1971-1980.

BEVAN, A. K., HUTCHINSON, K. R., FOUST, K. D., BRAUN, L., MCGOVERN, V. L., SCHMELZER, L., WARD, J. G., PETRUSKA, J. C., LUCCHESI, P. A., BURGHES, A. H. & KASPAR, B. K. 2010. Early heart failure in the SMNDelta7 model of spinal muscular atrophy and correction by postnatal scAAV9-SMN delivery. *Hum Mol Genet,* 19**,** 3895-905.

BIONDI, O., BRANCHU, J., BEN SALAH, A., HOUBEDINE, L., BERTIN, L., CHALI, F., DESSEILLE, C., WEILL, L., SANCHEZ, G., C., L., AÏD, S., LOPES, P., PARISET, C., LÉCOLLE, S., CÔTÉ, J., HOLZENBERGER, M., CHANOINE, C., MASSAAD, C. & CHARBONNIER, F. 2015. IGF-1R reduction triggers neuroprotective signaling pathways in spinal muscular atrophy mice. *J Neurosci,* 35**,** 12063-12079.

BIONDI, O., BRANCHU, J., SANCHEZ, G., LANCELIN, C., DEFORGES, S., LOPES, P., PARISET, C., LECOLLE, S., COTE, J., CHANOINE, C. & CHARBONNIER, F. 2010. In vivo NMDA receptor activation accelerates motor unit maturation, protects spinal motor neurons, and enhances SMN2 gene expression in severe spinal muscular atrophy mice. *J Neurosci,* 30**,** 11288-99.

BIONDI, O., GRONDARD, C., LECOLLE, S., DEFORGES, S., PARISET, C., LOPES, P., CIFUENTES-DIAZ, C., LI, H., DELLA GASPERA, B., CHANOINE, C. & CHARBONNIER, F. 2008. Exercise-induced activation of NMDA receptor promotes motor unit development and survival in a type 2 spinal muscular atrophy model mouse. *J Neurosci,* 28**,** 953-62.

BIRD, C. W., GARDINER, A. S., BOLOGNANI, F., TANNER, D. C., CHEN, C. Y., LIN, W. J., YOO, S., TWISS, J. L. & PERRONE-BIZZOZERO, N. I. 2013. KSRP modulation of GAP-43 mRNA stability restricts axonal outgrowth in embryonic hippocampal neurons. *PLoS One,* 8**,** e79255.

BOLOGNANI, F., CONTENTE-CUOMO, T. & PERRONE-BIZZOZERO, N. I. 2010. Novel recognition motifs and biological functions of the RNA-binding protein HuD revealed by genome-wide identification of its targets. *Nucleic Acids Res,* 38**,** 117-30.

BOLOGNANI, F., MERHEGE, M. A., TWISS, J. & PERRONE-BIZZOZERO, N. I. 2004. Dendritic localization of the RNA-binding protein HuD in hippocampal neurons: association with polysomes and upregulation during contextual learning. *Neurosci Lett,* 371**,** 152-7.

BORDET, T., BERNA, P., ABITBOL, J. L. & PRUSS, R. M. 2010. Olesoxime (TRO19622): A Novel Mitochondrial-Targeted Neuroprotective Compound. *Pharmaceuticals (Basel),* 3**,** 345-368.

BOWERMAN, M., ANDERSON, C. L., BEAUVAIS, A., BOYL, P. P., WITKE, W. & KOTHARY, R. 2009. SMN, profilin IIa and plastin 3: a link between the deregulation of actin dynamics and SMA pathogenesis. *Mol Cell Neurosci,* 42**,** 66-74.

BOWERMAN, M., BEAUVAIS, A., ANDERSON, C. L. & KOTHARY, R. 2010. Rho-kinase inactivation prolongs survival of an intermediate SMA mouse model. *Hum Mol Genet,* 19**,** 1468-78.

BOWERMAN, M., MICHALSKI, J. P., BEAUVAIS, A., MURRAY, L. M., DEREPENTIGNY, Y. & KOTHARY, R. 2014. Defects in pancreatic development and glucose metabolism in SMN-depleted mice independent of canonical spinal muscular atrophy neuromuscular pathology. *Hum Mol Genet,* 23**,** 3432-44.

BOWERMAN, M., MURRAY, L. M., BEAUVAIS, A., PINHEIRO, B. & KOTHARY, R. 2012a. A critical smn threshold in mice dictates onset of an intermediate spinal muscular atrophy phenotype associated with a distinct neuromuscular junction pathology. *Neuromuscul Disord,* 22**,** 263-276.

BOWERMAN, M., MURRAY, L. M., BOYER, J. G., ANDERSON, C. L. & KOTHARY, R. 2012b. Fasudil improves survival and promotes skeletal muscle development in a mouse model of spinal muscular atrophy. *BMC Med,* 10.

BOWERMAN, M., SHAFEY, D. & KOTHARY, R. 2007. Smn depletion alters profilin II expression and leads to upregulation of the RhoA/ROCK pathway and defects in neuronal integrity. *J Mol Neurosci,* 32**,** 120-131.

BRAHE, C., CLERMONT, O., ZAPPATA, S., TIZIANO, F., MELKI, J. & NERI, G. 1996. Frameshift mutation in the survival motor neuron gene in a severe case of SMA type I. *Hum Mol Genet,* 5**,** 1971-1976.

BRAHE, C., SERVIDEI, S., ZAPPATA, S., RICCI, E., TONALI, P. & NERI, G. 1995. Genetic homogeneity between childhood-onset and adult-onset autosomal recessive spinal muscular atrophy. *Lancet,* 346**,** 741-742.

BRAHE, C., VITALI, T., TIZIANO, F. D., ANGELOZZI, C., PINTO, A. M., BORGO, F., MOSCATO, U., BERTINI, E., MERCURI, E. & NERI, G. 2005. Phenylbutyrate increases SMN gene expression in spinal muscular atrophy patients. *Eur J Hum Genet,* 13**,** 256-9.

BRAHMS, H., MEHEUS, L., DE BRABANDERE, V., FISCHER, U. & LÜHRMANN, R. 2001. Symmetrical dimethylation of arginine residues in spliceosomal Sm protein B/B' and the Sm-like protein LSm4, and their interaction with the SMN protein. *RNA,* 7**,** 1531-1542.

BRANCHU, J., BIONDI, O., CHALI, F., COLLIN, T., LEROY, F., MAMCHAOUI, K., MAKOUKJI, J., PARISET, C., LOPES, P., MASSAAD, C., CHANOINE, C. & CHARBONNIER, F. 2013. Shift from extracellular signal-regulated kinase to AKT/cAMP response element-binding protein pathway increases survival-motor-neuron expression in spinal-muscular atrophy-like mice and patient cells. *J Neurosci,* 33**,** 4280-4294.

BRICHTA, L., HOFMANN, Y., HAHNEN, E., SIEBZEHNRUBL, F. A., RASCHKE, H., BLUMCKE, I., EYUPOGLU, I. Y. & WIRTH, B. 2003. Valproic acid increases the SMN2 protein level: a well-known drug as a potential therapy for spinal muscular atrophy. *Hum Mol Genet,* 12**,** 2481-9.

BRONICKI, L. M., BÉLANGER, G. & JASMIN, B. J. 2012. Characterization of multiple exon 1 variants in mammalian HuD mRNA and neuron-specific transcriptional control via neurogenin 2. *J Neurosci,* 32**,** 11164-11175.

BRZUSTOWICZ, L. M., LEHNER, T., CASTILLA, L. H., PENCHASZADEH, G. K., WILHEMSEN, K. C., DANIELS, R., DAVIES, K. E., LEPPERT, M., ZITER, F., WOOD, D., DUBOWITZ, V., ZERRES, K., HAUSMANOVA-PETRUSEWICZ, I.,

OTT, J., MUNSAT, T. L. & GILLIAM, T. C. 1990. Genetic mapping of chronic childhood-onset spinal muscular atrophy to chromosome 5q11.2-13.3. *Nature,* 344**,** 540-541.

BUCHER, T., COLLE, M. A., WAKELING, E., DUBREIL, L., FYFE, J., BRIOT-NIVARD, D., MAQUIGNEAU, M., RAOUL, S., CHEREL, Y., ASTORD, S., DUQUE, S., MARAIS, T., VOIT, T., MOULLIER, P., BARKATS, M. & JOUSSEMET, B. 2013. scAAV9 intracisternal delivery results in efficient gene transfer to the central nervous system of a feline model of motor neuron disease. *Hum Gene Ther,* 24**,** 670-82.

BÜHLER, D., RAKER, V., LÜHRMANN, R. & FISCHER, U. 1999. Essential role for the tudor domain of SMN in spliceosomal U snRNP assembly: implications for spinal muscular atrophy. *Hum Mol Genet,* 8**,** 2351-2357.

BURGHES, A. H. & SUMNER, C. J. 2011. Influence of housing, feeding, and handling conditions on SMA mouse performance. *TREAT-NMD Neuromuscular Network, Experimental protocols for SMA animal models,* SMA_M.2.2.003.

BÜRGLEN, L., LEFEBVRE, S., CLERMONT, O., BURLET, P., VIOLLET, L., CRUAUD, C., MUNNICH, A. & MELKI, J. 1996. Structure and organization of the human survival motor Neurone (SMN) gene. *Genomics,* 32**,** 479-482.

BURNETT, B. G., MUNOZ, E., TANDON, A., KWON, D. Y., SUMNER, C. J. & FISCHBECK, K. H. 2009. Regulation of SMN protein stability. *Mol Cell Biol,* 29**,** 1107-15.

BUTCHBACH, M. E., ROSE, F. F., JR., RHOADES, S., MARSTON, J., MCCRONE, J. T., SINNOTT, R. & LORSON, C. L. 2010. Effect of diet on the survival and phenotype of a mouse model for spinal muscular atrophy. *Biochem Biophys Res Commun,* 391**,** 835-40.

BUTCHBACH, M. E., SINGH, J., GURNEY, M. E. & BURGHES, A. H. 2014. The effect of diet on the protective action of D156844 observed in spinal muscular atrophy mice. *Exp Neurol,* 256**,** 1-6.

CAMPOS, A. R., GROSSMAN, D. & WHITE, K. 1985. Mutant alleles at the locus elav in Drosophila melanogaster lead to nervous system defects. A developmental-genetic analysis. *J Neurogenet,* 2**,** 197-218.

CARMODY, S. R. & WENTE, S. R. 2009. mRNA nuclear export at a glance. *J Cell Sci,* 122**,** 1933-7.

CARREL, T. L., MCWHORTER, M. L., WORKMAN, E., ZHANG, H., WOLSTENCROFT, E. C., LORSON, C. L., BASSELL, G. J., BURGHES, A. H. & BEATTIE, C. E. 2006. Survival motor neuron function in motor axons is independent of functions required for small nuclear ribonucleoprotein biogenesis. *J Neurosci,* 26**,** 11014-22.

CHAGNOVICH, D. & COHN, S. L. 1996. Binding of a 40-kDa protein to the N-myc 3'-untranslated region correlates with enhanced N-myc expression in human neuroblastoma. *J Biol Chem,* 271**,** 33580-33586.

CHOE, Y., LEE, B. J. & KIM, K. 2002. Participation of protein kinase C α isoform and extracellular signal-regulated kinase in neurite outgrowth of GT1 hypothalamic neurons. *J Neurochem,* 83**,** 1412-1422.

CHUNG, S., ECKRICH, M., PERRONE-BIZZOZERO, N., KOHN, D. T. & FURNEAUX, H. M. 1997. The Elav-like proteins bind to a conserved regulatory element in the 3'-untranslated region of GAP-43 mRNA. *272,* 10.

CHUNG, S., JIANG, L., CHENG, S. & FURNEAUX, H. M. 1996. Purification and properties of HuD, a neuronal RNA-binding protein. *Journal of Biological Chemistry,* 271**,** 11518-11524.

CLAYTON, G. H., PEREZ, G. M., SMITH, R. L. & OWENS, G. C. 1998. Expression of mRNA for the elav-like neural-specific RNA binding protein, HuD, during nervous system development. *Brain Res Dev Brain Res,* 109**,** 271-280.

ClinicalTrials.gov [Internet]. Bethesda (MD): National Library of Medicine (US). 2000 Feb 29 - Identifier NCT01302600, Safety and Efficacy of Olesoxime (TRO19622) in 3-25 Years SMA Patients; 2011 Feb 24 [cited 2017 Aug 22]; [about 9 screens]. Available from: https://clinicaltrials.gov/ct2/show/NCT01302600

ClinicalTrials.gov [Internet]. Bethesda (MD): National Library of Medicine (US). 2000 Feb 29 - Identifier NCT02628743, A Study to Evaluate Long Term Safety, Tolerability, and Effectiveness of Olesoxime in Participants With Spinal Muscular Atrophy (SMA); 2015 Dec 11 [cited 2017 Aug 22]; [about 8 screens]. Available from: https://clinicaltrials.gov/ct2/show/NCT02628743

ClinicalTrials.gov [Internet]. Bethesda (MD): National Library of Medicine (US). 2000 Feb 29 - Identifier NCT02644668, A Study of CK-2127107 in Patients With Spinal Muscular Atrophy; 2016 Jan 1 [cited 2017 Aug 22]; [about 11 screens]. Available from: https://clinicaltrials.gov/ct2/show/NCT02644668

COLOMBRITA, C., SILANI, V. & RATTI, A. 2013. ELAV proteins along evolution: back to the nucleus? *Mol Cell Neurosci,* 56**,** 447-455.

COOVERT, D. D., LE, T. T., MCANDREW, P. E., STRASSWIMMER, J., CRAWFORD, T. O., MENDELL, J. R., COULSON, S. E., ANDROPHY, E. J., PRIOR, T. W. & BURGHES, A. H. 1997. The survival motor neuron protein in spinal muscular atrophy. *Hum Mol Genet,* 6**,** 1205-1214.

CÔTÉ, J. & RICHARD, S. 2005. Tudor domains bind symmetrical dimethylated arginines. *J Biol Chem,* 280**,** 28476-83.

COUSSENS, L., PARKER, P. J., RHEE, L., YANG-FENG, T. L., CHEN, E., WATERFIELD, M. D., FRANCKE, U. & ULLRICH, A. 1986. Multiple, distinct forms of bovine and human protein kinase C suggest diversity in cellular signaling pathways. *Science,* 233**,** 859-866.

COUSSENS, L., RHEE, L., PARKER, P. J. & ULLRICH, A. 1987. Alternative splicing increases the diversity of the human protein kinase C family. *DNA,* 6**,** 389-394.

CRAWFORD, T. O. & PARDO, C. A. 1996. The neurobiology of childhood spinal muscular atrophy. *Neurobiol Dis,* 3**,** 97-110.

CROYLE, M. A., CHENG, X. & WILSON, J. M. 2001. Development of formulations that enhance physical stability of viral vectors for gene therapy. *Gene Ther,* 8**,** 1281-1290.

DAI, W., ZHANG, G. & MAKEYEV, E. V. 2012. RNA-binding protein HuR autoregulates its expression by promoting alternative polyadenylation site usage. *Nucleic Acids Res,* 40**,** 787-800.

DALMAU, J., FURNEAUX, H. M., GRALLA, R. J., KRIS, M. G. & POSNER, J. B. 1990. Detection of the anti-Hu antibody in the serum of patients with small cell lung cancer--a quantitative western blot analysis. *Ann Neurol,* 27**,** 544-552.

DARBAR, I., A., PLAGGERT, P. G., RESENDE, M. B., ZANOTELI, E. & REED, U. C. 2011. Evaluation of muscle strength and motor abilities in children with type II and III spinal muscle atrophy treated with valproic acid. *BMC Neurol,* 11**,** 1-5.

DEGUISE, M. O., DE REPENTIGNY, Y., MCFALL, E., AUCLAIR, N., SAD, S. & KOTHARY, R. 2017. Immune dysregulation may contribute to disease pathogenesis in spinal muscular atrophy mice. *Hum Mol Genet,* 26**,** 801-819.

DESCHENES-FURRY, J., BELANGER, G., PERRONE-BIZZOZERO, N. & JASMIN, B. J. 2003. Post-transcriptional regulation of acetylcholinesterase mRNAs in nerve growth factor-treated PC12 cells by the RNA-binding protein HuD. *J Biol Chem,* 278**,** 5710-7.

DESCHENES-FURRY, J., MOUSAVI, K., BOLOGNANI, F., NEVE, R. L., PARKS, R. J., PERRONE-BIZZOZERO, N. I. & JASMIN, B. J. 2007. The RNA-binding protein HuD binds acetylcholinesterase mRNA in neurons and regulates its expression after axotomy. *J Neurosci,* 27**,** 665-75.

DESCHENES-FURRY, J., PERRONE-BIZZOZERO, N. & JASMIN, B. J. 2006. The RNA-binding protein HuD: a regulator of neuronal differentiation, maintenance and plasticity. *Bioessays,* 28**,** 822-33.

DIDONATO, C. J. & BOGDANIK, L. 2011. Behavioral phenotyping for neonates: righting reflex. *TREAT-NMD Neuromuscular Network, Experimental protocols for SMA animal models,* MD_M.2.2.002.

DIDONATO, C. J., CHEN, X. N., NOYA, D., KORENBERG, J. R., NADEAU, J. H. & SIMARD, L. R. 1997. Cloning, characterization, and copy number of the murine survival motor neuron gene: homolog of the spinal muscular atrophy-determining gene. *Genome Res,* 7**,** 339-352.

DOMINGUEZ, E., MARAIS, T., CHATAURET, N., BENKHALIFA-ZIYYAT, S., DUQUE, S., RAVASSARD, P., CARCENAC, R., ASTORD, S., PEREIRA DE MOURA, A., VOLT, T. & BARKATS, M. 2011. Intravenous scAAV9 delivery of a codon-optimized SMN1 sequence rescues SMA mice. *Hum Mol Genet,* 20**,** 681-693.

DOWNWARD, J. 1998. Mechanisms and consequences of activation of protein kinase B/Akt. *Curr Opin Cell Biol,* 10**,** 262-267.

DUBOWITZ, V. 1999. Very severe spinal muscular atrophy (SMA type 0): An expanding clinical phenotype. *Eur J Paediatr Neurol,* 3**,** 49-51.

DUDEK, H., DATTA, S. R., FRANKE, T. F., BIRNBAUM, M. J., YAO, R., COOPER, G. M., SEGAL, R. A., KAPLAN, D. R. & GREENBERG, M. E. 1997. Dudek H et al. - Regulation of neuronal survival by the serine-threonine protein kinase Akt. *Science,* 275**,** 661-665.

DUQUE, S., JOUSSEMET, B., RIVIERE, C., MARAIS, T., DUBREIL, L., DOUAR, A. M., FYFE, J., MOULLIER, P., COLLE, M. A. & BARKATS, M. 2009. Intravenous administration of self-complementary AAV9 enables transgene delivery to adult motor neurons. *Mol Ther,* 17**,** 1187-96.

EGGERT, C., CHARI, A., LAGGERBAUER, B. & FISCHER, U. 2006. Spinal muscular atrophy: the RNP connection. *Trends Mol Med,* 12**,** 113-21.

EL-KHODOR, B. 2011. Behavioral phenotyping for neonates: hind limb suspension test (a.k.a. tube test). *TREAT-NMD Neuromuscular Network, Experimental protocols for SMA animal models,* SMA_M.2.2.001.

EL-KHODOR, B. F., EDGAR, N., CHEN, A., WINBERG, M. L., JOYCE, C., BRUNNER, D., SUAREZ-FARINAS, M. & HEYES, M. P. 2008. Identification of a battery of tests for drug candidate evaluation in the SMNDelta7 neonate model of spinal muscular atrophy. *Exp Neurol,* 212**,** 29-43.

EVES, E. M., XIONG, W., BELLACOSA, A., KENNEDY, S. G., TSICHLIS, P. N., ROSNER, M. R. & HAY, N. 1998. Akt, a target of phosphatidylinositol 3-kinase, inhibits apoptosis in a differentiating neuronal cell line. *Mol Cell Biol,* 18**,** 2143-2152.

FALLINI, C., BASSELL, G. J. & ROSSOLL, W. 2012. Spinal muscular atrophy: the role of SMN in axonal mRNA regulation. *Brain Res,* 1462**,** 81-92.

FALLINI, C., ROUANET, J. P., DONLIN-ASP, P. G., GUO, P., ZHANG, H., SINGER, R. H., ROSSOLL, W. & BASSELL, G. J. 2014. Dynamics of survival of motor neuron (SMN) protein interaction with the mRNA-binding protein IMP1 facilitates its trafficking into motor neuron axons. *Dev Neurobiol,* 74**,** 319-332.

FALLINI, C., ZHANG, H., SILANI, V., SINGER, R. H., ROSSOLL, W. & BASSELL, G. J. 2011. The survival of motor neuron (SMN) protein interacts with the mRNA-

binding protein HuD and regulates localization of poly(A) mRNA in primary motor neuron axons. *J Neurosci,* 31**,** 3914-3925.

FAN, L. & SIMARD, L. R. 2002. Survival motor neuron (SMN) protein role in neurite outgrowth and neuromuscular maturation during neuronal differentiation and development. *Hum Mol Genet,* 11**,** 1605-1614.

FAN, Y., XIE, P., ZHANG, H., GUO, S., GU, D., SHE, M. & LI, H. 2008. Proteasome-dependent inactivation of Akt is essential for 12-O-tetradecanoylphorbol 13-acetate-induced apoptosis in vascular smooth muscle cells. *Apoptosis,* 13**,** 1401-9.

FAUSTINO, N. A. & COOPER, T. A. 2003. Pre-mRNA splicing and human disease. *Genes Dev,* 17**,** 419-437.

FENG, Q., HE, B., JUNG, S. Y., SONG, Y., QIN, J., TSAI, S. Y., TSAI, M. J. & O'MALLEY, B. W. 2009. Biochemical control of CARM1 enzymatic activity by phosphorylation. *J Biol Chem,* 284**,** 36167-74.

FENG, Y., MAITY, R., WHITELEGGE, J. P., HADJIKYRIACOU, A., LI, Z., ZURITA-LOPEZ, C., AL-HADID, Q., CLARK, A. T., BEDFORD, M. T., MASSON, J. Y. & CLARKE, S. G. 2013. Mammalian protein arginine methyltransferase 7 (PRMT7) specifically targets RXR sites in lysine- and arginine-rich regions. *J Biol Chem,* 288**,** 37010-37025.

FERRARI, F. K., SAMULSKI, T., SHENK, T. & SAMULSKI, R. J. 1996. Second-strand synthesis is a rate-limiting step for efficient transduction by recombinant adeno-associated virus vectors. *J Virol,* 70**,** 3227-3234.

FINKEL, R. S., CHIRIBOGA, C. A., VAJSAR, J., DAY, J. W., MONTES, J., DE VIVO, D. C., YAMASHITA, M., RIGO, F., HUNG, G., SCHNEIDER, E., NORRIS, D. A., XIA, S., BENNETT, C. F. & BISHOP, K. M. 2016. Treatment of infantile-onset spinal muscular atrophy with nusinersen: a phase 2, open-label, dose-escalation study. *The Lancet,* 388**,** 3017-3026.

FISCHER, U., LIU, Q. & DREYFUSS, G. 1997. The SMN–SIP1 complex has an essential role in spliceosomal snRNP biogenesis. *Cell,* 90**,** 1023-1029.

FISHER, K. J., GAO, G. P., WEITZMAN, M. D., DEMATTEO, R., BURDA, J. F. & WILSON, J. M. 1996. Transduction with recombinant adeno-associated virus for gene therapy is limited by leading-strand synthesis. *J Virol,* 70**,** 520-532.

FOUST, K. D., NURRE, E., MONTGOMERY, C. L., HERNANDEZ, A., CHAN, C. M. & KASPAR, B. K. 2009. Intravascular AAV9 preferentially targets neonatal neurons and adult astrocytes. *Nat Biotechnol,* 27**,** 59-65.

FOUST, K. D., WANG, X., MCGOVERN, V. L., BRAUN, L., BEVAN, A. K., HAIDET, A. M., LE, T. T., MORALES, P. R., RICH, M. M., BURGHES, A. H. & KASPAR, B. K. 2010. Rescue of the spinal muscular atrophy phenotype in a mouse model by early postnatal delivery of SMN. *Nat Biotechnol,* 28**,** 271-274.

FRANKE, T. F., KAPLAN, D. R., CANTLEY, L. C. & TOKER, A. 1997. Direct regulation of the Akt proto-oncogene product by phosphatidylinositol-3,4-bisphosphate. *Science,* 275**,** 665-668.

FUJIWARA, T., MORI, Y., CHU, D. L., KOYAMA, Y., MIYATA, S., TANAKA, H., YACHI, K., KUBO, T., YOSHIKAWA, H. & TOHYAMA, M. 2006. CARM1 regulates proliferation of PC12 cells by methylating HuD. *Mol Cell Biol,* 26**,** 2273-85.

FUKAO, A., MISHIMA, Y., TAKIZAWA, N., OKA, S., IMATAKA, H., PELLETIER, J., SONENBERG, N., THOMA, C. & FUJIWARA, T. 2014. MicroRNAs trigger dissociation of eIF4AI and eIF4AII from target mRNAs in humans. *Mol Cell,* 56**,** 79-89.

FUKAO, A., SASANO, Y., IMATAKA, H., INOUE, K., SAKAMOTO, H., SONENBERG, N., THOMA, C. & FUJIWARA, T. 2009. The ELAV protein HuD stimulates cap-dependent translation in a Poly(A)- and eIF4A-dependent manner. *Mol Cell,* 36**,** 1007-17.

GABANELLA, F., BUTCHBACH, M. E., SAIEVA, L., CARISSIMI, C., BURGHES, A. H. & PELLIZZONI, L. 2007. Ribonucleoprotein assembly defects correlate with spinal muscular atrophy severity and preferentially affect a subset of spliceosomal snRNPs. *PLoS One,* 2**,** e921.

GARY, J. D. & CLARKE, S. 1998. RNA and Protein Interactions Modulated by Protein Arginine Methylation. 61**,** 65-131.

GIBSON, D. G., YOUNG, L., CHUANG, R. Y., VENTER, J. C., HUTCHISON, C. A., 3RD & SMITH, H. O. 2009. Enzymatic assembly of DNA molecules up to several hundred kilobases. *Nat Methods,* 6**,** 343-5.

GLASCOCK, J. J., OSMAN, E. Y., WETZ, M. J., KROGMAN, M. M., SHABABI, M. & LORSON, C. L. 2012a. Decreasing disease severity in symptomatic, Smn(-/-);SMN2 (+/+), spinal muscular atrophy mice following scAAV9-SMN delivery. *Hum Gene Ther,* 23**,** 330-335.

GLASCOCK, J. J., SHABABI, M., WETZ, M. J., KROGMAN, M. M. & LORSON, C. L. 2012b. Direct central nervous system delivery provides enhanced protection following vector mediated gene replacement in a severe model of spinal muscular atrophy. *Biochem Biophys Res Commun,* 417**,** 376-381.

GOGLIOTTI, R. G., HAMMOND, S. M., LUTZ, C. & DIDONATO, C. J. 2010. Molecular and phenotypic reassessment of an infrequently used mouse model for spinal muscular atrophy. *Biochem Biophys Res Commun,* 391**,** 517-522.

GOMBASH, S. E., COWLEY, C. J., FITZGERALD, J. A., IYER, C. C., FRIED, D., MCGOVERN, V. L., WILLIAMS, K. C., BURGHES, A. H., CHRISTOFI, F. L., GULBRANSEN, B. D. & FOUST, K. D. 2015. SMN deficiency disrupts gastrointestinal and enteric nervous system function in mice. *Hum Mol Genet,* 24**,** 3847-3860.

GOOD, P. J. 1995. A conserved family of elav-like genes in vertebrates. *Proc Natl Acad Sci U S A,* 92**,** 4557-4561.

GOOD, P. J. 1997. The role of elav-like genes, a conserved family encoding RNA-binding proteins, in growth and development. *Semin Cell Dev Biol,* 8**,** 577-584.

GOULET, B. B., MCFALL, E. M., WONG, C. M., KOTHARY, R. & PARKS, R. J. 2012. Supraphysiological expression of survival motor neuron protein from an adenovirus vector does not adversely affect cell function. *Biochem Cell Biol,* 91**,** 252-264.

GRONDARD, C., BIONDI, O., ARMAND, A. S., LECOLLE, S., DELLA GASPERA, B., PARISET, C., LI, H., GALLIEN, C. L., VIDAL, P. P., CHANOINE, C. & CHARBONNIER, F. 2005. Regular exercise prolongs survival in a type 2 spinal muscular atrophy model mouse. *J Neurosci,* 25**,** 7615-22.

GSCHWEND, J. E., FAIR, W. R. & POWELL, C. T. 2000. Bryostatin 1 induces prolonged activation of extracellular regulated protein kinases in and apoptosis of LNCaP human prostate cancer cells overexpressing protein kinase calpha. *Mol Pharmacol,* 57**,** 1224-1234.

HAHNEN, E., EYUPOGLU, I. Y., BRICHTA, L., HAASTERT, K., TRANKLE, C., SIEBZEHNRUBL, F. A., RIESSLAND, M., HOLKER, I., CLAUS, P., ROMSTOCK, J., BUSLEI, R., WIRTH, B. & BLUMCKE, I. 2006. In vitro and ex vivo evaluation of second-generation histone deacetylase inhibitors for the treatment of spinal muscular atrophy. *J Neurochem,* 98**,** 193-202.

HAN, K. J., FOSTER, D. G., ZHANG, N. Y., KANISHA, K., DZIECIATKOWSKA, M., SCLAFANI, R. A., HANSEN, K. C., PENG, J. & LIU, C. W. 2012. Ubiquitin-specific protease 9x deubiquitinates and stabilizes the spinal muscular atrophy protein-survival motor neuron. *J Biol Chem,* 287**,** 43741-52.

HANNUS, S., BÜHLER, D., ROMANO, M., SERAPHIN, B. & FISCHER, U. 2000. The Schizosaccharomyces pombe protein Yab8p and a novel factor, Yip1p, share structural and functional similarity with the spinal muscular atrophy-associated proteins SMN and SIP1. *Hum Mol Genet,* 9**,** 663-674.

HAO LE, T., WOLAMN, M., GRANATO, M. & BEATTIE, C. E. 2012. Survival motor neuron affects plastin 3 protein levels leading to motor defects. *J Neurosci,* 32**,** 5074-5084.

HARAHAP, I. S., SAITO, T., SAN, L. P., SASAKI, N., GUNADI, NURPUTRA, D. K., YUSOFF, S., YAMAMOTO, T., MORIKAWA, S., NISHIMURA, N., LEE, M. J., TAKESHIMA, Y., MATSUO, M. & NISHIO, H. 2012. Valproic acid increases SMN2 expression and modulates SF2/ASF and hnRNPA1 expression in SMA fibroblast cell lines. *Brain Dev,* 34**,** 213-222.

HAUKE, J., RIESSLAND, M., LUNKE, S., EYUPOGLU, I. Y., BLUMCKE, I., EL-OSTA, A., WIRTH, B. & HAHNEN, E. 2009. Survival motor neuron gene 2 silencing by DNA methylation correlates with spinal muscular atrophy disease severity and can be bypassed by histone deacetylase inhibition. *Hum Mol Genet,* 18**,** 304-17.

HEIER, C. R. & DIDONATO, C. J. 2009. Translational readthrough by the aminoglycoside geneticin (G418) modulates SMN stability in vitro and improves motor function in SMA mice in vivo. *Hum Mol Genet,* 18**,** 1310-22.

HEIER, C. R., SATTA, R., LUTZ, C. & DIDONATO, C. J. 2010. Arrhythmia and cardiac defects are a feature of spinal muscular atrophy model mice. *Hum Mol Genet,* 19**,** 3906-3918.

HELMKEN, C., HOFMANN, Y., SCHOENEN, F., OPREA, G., RASCHKE, H., RUDNIK-SCHÖNEBORN, S. S., ZERRES, K. & WIRTH, B. 2003. Evidence for a modifying pathway in SMA discordant families: reduced SMN level decreases the amount of its interacting partners and Htra2-beta1. *Hum Genet,* 114**,** 11-21.

HIGASHIMOTO, K., KUHN, P., DESAI, D., CHENG, X. & XU, W. 2007. Phosphorylation-mediated inactivation of coactivator-associated arginine methyltransferase 1. *Proc Natl Acad Sci U S A,* 104**,** 12318-12323.

HINMAN, M. N. & LOU, H. 2008. Diverse molecular functions of Hu proteins. *Cell Mol Life Sci,* 65**,** 3168-81.

HOFFMANN, J. 1893. Über chronische spinale Muskelatrophie im Kindesalter, auf familiärer Basis. 3**,** 427-470.

HOFFMANN, J. 1897. Weiterer Beitrag zur Lehre von der hereditären progressiven spinalen Muskelatrophie im Kindesalter. *Dtsch Z Nervenheilkd,* 10**,** 292-320.

HOFFMANN, J. 1900. Dritter Beitrag zur Lehre von der hereditären progressiven spinalen Muskelatrophie im Kindesalter. *Dtsch Z Nervenheilkd,* 18**,** 217-224.

HONGPAISAN, J., SUN, M. K. & ALKON, D. L. 2011. PKC epsilon activation prevents synaptic loss, Abeta elevation, and cognitive deficits in Alzheimer's disease transgenic mice. *J Neurosci,* 31**,** 630-43.

HONGPAISAN, J., XU, C., SEN, A., NELSON, T. J. & ALKON, D. L. 2013. PKC activation during training restores mushroom spine synapses and memory in the aged rat. *Neurobiol Dis,* 55**,** 44-62.

HOSSEINIBARKOOIE, S., PETERS, M., TORRES-BENITO, L., RASTETTER, R. H., HUPPERICH, K., HOFFMANN, A., MENDOZA-FERREIRA, N., KACZMAREK, A., JANZEN, E., MILBRADT, J., LAMKEMEYER, T., RIGO, F., BENNETT, C. F., GUSCHLBAUER, C., BUSCHGES, A., HAMMERSCHMIDT, M., RIESSLAND, M., KYE, M. J., CLEMEN, C. S. & WIRTH, B. 2016. The Power of Human Protective Modifiers: PLS3 and CORO1C Unravel Impaired Endocytosis in Spinal Muscular Atrophy and Rescue SMA Phenotype. *Am J Hum Genet,* 99**,** 647-665.

HSIEH-LI, H. M., CHANG, J. G., JONG, Y. J., WU, M. H., WANG, N. M., TSAI, C. H. & LI, H. 2000. A mouse model for spinal muscular atrophy. *Nat Genet,* 24**,** 66-70.

HSU, S. H., LAI, M. C., ER, T. K., YANG, S. N., HUNG, C. H., TSAI, H. H., LIN, Y. C., CHANG, J. G., LO, Y. C. & JONG, Y. J. 2010. Ubiquitin carboxyl-terminal hydrolase L1 (UCHL1) regulates the level of SMN expression through ubiquitination in primary spinal muscular atrophy fibroblasts. *Clin Chim Acta,* 411**,** 1920-8.

HU, Z. B., GIGNAC, S. M., UPHOFF, C. C., QUENTMEIER, H., STEUBE, K. G. & DREXLER, H. G. 1993. Induction of differentiation of B-cell leukemia cell lines JVM-2 and EHEB by bryostatin 1. *Leuk Lymphoma,* 10**,** 135-42.

HU, Z. B., MA, W., UPHOFF, C. C., QUENTMEIER, H. & DREXLER, H. G. 1994. c-kit expression in human megakaryoblastic leukemia cell lines. *Blood,* 83**,** 2133-2144.

HUA, Y., SAHASHI, K., HUNG, G., RIGO, F., PASSINI, M. A., BENNETT, C. F. & KRAINER, A. R. 2010. Antisense correction of SMN2 splicing in the CNS rescues necrosis in a type III SMA mouse model. *Genes Dev,* 24**,** 1634-1644.

HUA, Y., VICKERS, T. A., BAKER, B. F., BENNETT, C. F. & KRAINER, A. R. 2007. Enhancement of SMN2 exon 7 inclusion by antisense oligonucleotides targeting the exon. *PLoS Biol,* 5**,** e73.

HUA, Y., VICKERS, T. A., OKUNOLA, H. L., BENNETT, C. F. & KRAINER, A. R. 2008. Antisense masking of an hnRNP A1/A2 intronic splicing silencer corrects SMN2 splicing in transgenic mice. *Am J Hum Genet,* 82**,** 834-848.

HUBERS, L., VALDERRAMA-CARVAJAL, H., LAFRAMBOISE, J., TIMBERS, J., SANCHEZ, G. & CÔTÉ, J. 2011. HuD interacts with survival motor neuron protein and can rescue spinal muscular atrophy-like neuronal defects. *Hum Mol Genet,* 20**,** 553-579.

HWEE, D. T., KENNEDY, A. R., HARTMAN, J. J., RYANS, J., DURHAM, N., MALIK, F. I. & JASPER, J. R. 2015. The small-molecule fast skeletal troponin activator, CK-2127107, improves exercise tolerance in a rat model of heart failure. *J Pharmacol Exp Ther,* 353**,** 159-68.

INCE-DUNN, G., OKANO, H. J., JENSEN, K. B., PARK, W. Y., ZHONG, R., ULE, J., MELE, A., FAK, J. J., YANG, C. C., ZHANG, C., YOO, J., HERRE, M., OKANO, H., NOEBELS, J. L. & DARNELL, R. B. 2012. Neuronal Elav-like (Hu) proteins regulate RNA splicing and abundance to control glutamate levels and neuronal excitability. *Neuron,* 75**,** 1067-1080.

INMAN, M. V., LEVY, S., MOCK, B. A. & OWENS, G. C. 1998. Gene organization and chromosome location of the neural-specific RNA binding protein Elavl4. *Gene,* 208**,** 139-145.

JABLONKA, S., BANDILLA, M., WIESE, S., BÜHLER, D., WIRTH, B., SENDTNER, M. & FISCHER, U. 2001. Co-regulation of survival of motor neuron (SMN) protein and its interactor SIP1 during developmend and in spinal muscular atrophy. *Hum Mol Genet,* 10**,** 497-505.

JALAVA, A. M., HEIKKILÄ, J., AKERLIND, G., PETTIT, G. R. & AKERMAN, K. E. 1990. Effects of bryostatins 1 and 2 on morphological and functional differentiation of SH-SY5Y human neuroblastoma cells. *Cancer Res,* 50**,** 3422-3428.

JODELKA, F. M., EBERT, A. D., DUELLI, D. M. & HASTINGS, M. L. 2010. A feedback loop regulates splicing of the spinal muscular atrophy-modifying gene, SMN2. *Hum Mol Genet,* 19**,** 4906-4917.

JOSEPH, B., ORLIAN, M. & FURNEAUX, H. M. 1998. p21(waf1) mRNA contains a conserved element in its 3'-untranslated region that is bound by the Elav-like mRNA-stabilizing proteins. *J Biol Chem,* 273**,** 20511-20516.

KAIBUCHI, K., FUKUMOTO, Y., OKU, N., TAKAI, Y., ARAI, K. & MURAMATSU, M. 1989. Molecular genetic analysis of the regulatory and catalytic domains of protein kinase C. *J Biol Chem,* 264**,** 13489-13496.

KAIFER, K. A., VILLALON, E., OSMAN, E. Y., GLASCOCK, J. J., ARNOLD, L. L., CORNELISON, D. D. & LORSON, C. L. 2017. Plastin-3 extends survival and reduces severity in mouse models of spinal muscular atrophy. *JCI Insight,* 2**,** e89970.

KASASHIMA, K., SAKASHITA, E., SAITO, K. & SAKAMOTO, H. 2002. Complex formation of the neuron-specific ELAV-like Hu RNA-binding proteins. *Nucleic Acids Res,* 30**,** 4519-4526.

KASASHIMA, K., TERASHIMA, K., YAMAMOTO, K., SAKASHITA, E. & SAKAMOTO, H. 1999. Cytoplasmic localization is required for the mammalian ELAV-like protein HuD to induce neuronal differentiation. *Genes Cells,* 4**,** 667-683.

KAWAKAMI, Y., NISHIMOTO, H., KITAURA, J., MAEDA-YAMAMOTO, M., KATO, R. M., LITTMAN, D. R., LEITGES, M., RAWLINGS, D. J. &

KAWAKAMI, T. 2004. Protein kinase C betaII regulates Akt phosphorylation on Ser-473 in a cell type- and stimulus-specific fashion. *J Biol Chem,* 279**,** 47720-5.

KENNEDY, S. G., WAGNER, A. J., CONZEN, S. D., JORDAN, J., BELLACOSA, A., TSICHLIS, P. N. & HAY, N. 1997. The PI 3-kinase/Akt signaling pathway delivers an anti-apoptotic signal. *Genes Dev,* 11**,** 701-713.

KIM, H. H., KUWANO, Y., SRIKANTAN, S., LEE, E. K., MARTINDALE, J. L. & GOROSPE, M. 2009. HuR recruits let-7/RISC to repress c-Myc expression. *Genes Dev,* 23**,** 1743-1748.

KIM, H. H., LEE, S. J., GARDINER, A. S., PERRONE-BIZZOZERO, N. I. & YOO, S. 2015. Different motif requirements for the localization zipcode element of β-actin mRNA binding by HuD and ZBP1. *Nucleic Acids Res,* 43**,** 7432-7446.

KIM, Y. J. & BAKER, B. S. 1993. The Drosophila gene rbp9 encodes a protein that is a member of a conserved group of putative RNA binding proteins that are nervous system-specific in both flies and humans. *J Neurosci,* 13**,** 1045-1056.

KOLLAR, P., RAJCHARD, J., BALOUNOVA, Z. & PAZOUREK, J. 2014. Marine natural products: bryostatins in preclinical and clinical studies. *Pharm Biol,* 52**,** 237-42.

KOTHARY, R. 2010. Use of pen test (balance beam) to assess motor balance and coordination in mice. *TREAT-NMD Neuromuscular Network, Experimental protocols for SMA animal models,* SMA_M.2.1.001.

KRAFT, A. S., BAKER, V. V. & MAY, W. S. 1987. Bryostatin induces changes in protein kinase C location and activity without altering c-myc gene expression in human promyelocytic leukemia cells (HL-60). *Oncogene,* 1**,** 111-118.

KRAFT, A. S., SMITH, J. B. & BERKOW, R. L. 1986. Bryostatin, an activator of the calcium phospholipid-dependent protein kinase, blocks phorbol ester-induced differentiation of human promyelocytic leukemia cells HL-60. *Proc Natl Acad Sci U S A,* 83**,** 1334-1338.

KRAFT, A. S., WILLIAM, F., PETTIT, G. R. & LILLY, M. B. 1989. Varied differentiation responses of human leukemias to bryostatin 1. *Cancer Res,* 49**,** 1287-1293.

KRISHNA, M. & NARANG, H. 2008. The complexity of mitogen-activated protein kinases (MAPKs) made simple. *Cell Mol Life Sci,* 65**,** 3525-44.

KUGELBERG, E. & WELANDER, L. 1956. Heredofamilial juvenile muscular atrophy simulating muscular dystrophy. *AMA Arch Neurol Psy,* 75**,** 500-509.

KULLMANN, M., GÖPERT, U., SIEWE, B. & HENGST, L. 2002. ELAV/Hu proteins inhibit p27 translation via an IRES element in the p27 5'UTR. *Genes Dev,* 16**,** 3087-3099.

LE, T. T., PHAM, L. T., BUTCHBACH, M. E., ZHANG, H. L., MONANI, U. R., COOVERT, D. D., GAVRILINA, T. O., XING, L., BASSELL, G. J. & BURGHES, A. H. 2005. SMNDelta7, the major product of the centromeric survival motor neuron (SMN2) gene, extends survival in mice with spinal muscular atrophy and associates with full-length SMN. *Hum Mol Genet,* 14**,** 845-57.

LEE, E. K., KIM, W., TOMINAGA, K., MARTINDALE, J. L., YANG, X., SUBARAN, S. S., CARLSON, O. D., MERCKEN, E. M., KULKARNI, R. N., AKAMATSU, W., OKANO, H., PERRONE-BIZZOZERO, N. I., DE CABO, R., EGAN, J. M. & GOROSPE, M. 2012. RNA-binding protein HuD controls insulin translation. *45,* 6.

LEE, H. W., SMITH, L., PETTIT, G. R., VINITSKY, A. & SMITH, J. B. 1996. Ubiquitination of protein kinase C-alpha and degradation by the proteasome. *J Biol Chem,* 271**,** 20973-20976.

LEFEBVRE, S., BÜRGLEN, L., REBOULLET, S., CLERMONT, O., BURLET, P., VIOLLET, L., BENICHOU, B., CRUAUD, C., MILLASSEAU, P., ZEVIANI, M., LE PASLIER, D., PRÉZAL, J., COHEN, D., WEISSENBACH, J., MUNNICH, A. & MELKI, J. 1995. Identification and characterization of a spinal muscular atrophy-determining gene. *Cell,* 80**,** 155-165.

LEFEBVRE, S., BURLET, P., LIU, Q., BERTRANDY, S., CLERMONT, O., MUNNICH, A., DREYFUSS, G. & MELKI, J. 1997. Correlation between severity and SMN protein level in spinal muscular atrophy. *Nat Genet,* 16**,** 265-269.

LI, Y., MOHAMMAD, R. M., AL-KATIB, A., VARTERASIAN, M. L. & CHEN, B. 1997. Bryostatin 1 (bryo1)-induced monocytic differentiation in THP-1 human leukemia cells is associated with enhanced c-fyn tyrosine kinase and M-CSF receptors. *Leuk Res,* 21**,** 391-397.

LILLY, M. B., TOMPKINS, C., BROWN, C., PETTIT, G. R. & KRAFT, A. S. 1990. Differentiation and growth modulation of chronic myelogenous leukemia cells by bryostatin. *Cancer Res,* 50**,** 5520-5525.

LIM, C. S. & ALKON, D. L. 2012. Protein kinase C stimulates HuD-mediated mRNA stability and protein expression of neurotrophic factors and enhances dendritic maturation of hippocampal neurons in culture. *Hippocampus,* 22**,** 2303-2319.

LIM, C. S. & ALKON, D. L. 2014. PKCε promotes HuD-mediated neprilysin mRNA stability and enhances Neprilysin-Induced Aβ degradation in brain neurons. *PLoS One,* 9**,** e98856.

LIU, H., QIU, Y., XIAO, L. & DONG, F. 2006. Involvement of Protein Kinase C in the Negative Regulation of Akt Activation Stimulated by Granulocyte Colony-Stimulating Factor. *The Journal of Immunology,* 176**,** 2407-2413.

LIU, J., DALMAU, J., SZABO, A., ROSENFELD, M., HUBER, J. & FURNEAUX, H. M. 1995. Paraneoplastic encephalomyelitis antigens bind to the AU-rich elements of mRNA. *Neurology,* 45**,** 544-550.

LIU, Q. & DREYFUSS, G. 1996. A novel nuclear structure containing the survival of motor neurons protein. *EMBO J,* 15**,** 3555-3565.

LIU, Q., FISCHER, U., WANG, F. & DREYFUSS, G. 1997. The spinal muscular atrophy disease gene product, SMN, and its associated protein SIP1 are in a complex with spliceosomal snRNP proteins. *Cell,* 90**,** 1013-1021.

LORENZO, P. S., BÖGI, K., ACS, P., PETTIT, G. R. & BLUMBERG, P. M. 1997. The catalytic domain of protein kinase Cdelta confers protection from down-regulation induced by bryostatin 1. *J Biol Chem,* 272**,** 33338-33343.

LORSON, C. L. & ANDROPHY, E. J. 1998a. The domain encoded by exon 2 of the survival motor neuron protein mediates nucleic acid binding. *Hum Mol Genet,* 7**,** 1269-1275.

LORSON, C. L., HAHNEN, E., ANDROPHY, E. J. & WIRTH, B. 1999. A single nucleotide in the SMN gene regulates splicing and is responsible for spinal muscular atrophy. *Proc Natl Acad Sci U S A,* 96**,** 6307-6311.

LORSON, C. L., STRASSWIMMER, J., YAO, J. M., BALEJA, J. D., HAHNEN, E., WIRTH, B., LE, T. T., BURGHES, A. H. & ANDROPHY, E. J. 1998b. SMN oligomerization defect correlates with SMA severity. *Nat Genet,* 19**,** 63-66.

LU, J. Y. & SCHNEIDER, R. J. 2004. Tissue distribution of AU-rich mRNA-binding proteins involved in regulation of mRNA decay. *J Biol Chem,* 279**,** 12974-9.

LUCKE-WOLD, B. P., LOGSDON, A. F., SMITH, K. E., TURNER, R. C., ALKON, D. L., TAN, Z., NASER, Z. J., KNOTTS, C. M., HUBER, J. D. & ROSEN, C. L. 2015. Bryostatin-1 Restores Blood Brain Barrier Integrity following Blast-Induced Traumatic Brain Injury. *Mol Neurobiol,* 52**,** 1119-1134.

LYON, A. N., PINEDA, R. H., HAO LE, T., KUDRYASHOVA, E., KUDRYASHOV, D. S. & BEATTIE, C. E. 2014. Calcium binding is essential for plastin 3 function in Smn-deficient motoneurons. *Hum Mol Genet,* 23**,** 1990-2004.

MA, W. J., CHENG, S., CAMPBELL, C., WRIGHT, A. & FURNEAUX, H. M. 1996. Cloning and characterization of HuR, a ubiquitously expressed Elav-like protein. *J Biol Chem,* 271**,** 8144-8151.

MA, W. J., CHUNG, S. & FURNEAUX, H. M. 1997. The Elav-like proteins bind to AU-rich elements and to the poly(A) tail of mRNA. *Nucleic Acids Res,* 25**,** 3564-3569.

MANSFIELD, K. D. & KEENE, J. D. 2012. Neuron-specific ELAV/Hu proteins suppress HuR mRNA during neuronal differentiation by alternative polyadenylation. *Nucleic Acids Res,* 40**,** 2734-2746.

MARCHESI, N., AMADIO, M., COLOMBRITA, C., GOVONI, S., RATTI, A. & PASCALE, A. 2016. PKC Activation Counteracts ADAM10 Deficit in HuD-Silenced Neuroblastoma Cells. *J Alzheimers Dis,* 54**,** 535-47.

MATERA, A. G. & SHPARGEL, K. B. 2006. Pumping RNA: nuclear bodybuilding along the RNP pipeline. *Curr Opin Cell Biol,* 18**,** 317-24.

MATSUMOTO, E., HATANAKA, M., BOHGAKI, M. & MAEDA, S. 2006. PKC pathway and ERK/MAPK pathway are required for induction of cyclin D1 and p21Waf1 during 12-o-tetradecanoylphorbol 13-acetate-induced differentiation of myeloleukemia cells. *Kobe J Med Sci,* 52**,** 181-194.

MATTIS, V. B., EBERT, A. D., FOSSO, M. Y., CHANG, C. W. & LORSON, C. L. 2009. Delivery of a read-through inducing compound, TC007, lessens severity of a spinal muscular atrophy animal model. *Hum Mol Genet,* 18**,** 3906-3913.

MCANDREW, P. E., PARSONS, D. W., SIMARD, L. R., ROCHETTE, C., RAY, P. N., MENDELL, J. R., PRIOR, T. W. & BURGHES, A. H. 1997. Identification of proximal spinal muscular atrophy carriers and patients by analysis of SMNT and SMNC gene copy number. *Am J Hum Genet,* 60**,** 1411-22.

MCCARTY, D. M., MONAHAN, P. E. & SAMULSKI, R. J. 2001. Self-complementary recombinant adeno-associated virus (scAAV) vectors promote efficient transduction independently of DNA synthesis. *Gene Ther,* 8**,** 1248-1254.

MCCUBREY, J. A., STEELMAN, L. S., CHAPPELL, W. H., ABRAMS, S. L., WONG, E. W., CHANG, F., LEHMANN, B., TERRIAN, D. M., MILELLA, M., TAFURI, A., STIVALA, F., LIBRA, M., BASECKE, J., EVANGELISTI, C., MARTELLI, A. M. & FRANKLIN, R. A. 2007. Roles of the Raf/MEK/ERK pathway in cell growth, malignant transformation and drug resistance. *Biochim Biophys Acta,* 1773**,** 1263-84.

MCGOVERN, V. L., MASSONI-LAPORTE, A., WANG, X., LE, T. T., LE, H. T., BEATTIE, C. E., RICH, M. M. & BURGHES, A. H. 2015. Plastin 3 Expression Does Not Modify Spinal Muscular Atrophy Severity in the 7 SMA Mouse. *PLoS One,* 10**,** e0132364.

MCWHORTER, M. L., MONANI, U. R., BURGHES, A. H. & BEATTIE, C. E. 2003. Knockdown of the survival motor neuron (Smn) protein in zebrafish causes defects in motor axon outgrowth and pathfinding. *J Cell Biol,* 162**,** 919-31.

MEBRATU, Y. & TESFAIGZI, Y. 2009. How ERK1/2 activation controls cell proliferation and cell death: Is subcellular localization the answer? *Cell Cycle,* 8**,** 1168-75.

MELKI, J., ABDELHAK, S., SHETH, P., BACHELOT, M. F., BURLET, P., MARCADET, A., AICARDI, J., BAROIS, A., CARRIERE, J. P., FARDEAU, M., FONTAN, D., PONSOT, G., BILLETTE, T., ANGELINI, C., BARBOSA, C., FERRIERE, G., LANZI, G., OTTOLINI, A., BABRON, M. C., COHEN, D., HANAUER, A., CLERGET-DARPOUX, F., LATHROP, M., MUNNICH, A. & FREZAL, J. 1990a. Gene for chronic proximal spinal muscular atrophies maps to chromosome 5q. *Nature,* 344**,** 767-768.

MELKI, J., SHETH, P., ABDELHAK, S., BURLET, P., BACHELOT, M. F., LATHROP, M. G., FREZAL, J. & MUNNICH, A. 1990b. Mapping of acute (type I) spinal muscular atrophy to chromosome 5q12-q14. The French Spinal Muscular Atrophy Investigators. *Lancet,* 336**,** 271-273.

MELLOR, H. & PARKER, P. J. 1998. The extended protein kinase C superfamily. *Biochem J,* 332**,** 281-292.

MEYER, K., FERRAIUOLO, L., SCHMELZER, L., BRAUN, L., MCGOVERN, V., LIKHITE, S., MICHELS, O., GOVONI, A., FITZGERALD, J., MORALES, P., FOUST, K. D., MENDELL, J. R., BURGHES, A. H. & KASPAR, B. K. 2015. Improving single injection CSF delivery of AAV9-mediated gene therapy for SMA: a dose-response study in mice and nonhuman primates. *Mol Ther,* 23**,** 477-87.

MICHAUD, M., ARNOUX, T., BIELLI, S., DURAND, E., ROTROU, Y., JABLONKA, S., ROBERT, F., GIRAUDON-PAOLI, M., RIESSLAND, M., MATTEI, M. G., ANDRIAMBELOSON, E., WIRTH, B., SENDTNER, M., GALLEGO, J., PRUSS, R. M. & BORDET, T. 2010. Neuromuscular defects and breathing disorders in a new mouse model of SMA. *Neurobiol Dis,* 38**,** 125-135.

MIZUTANI, K., SONODA, S., WAKITA, H. & SHIMPO, K. 2015. Protein kinase C activator, bryostatin-1, promotes exercise-dependent functional recovery in rats with cerebral infarction. *Am J Phys Med Rehabil,* 94**,** 239-43.

MOBARAK, C. D., ANDERSON, K. D., MORIN, M., BECKEL-MITCHENER, A. C., ROGERS, S. L., FURNEAUX, H. M., KING, P. H. & PERRONE-BIZZOZERO, N. 2000. The RNA-binding Protein HuD Is Required for GAP- 43 mRNA Stability, GAP-43 Gene Expression, and PKC-dependent Neurite Outgrowth in PC12 Cells. *Mol Biol Cell* 11**,** 3191-3203.

MONANI, U. R., LORSON, C. L., PARSONS, D. W., PRIOR, T. W., ANDROPHY, E. J., BURGHES, A. H. & MCPHERSON, J. D. 1999. A single nucleotide difference that alters splicing patterns distinguishes the SMA gene SMN1 from the copy gene SMN2. *Hum Mol Genet,* 8**,** 1177-1183.

MONANI, U. R., PASTORE, M. T., GAVRILINA, T. O., JABLONKA, S., LE, T. T., ANDREASSI, C., DICOCCO, J. M., LORSON, C. L., ANDROPHY, E. J., SENDTNER, M., PODELL, M. & BURGHES, A. H. 2003. A transgene carrying an A2G missense mutation in the SMN gene modulates phenotypic severity in mice with severe (type I) spinal muscular atrophy. *J Cell Biol,* 160**,** 41-52.

MONANI, U. R., SENDTNER, M., COOVERT, D. D., PARSONS, D. W., ANDREASSI, C., LE, T. T., JABLONKA, S., SCHRANK, B., ROSSOLL, W., PRIOR, T. W., MORRIS, G. E. & BURGHES, A. H. 2000. The human centromeric survival motor neuron gene rescues embryonic lethality in smn-- mice and results in a mouse with SMA. *Hum Mol Genet,* 9**,** 333-339.

MOULARD, B., SALACHAS, F., CHASSANDE, B., BRIOLOTTI, V., MEININGER, V., MALAFOSSE, A. & CAMU, W. 1998. Association between centromeric deletions of the SMN gene and sporadic adult-onset lower motor neuron disease. *Ann Neurol,* 43**,** 640-644.

MUNSAT, T. L. 1991. Workshop report: International SMA collaboration. *Neuromuscul Disord,* 1**,** 81.

MUNSAT, T. L. & DAVIES, K. E. 1992. International SMA Consortium Meeting. *Neuromuscul Disord,* 2**,** 423-428.

MURESU, R., BALDINI, A., GRESS, T., POSNER, J. B., FURNEAUX, H. M. & SINISCALCO, M. 1994. Mapping of the gene coding for a paraneoplastic encephalomyelitis antigen (HuD) to human chromosome site 1p34. *Cytogenet Cell Genet,* 65**,** 177-178.

MUTTER, R. & WILLS, M. 2000. Chemistry and clinical biology of the bryostatins. *Bioorg Med Chem,* 8**,** 1841-1860.

NARVER, H. L., KONG, L., BURNETT, B. G., CHOE, D. W., BOSCH-MARCE, M., TAYE, A. A., ECKHAUS, M. A. & SUMNER, C. J. 2008. Sustained improvement of spinal muscular atrophy mice treated with trichostatin A plus nutrition. *Ann Neurol,* 64**,** 465-70.

NEWTON, A. C. 2001. Protein Kinase C: Structural and Spatial Regulation by Phosphorylation, Cofactors, and Macromolecular Interactions. *Chemical Reviews,* 101**,** 2353-2364.

OKANO, H. J. & DARNELL, R. B. 1997. A hierarchy of Hu RNA binding proteins in developing and adult neurons. *J Neurosci,* 17**,** 3024-3037.

ONO, Y., FUJII, T., OGITA, K., KIKKAWA, U., IGARASHI, K. & NISHIZUKA, Y. 1987. Identification of three additional members of rat protein kinase C family: delta-, epsilon- and zeta-subspecies. *FEBS Lett,* 226**,** 125-128.

ONO, Y., FUJJI, T., IGARASHI, K., KUNO, T., TANAKA, C., KIKKAWA, U. & NISHIZUKA, Y. 1989a. Phorbol ester binding to protein kinase C requires a cysteine-rich zinc-finger-like sequence. *Proc Natl Acad Sci U S A,* 86**,** 4868-4871.

ONO, Y., FUJJI, T., OGITA, K., KIKKAWA, U., IGARASHI, K. & NISHIZUKA, Y. 1989b. Protein kinase C zeta subspecies from rat brain: its structure, expression, and properties. *Proc Natl Acad Sci U S A,* 86**,** 3099-3103.

OPREA, G. E., KRÖBER, S., MCWHORTER, M. L., ROSSOLL, W., MÜLLER, S., KRAWCZAK, M., BASSELL, G. J., BEATTIE, C. E. & WIRTH, B. 2008. Plastin 3 is a protective modifier of autosomal recessive spinal muscular atrophy. *Science,* 320**,** 524-527.

OSADA, S., MIZUNO, K., SAIDO, T. C., AKITA, Y., SUZUKI, K., KUROKI, T. & OHNO, S. 1990. A phorbol ester receptor/protein kinase, nPKC eta, a new member of the protein kinase C family predominantly expressed in lung and skin. *J Biol Chem,* 265**,** 22343-22440.

OSADA, S., MIZUNO, K., SAIDO, T. C., SUZUKI, K., KUROKI, T. & OHNO, S. 1992. A new member of the protein kinase C family, nPKC theta, predominantly expressed in skeletal muscle. *Mol Cell Biol,* 12**,** 3930-3938.

OSKOUI, M., LEVY, G., GARLAND, C. J., GRAY, J. M., O'HAGEN, J., DE VIVO, D. C. & KAUFMANN, P. 2007. The changing natural history of spinal muscular atrophy type 1. *Neurology,* 69**,** 1931-1936.

OSMAN, E. Y., WASHINGTON, C. W., SIMON, M. E., MEGIDDO, D., GREIF, H. & LORSON, C. L. 2017. Analysis of azithromycin monohydrate as a single or a combinatorial therapy in a mouse model of severe spinal muscular atrophy. *J Neuromuscul Dis,* Preprint**,** 1-13.

OTTESEN, E. W. 2017. ISS-N1 makes the First FDA-approved Drug for Spinal Muscular Atrophy. *Transl Neurosci,* 8**,** 1-6.

OTTESEN, E. W., HOWELL, M. D., SINGH, N. N., SEO, J., WHITLEY, E. M. & SINGH, R. N. 2016. Severe impairment of male reproductive organ development in a low SMN expressing mouse model of spinal muscular atrophy. *Sci Rep,* 6**,** 20193.

PAGLIARDINI, S., GIAVAZZI, A., SETOLA, V., LIZIER, C., DI LUCA, M., DEBIASI, S. & BATTAGLIA, G. 2000. Subcellular localization and axonal transport

of the survival motor neuron (SMN) protein in the developing rat spinal cord. *Hum Mol Genet,* 9**,** 47-56.

PARK, S., MYSZKA, D. G., YU, M., LITTLER, S. J. & LAIRD-OFFRINGA, I. A. 2000. HuD RNA recognition motifs play distinct roles in the formation of a stable complex with AU-Rich RNA. *Molecular and Cellular Biology,* 20**,** 4765-4772.

PARKER, P. J., COUSSENS, L., TOTTY, N., RHEE, L., YOUNG, S., CHEN, E., STABEL, S., WATERFIELD, M. D. & ULLRICH, A. 1986. The complete primary structure of protein kinase C-the major phorbol ester receptor. *Science,* 233**,** 853-859.

PASCALE, A., AMADIO, M., SCAPAGNINI, G., LANNI, C., RACCHI, M., PROVENZANI, A., GOVONI, S., ALKON, D. L. & QUATTRONE, A. 2005. Neuronal ELAV proteins enhance mRNA stability by a PKCalpha-dependent pathway. *Proc Natl Acad Sci U S A,* 102**,** 12065-12070.

PASCALE, A., GUSEV, P. A., AMADIO, M., DOTTORINI, T., GOVONI, S., ALKON, D. L. & QUATTRONE, A. 2004. Increase of the RNA-binding protein HuD and posttranscriptional up-regulation of the GAP-43 gene during spatial memory. *Proc Natl Acad Sci U S A,* 101**,** 1217-1222.

PASSINI, M. A. 2011. Antisense oligonucleotides delivered to the mouse CNS ameliorate symptoms of severe spinal muscular atrophy. *Sci Transl Med,* 3**,** 72ra18.

PEARN, J. H., HUDGSON, P. & WALTON, J. N. 1978. A clinical and genetic study of spinal muscular atrophy of adult onset: the autosomal recessive form as a discrete disease entity. *Brain,* 101**,** 591-606.

PELLIZZONI, L., CHARROUX, B. & DREYFUSS, G. 1999. SMN mutants of spinal muscular atrophy patients are defective in binding to snRNP proteins. *Proc Natl Acad Sci U S A,* 96**,** 11167-11172.

PELLIZZONI, L., KATAOKA, N., CHARROUX, B. & DREYFUSS, G. 1998. A novel function for SMN, the spinal muscular atrophy disease gene product, in pre-mRNA splicing. *Cell,* 95**,** 615-624.

PERRONE-BIZZOZERO, N. I., CANSINO, V. V. & KOHN, D. T. 1993. Posttranscriptional regulation of GAP-43 gene expression in PC12 cells through protein kinase C-dependent stabilization of the mRNA. *J Cell Biol,* 120**,** 1263-1270.

PETTIT, G. R., HERALD, C. L., DOUBEK, D. L., HERALD, D. L., ARNOLD, E. & CLARDY, J. 1982. Isolation and structure of bryostatin 1. *J Am Chem Soc,* 104**,** 6846-6848.

PIAZZON, N., RAGE, F., SCHLOTTER, F., MOINE, H., BRANLANT, C. & MASSENET, S. 2008. In vitro and in cellulo evidences for association of the survival of motor neuron complex with the fragile X mental retardation protein. *J Biol Chem,* 283**,** 5598-610.

PIEPERS, S., COBBEN, J. M., SODAAR, P., JANSEN, M. D., WADMAN, R. I., MEESTER-DELVER, A., POLL-THE, B. T., LEMMINK, H. H., WOKKE, J. H., VAN DER POL, W. L. & VAN DEN BERG, L. H. 2011. Quantification of SMN protein in leucocytes from spinal muscular atrophy patients: effects of treatment with valproic acid. *J Neurol Neurosurg Psychiatry,* 82**,** 850-2.

PRIOR, T. W., KRAINER, A. R., HUA, Y., SWOBODA, K. J., SNYDER, P. C., BRIDGEMAN, S. J., BURGHES, A. H. & KISSEL, J. T. 2009. A positive modifier of spinal muscular atrophy in the SMN2 gene. *Am J Hum Genet,* 85**,** 408-13.

QUATTRONE, A., PASCALE, A., NOGUES, X., ZHAO, W., GUSEV, P., PACINI, A. & ALKON, D. L. 2001. Posttranscriptional regulation of gene expression in learning by the neuronal ELAV-like mRNA-stabilizing proteins. *Proc Natl Acad Sci U S A,* 98**,** 11668-11673.

RACKE, F. K., LEWANDOWSKA, K., GOUELI, S. & GOLDFARB, A. N. 1997. Sustained activation of the extracellular signal-regulated kinase/mitogen-activated protein kinase pathway is required for megakaryocytic differentiation of K562 cells. *J Biol Chem,* 272**,** 23366-23370.

RAGE, F., BOULISFANE, N., RIHAN, K., NEEL, H., GOSTAN, T., BERTRAND, E., BORDONNÉ, R. & SORET, J. 2013. Genome-wide identification of mRNAs associated with the protein SMN whose depletion decreases their axonal localization. *RNA,* 19**,** 1755-1766.

RAMSDELL, J. S., PETTIT, G. R. & TASHJIAN, A. H. J. 1986. Three activators of protein kinase C, bryostatins, dioleins, and phorbol esters, show differing specificities of action on GH, pituitary cells. *J Biol Chem,* 261**,** 17073-17080.

RATTI, A., FALLINI, C., COLOMBRITA, C., PASCALE, A., LAFORENZA, U., QUATTRONE, A. & SILANI, V. 2008. Post-transcriptional regulation of neuro-

oncological ventral antigen 1 by the neuronal RNA-binding proteins ELAV. *J Biol Chem,* 283**,** 7531-41.

RIESSLAND, M., BRICHTA, L., HAHNEN, E. & WIRTH, B. 2006. The benzamide M344, a novel histone deacetylase inhibitor, significantly increases SMN2 RNA/protein levels in spinal muscular atrophy cells. *Hum Genet,* 120**,** 101-10.

RIESSLAND, M., KACZMAREK, A., SCHNEIDER, S., SWOBODA, K. J., LOHR, H., BRADLER, C., GRYSKO, V., DIMITRIADI, M., HOSSEINIBARKOOIE, S., TORRES-BENITO, L., PETERS, M., UPADHYAY, A., BIGLARI, N., KROBER, S., HOLKER, I., GARBES, L., GILISSEN, C., HOISCHEN, A., NURNBERG, G., NURNBERG, P., WALTER, M., RIGO, F., BENNETT, C. F., KYE, M. J., HART, A. C., HAMMERSCHMIDT, M., KLOPPENBURG, P. & WIRTH, B. 2017. Neurocalcin Delta Suppression Protects against Spinal Muscular Atrophy in Humans and across Species by Restoring Impaired Endocytosis. *Am J Hum Genet,* 100**,** 297-315.

ROBBINS, K. L., GLASCOCK, J. J., OSMAN, E. Y., MILLER, M. R. & LORSON, C. L. 2014. Defining the therapeutic window in a severe animal model of spinal muscular atrophy. *Hum Mol Genet,* 23**,** 4559-4568.

ROBINOW, S. & WHITE, K. 1988. The locus elav of Drosophila melanogaster is expressed in neurons at all developmental stages. *Dev Biol,* 126**,** 294-303.

ROSS, R. A., LAZAROVA, D. L., MANLEY, G. T., SMITT, P. S., SPENGLER, B. A., POSNER, J. B. & BIEDLER, J. L. 1997. HuD, a neuronal-specific RNA-binding protein, is a potential regulator of MYCN expression in human neuroblastoma cells. *Eur J Cancer,* 33**,** 2071-2074.

ROSSOLL, W., JABLONKA, S., ANDREASSI, C., KRONING, A. K., KARLE, K., MONANI, U. R. & SENDTNER, M. 2003. Smn, the spinal muscular atrophy-determining gene product, modulates axon growth and localization of beta-actin mRNA in growth cones of motoneurons. *J Cell Biol,* 163**,** 801-12.

ROSSOLL, W., KRÖNING, A. K., OHNDORF, U. M., STEEGBORN, C., JABLONKA, S. & SENDTNER, M. 2002. Specific interaction of Smn with hnRNP-R and gry-rbphnRNP-Q a role for Smn in RNA processing in motor axons. *Hum Mol Genet,* 11**,** 93-105.

RUSSMAN, B. S. 2007. Spinal muscular atrophy: clinical classification and disease heterogeneity. *J Child Neurol,* 22**,** 946-51.

SAAL, L., BRIESE, M., KNEITZ, S., GLINKA, M. & SENDTNER, M. 2014. Subcellular alterations in a cell culture model of spinal muscular atrophy point to widespread defects in axonal growth and presynaptic. *RNA,* 20**,** 1789-1802.

SAITO, K., FUJIWARA, T., KATASHIRA, J., INOUE, K. & SAKAMOTO, H. 2004. TAP/NXF1, the primary mRNA export receptor, specifically interacts with a neuronal RNA-binding protein HuD. *Biochem Biophys Res Commun,* 321**,** 291-297.

SAKO, T., YUSPA, S. H., HERALD, C. L., PETTIT, G. R. & BLUMBERG, P. M. 1987. Partial parallelism and partial blockade by bryostatin 1 of effects of phorbol ester tumor promoters on primary mouse epidermal cells. *Cancer Res,* 47**,** 5445-5450.

SALAZAR-GRUESO, E. F., KIM, S. & KIM, H. 1991. Embryonic mouse spinal cord motor neuron hybrid cells. *Neuroreport,* 2**,** 505-508.

SAMSON, M.-L. & CHALVET, F. 2003. found in neurons, a third member of the Drosophila elav gene family, encodes a neuronal protein and interacts with elav. *Mechanisms of Development,* 120**,** 373-383.

SANCHEZ, G., DURY, A. Y., MURRAY, L. M., BIONDI, O., TADESSE, H., EL FATIMY, R., KOTHARY, R., CHARBONNIER, F., KHANDJIAN, E. W. & CÔTÉ, J. 2013. A novel function for the survival motoneuron protein as a translational regulator. *Hum Mol Genet,* 22**,** 668-684.

SCHRANK, B., GÖTZ, R., GUNNERSEN, J. M., URE, J. M., TOYKA, K. V., SMITH, A. G. & SENDTNER, M. 1997. Inactivation of the SMN gene, a candidate gene for human spinal muscular atrophy, leads to massive cell death in early mouse embryos. *Proc Natl Acad Sci U S A,* 94**,** 9920-9925.

SCHREML, J., RIESSLAND, M., PATERNO, M., GARBES, L., ROSSBACH, K., ACKERMANN, B., KRAMER, J., SOMERS, E., PARSON, S. H., HELLER, R., BERKESSEL, A., STERNER-KOCK, A. & WIRTH, B. 2013. Severe SMA mice show organ impairment that cannot be rescued by therapy with the HDACi JNJ-26481585. *Eur J Hum Genet,* 21**,** 643-52.

SCHROTT, L. M., JACKSON, K., YI, P., DIETZ, F., JOHNSON, G. S., BASTING, T. F., PURDUM, G., TYLER, T., RIOS, J. D., CASTOR, T. P. & ALEXANDER, J. S. 2015. Acute oral Bryostatin-1 administration improves learning deficits in the APP/PS1 transgenic mouse model of Alzheimer's disease. *Curr Alzheimer Res,* 12**,** 22-31.

SCOTO, M., FINKEL, R. S., MERCURI, E. & MUNTONI, F. 2017. Therapeutic approaches for spinal muscular atrophy (SMA). *Gene Ther*.

SEKIDO, Y., BADER, S. A., CARBONE, D. P., JOHNSON, B. E. & MINNA, J. D. 1994. Molecular analysis of the HuD gene encoding a paraneoplastic encephalomyelitis antigen in human lung cancer cell lines. *Cancer Res,* 54**,** 4988-4992.

SELENKO, P., SPRANGERS, R., STIER, G., BÜHLER, D., FISCHER, U. & SATTLER, M. 2001. SMN Tudor domain structure and its interaction with the Sm proteins. *Nat Struct Biol,* 8**,** 27-31.

SHABABI, M., HABIBI, J., YANG, H. T., VALE, S. M., SEWELL, W. A. & LORSON, C. L. 2010. Cardiac defects contribute to the pathology of spinal muscular atrophy models. *Hum Mol Genet,* 19**,** 4059-4071.

SHANMUGARAJAN, S., TSURUGA, E., SWOBODA, K. J., MARIA, B. L., RIES, W. L. & REDDY, S. V. 2009. Bone loss in survival motor neuron (Smn(-/-) SMN2) genetic mouse model of spinal muscular atrophy. *J Pathol,* 219**,** 52-60.

SHARMA, A., LAMBRECHTS, A., HAO LE, T., LE, T. T., SEWRY, C. A., AMPE, C., BURGHES, A. H. & MORRIS, G. E. 2005. A role for complexes of survival of motor neurons (SMN) protein with gemins and profilin in neurite-like cytoplasmic extensions of cultured nerve cells. *Exp Cell Res,* 309**,** 185-97.

SHAUL, Y. D. & SEGER, R. 2007. The MEK/ERK cascade: from signaling specificity to diverse functions. *Biochim Biophys Acta,* 1773**,** 1213-26.

SINGH, N. K., SINGH, N. N., ANDROPHY, E. J. & SINGH, R. N. 2006. Splicing of a critical exon of human Survival Motor Neuron is regulated by a unique silencer element located in the last intron. *Mol Cell Biol,* 26**,** 1333-46.

SINGH, N. N., HOWELL, M. D., ANDROPHY, E. J. & SINGH, R. N. 2017. How the discovery of ISS-N1 led to the first medical therapy for spinal muscular atrophy. *Gene Ther*.

SINGH, N. N., LAWLER, M. N., OTTESEN, E. W., UPRETI, D., KACZYNSKI, J. R. & SINGH, R. N. 2013. An intronic structure enabled by a long-distance interaction serves as a novel target for splicing correction in spinal muscular atrophy. *Nucleic Acids Res,* 41**,** 8144-65.

SINGH, N. N., LEE, B. M., DIDONATO, C. J. & SINGH, R. N. 2015. Mechanistic principles of antisense targets for the treatment of spinal muscular atrophy. *Future Med Chem,* 7**,** 1793-1808.

SINGH, N. N. & SINGH, R. N. 2011. Alternative splicing in spinal muscular atrophy underscores the role of an intron definition model. *RNA Biol,* 8**,** 600-6.

SINTUSEK, P., CATAPANO, F., ANGKATHUNKAYUL, N., MARROSU, E., PARSON, S. H., MORGAN, J. E., MUNTONI, F. & ZHOU, H. 2016. Histopathological Defects in Intestine in Severe Spinal Muscular Atrophy Mice Are Improved by Systemic Antisense Oligonucleotide Treatment. *PLoS One,* 11**,** e0155032.

SMITH, C. L., AFROZ, R., BASSELL, G. J., FURNEAUX, H. M., PERRONE-BIZZOZERO, N. I. & BURRY, R. W. 2004. GAP-43 mRNA in growth cones is associated with HuD and ribosomes. *J Neurobiol,* 61**,** 222-235.

SMITH, J. B., SMITH, L. & PETTIT, G. R. 1985. Bryostatins: potent, new mitogens that mimic phorbol ester tumor promoters. *Biochem Biophys Res Commun,* 132**,** 939-945.

SOLLER, M. & WHITE, K. 2003. ELAV inhibits 3'-end processing to promote neural splicing of ewg pre-mRNA. *Genes Dev,* 17**,** 2526-38.

SOSANYA, N. M., CACHEAUX, L. P., WORKMAN, E. R., NIERE, F., PERRONE-BIZZOZERO, N. I. & RAAB-GRAHAM, K. F. 2015. Mammalian target of rapamycin (mTOR) tagging promotes dendritic branch variability through the capture of Ca2+/Calmodulin-dependent Protein Kinase II α (CaMKIIα) mRNAs by the RNA-binding Protein HuD. *J Biol Chem,* 290**,** 16357-16371.

SOSANYA, N. M., HUANG, P. P., CACHEAUX, L. P., CHEN, C. J., NGUYEN, K., PERRONE-BIZZOZERO, N. I. & RAAB-GRAHAM, K. F. 2013. Degradation of high affinity HuD targets releases Kv1.1 mRNA from miR-129 repression by mTORC1. *J Cell Biol,* 202**,** 53-69.

STRATIGOPOULOS, G., LANZANO, P., DENG, L., GUO, J., KAUFMANN, P., DARRAS, B., FINKEL, R. S., TAWIL, R., MCDERMOTT, M. P., MARTENS, W., DEVIVO, D. C. & CHUNG, W. K. 2010. Association of plastin 3 expression with disease severity in spinal muscular atrophy only in postpubertal females. *Arch Neurol,* 67**,** 1252-1256.

SUMNER, C. J., HUYNH, T. N., MARKOWITZ, J. A., PERHAC, J. S., HILL, B., COOVERT, D. D., SCHUSSLER, K., CHEN, X., JARECKI, J., BURGHES, A. H., TAYLOR, J. P. & FISCHBECK, K. H. 2003. Valproic acid increases SMN levels in spinal muscular atrophy patient cells. *Ann Neurol,* 54**,** 647-654.

SUN, M. K. & ALKON, D. L. 2005a. Dual effects of bryostatin-1 on spatial memory and depression. *Eur J Pharmacol,* 512**,** 43-51.

SUN, M. K., HONGPAISAN, J., LIM, C. S. & ALKON, D. L. 2014. Bryostatin-1 restores hippocampal synapses and spatial learning and memory in adult fragile x mice. *J Pharmacol Exp Ther,* 349**,** 393-401.

SUN, Y., GRIMMLER, M., SCHWARZER, V., SCHOENEN, F., FISCHER, U. & WIRTH, B. 2005b. Molecular and functional analysis of intragenic SMN1 mutations in patients with spinal muscular atrophy. *Hum Mutat,* 25**,** 64-71.

SWOBODA, K. J., SCOTT, C. B., CRAWFORD, T. O., SIMARD, L. R., REYNA, S. P., KROSSCHELL, K. J., ACSADI, G., ELSHEIK, B., SCHROTH, M. K., D'ANJOU, G., LASALLE, B., PRIOR, T. W., SORENSON, S. L., MACZULSKI, J. A., BROMBERG, M. B., CHAN, G. M., KISSEL, J. T. & PROJECT CURE SPINAL MUSCULAR ATROPHY INVESTIGATORS, N. 2010. SMA CARNI-VAL trial part I: double-blind, randomized, placebo-controlled trial of L-carnitine and valproic acid in spinal muscular atrophy. *PLoS One,* 5**,** e12140.

SZABO, A., DALMAU, J., MANLEY, G., ROSENFELD, M., WONG, E., HENSON, J., POSNER, J. B. & FURNEAUX, H. M. 1991. HuD, a paraneoplastic encephalomyelitis antigen, contains RNA-binding domains and is homologous to Elav and sex-lethal. *Cell,* 67**,** 325-333.

SZUNYOGOVA, E., ZHOU, H., MAXWELL, G. K., POWIS, R. A., FRANCESCO, M., GILLINGWATER, T. H. & PARSON, S. H. 2016. Survival Motor Neuron (SMN) protein is required for normal mouse liver development. *Sci Rep,* 6**,** 34635.

TADESSE, H., DESCHENES-FURRY, J., BOISVENUE, S. & COTE, J. 2008. KH-type splicing regulatory protein interacts with survival motor neuron protein and is misregulated in spinal muscular atrophy. *Hum Mol Genet,* 17**,** 506-24.

TAN, Z., TURNER, R. C., LEON, R. L., LI, X., HONGPAISAN, J., ZHENG, W., LOGSDON, A. F., NASER, Z. J., ALKON, D. L., ROSEN, C. L. & HUBER, J. D. 2013. Bryostatin improves survival and reduces ischemic brain injury in aged rats after acute ischemic stroke. *Stroke,* 44**,** 3490-7.

THOMSON, A. K., SOMERS, E., POWIS, R. A., SHORROCK, H. K., MURPHY, K., SWOBODA, K. J., GILLINGWATER, T. H. & PARSON, S. H. 2017. Survival of motor neurone protein is required for normal postnatal development of the spleen. *J Anat,* 230**,** 337-346.

TIRUCHINAPALLI, D. M., EHLERS, M. D. & KEENE, J. D. 2008. Activity-dependent expression of RNA binding protein HuD and its association with mRNAs in neurons. *RNA Biol,* 5**,** 157-168.

TOMINAGA, K., SRIKANTAN, S., LEE, E. K., SUBARAN, S. S., MARTINDALE, J. L., ABDELMOHSEN, K. & GOROSPE, M. 2011. Competitive regulation of nucleolin expression by HuR and miR-494. *Mol Cell Biol,* 31**,** 4219-31.

TRIPSIANES, K., MADL, T., MACHYNA, M., FESSAS, D., ENGLBRECHT, C., FISCHER, U., NEUGEBAUER, K. M. & SATTLER, M. 2011. Structural basis for dimethylarginine recognition by the Tudor domains of human SMN and SPF30 proteins. *Nat Struct Mol Biol,* 18**,** 1414-20.

TSAI, K. C., CANSINO, V. V., KOHN, D. T., NEVE, R. L. & PERRONE-BIZZOZERO, N. I. 1997. Post-transcriptional regulation of the GAP-43 gene by specific sequences in the 3' untranslated region of the mRNA. *J Neurosci,* 17**,** 1950-1958.

TSAI, L. K., TSAI, M. S., LIN, T. B., HWU, W. L. & LI, H. 2006. Establishing a standardized therapeutic testing protocol for spinal muscular atrophy. *Neurobiol Dis,* 24**,** 286-95.

VALORI, C. F., NING, K., WYLES, M., MEAD, R. J., GRIERSON, A. J., SHAW, P. J. & AZZOUZ, M. 2010. Systemic delivery of scAAV9 expressing SMN prolongs survival in a model of spinal muscular atrophy. *Sci Transl Med,* 2**,** 35ra42.

VEZAIN, M., SAUGIER-VEBER, P., GOINA, E., TOURAINE, R., MANEL, V., TOUTAIN, A., FEHRENBACH, S., FREBOURG, T., PAGANI, F., TOSI, M. & MARTINS, A. 2010. A rare SMN2 variant in a previously unrecognized composite splicing regulatory element induces exon 7 inclusion and reduces the clinical severity of spinal muscular atrophy. *Hum Mutat,* 31**,** E1110-25.

VIOLLET, L., BERTRANDY, S., BUENO BRUNIALTI, A. L., LEFEBVRE, S., BURLET, P., CLERMONT, O., CRUAUD, C., GUÉNET, J. L., MUNNICH, A. & MELKI, J. 1997. cDNA isolation, expression, and chromosomal localization of the mouse survival motor neuron gene (Smn). *Genomics,* 40**,** 185-188.

VITTE, J. M., DAVOULT, B., ROBLOT, N., MAYER, M., JOSHI, V., COURAGEOT, S., TRONCHE, F., VADROT, J., MOREAU, M. H., KEMENY, F. & MELKI, J. 2004. Deletion of murine Smn exon 7 Directed to liver leads to severe defect of liver development associated with iron overload. *Am J Pathol,* 165**,** 1731-1741.

WALL, N. R., MOHAMMAD, R. M. & AL-KATIB, A. 2001. Mitogen-activated protein kinase is required for bryostatin 1-induced differentiation of the human acute lymphoblastic leukemia cell line Reh. *Cell Growth Differ,* 12**,** 641-647.

WALTER, L. M., BETTS, C. A., MEJIBOOM, K. E., VAN WESTERING, T., HAZELL, G., WOOD, M. J. A. & BOWERMAN, M. SMN around the clock: Circadian dysregulation in SMA metabolic tissues [abstract]. 21st SMA Researcher Meeting, June 30th, 2017 2017 Orlando, FL.

WAN, L., BATTLE, D. J., YONG, J., GUBITZ, A. K., KOLB, S. J., WANG, J. & DREYFUSS, G. 2005. The survival of motor neurons protein determines the capacity for snRNP assembly: biochemical deficiency in spinal muscular atrophy. *Mol Cell Biol,* 25**,** 5543-51.

WANG, H., MOLFENTER, J., ZHU, H. & LOU, H. 2010. Promotion of exon 6 inclusion in HuD pre-mRNA by Hu protein family members. *Nucleic Acids Res,* 38**,** 3760-3770.

WANG, X. & TANAKA HALL, T. M. 2001. Structural basis for recognition of AU-rich element RNA by the HuD protein. *Nat Struct Biol,* 8**,** 141-145.

WANG, Z., MA, H. I., LI, J., SUN, L., ZHANG, J. & XIAO, X. 2003. Rapid and highly efficient transduction by double-stranded adeno-associated virus vectors in vitro and in vivo. *Gene Ther,* 10**,** 2105-2111.

WEN, H. C., HUANG, W. C., ALI, A., WOODGETT, J. R. & LIN, W. W. 2002. Negative regulation of phosphatidylinositol 3-kinase and Akt signalling pathway by PKC. *Cell Signal,* 15**,** 37-45.

WERDNIG, G. 1891. Zwei frühinfantile hereditäre Fälle von progressiver Muskelatrophie unter dem Bilde der Dystrophie, aber anf neurotischer Grundlage. *Arch Psychiat Nerven,* 22**,** 437-481.

WERDNIG, G. 1894. Die frühinfantile progressive spinale Amyotrophie. *Arch Psychiat Nerven,* 26**,** 706-744.

WOLSTENCROFT, E. C., MATTIS, V. B., BAJER, A. A., YOUNG, P. J. & LORSON, C. L. 2005. A non-sequence-specific requirement for SMN protein activity: the role of aminoglycosides in inducing elevated SMN protein levels. *Hum Mol Genet,* 14**,** 1199-1210.

WORKMAN, E., SAIEVA, L., CARREL, T. L., CRAWFORD, T. O., LIU, D., LUTZ, C., BEATTIE, C. E., PELLIZZONI, L. & BURGHES, A. H. 2009. A SMN missense mutation complements SMN2 restoring snRNPs and rescuing SMA mice. *Hum Mol Genet,* 18**,** 2215-29.

YOO, S., KIM, H. H., KIM, P., DONNELLY, C. J., KALINSKI, A. L., VUPPALANCHI, D., PARK, M., LEE, S. J., MERIANDA, T. T., PERRONE-BIZZOZERO, N. I. & TWISS, J. L. 2013. A HuD-ZBP1 ribonucleoprotein complex localizes GAP-43 mRNA into axons through its 3' untranslated region AU-rich regulatory element. *J Neurochem,* 126**,** 792-804.

YOUNG, L. E., MOORE, A. E., SOKOL, L., MEISNER-KOBER, N. & DIXON, D. A. 2012. The mRNA stability factor HuR inhibits microRNA-16 targeting of COX-2. *Mol Cancer Res,* 10**,** 167-80.

YOUNG, P. J., MAN, N. T., LORSON, C. L., LE, T. T., ANDROPHY, E. J., BURGHES, A. H. & MORRIS, G. E. 2000. The exon 2b region of the spinal muscular atrophy protein, SMN, is involved in self-association and SIP1 binding. *Hum Mol Genet,* 9**,** 2869-2877.

ZERRES, K., RUDNIK-SCHÖNEBORN, S., FORREST, E., LUSAKOWSKA, A., BORKOWSKA, A. & HAUSMANOVA-PETRUSEWICZ, I. 1997. A collaborative study on the natural history of childhood and juvenile onset proximal spinal muscular atrophy (type II and III SMA): 569 patients. *J Neurol Sci,* 146**,** 67-72.

ZERRES, K., RUDNIK-SCHÖNEBORN, S. S., FORKERT, R. & WIRTH, B. 1995. Genetic basis of adult-onset spinal muscular atrophy. *Lancet,* 346**,** 1162.

ZHANG, H., XING, L., ROSSOLL, W., WICHTERLE, H., SINGER, R. H. & BASSELL, G. J. 2006. Multiprotein complexes of the survival of motor neuron protein SMN with Gemins traffic to neuronal processes and growth cones of motor neurons. *J Neurosci,* 26**,** 8622-32.

ZHANG, H. L., PAN, F., HONG, D., SHENOY, S. M., SINGER, R. H. & BASSELL, G. J. 2003. Active transport of the survival motor neuron protein and the role of exon-7 in cytoplasmic localization. *J Neurosci,* 23**,** 6627-6637.

ZHANG, Z., LOTTI, F., DITTMAR, K., YOUNIS, I., WAN, L., KASIM, M. & DREYFUSS, G. 2008. SMN deficiency causes tissue-specific perturbations in the repertoire of snRNAs and widespread defects in splicing. *Cell,* 133**,** 585-600.

ZHOU, H. L., HINMAN, M. N., BARRON, V. A., GENG, C., ZHOU, G., LUO, G., SIEGEL, R. E. & LOU, H. 2011. Hu proteins regulate alternative splicing by inducing localized histone hyperacetylation in an RNA-dependent manner. *Proc Natl Acad Sci U S A,* 108**,** E627-35.

ZHU, H., HASMAN, R. A., BARRON, V. A., LUO, G. & LOU, H. 2006. A nuclear function of Hu proteins as neuron-specific alternative RNA processing regulators. *Mol Biol Cell,* 17**,** 5105-5114.

ZHU, H., HINMAN, M. N., HASMAN, R. A., MEHTA, P. & LOU, H. 2008. Regulation of neuron-specific alternative splicing of neurofibromatosis type 1 pre-mRNA. *Mol Cell Biol,* 28**,** 1240-51.

ZURITA-LOPEZ, C. I., SANDBERG, T., KELLY, R. & CLARKE, S. G. 2012. Human Protein Arginine Methyltransferase 7 (PRMT7) Is a Type III Enzyme Forming ω-NG-Monomethylated Arginine Residues. *Journal of Biological Chemistry,* 287**,** 7859-7870.